

NASA TECHNICAL NOTE



NASA TN D-3798

NASA TN D-3798

C.1



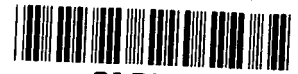
LOAN COPY: RETURN TO
AFWL (WLIL-2)
KIRTLAND AFB, N MEX

DIGITAL CODES FOR DESIGN AND
EVALUATION OF CONVECTIVELY COOLED
ROCKET NOZZLE WITH APPLICATION
TO NUCLEAR-TYPE ROCKET

by John E. Rohde, Rudolph A. Duscha, and George Derderian

*Lewis Research Center
Cleveland, Ohio*





DIGITAL CODES FOR DESIGN AND EVALUATION OF CONVECTIVELY COOLED
ROCKET NOZZLE WITH APPLICATION TO NUCLEAR-TYPE ROCKET

By John E. Rohde, Rudolph A. Duscha, and George Derderian

Lewis Research Center
Cleveland, Ohio

NATIONAL AERONAUTICS AND SPACE ADMINISTRATION

For sale by the Clearinghouse for Federal Scientific and Technical Information
Springfield, Virginia 22151 - Price \$2.50

CONTENTS

	Page
SUMMARY	1
INTRODUCTION	1
DESCRIPTION OF COMPUTER CODES	3
Basic Analytical Procedure	3
Design procedure	3
Evaluation procedure	5
Variations of design and evaluation procedures	6
Heat-Transfer Equations Utilized	6
Hot-gas side	6
Coolant side	9
Heat-transfer model	10
Fluid-Flow Equations Utilized	13
Pressure drop	13
Determination of coolant stagnation and static conditions	14
Coolant-Passage Stress Analysis Utilized	16
APPLICATION OF CODES TO NUCLEAR-ROCKET-TYPE NOZZLE	18
Design Procedure	18
Nozzle conditions	19
Temperatures and heights of coolant passages	20
Coolant-passage stresses	24
Variation in number of coolant tubes	24
Effect of Assumptions on Design	26
Heat-transfer-correlation effects	27
Curvature heat-transfer-correction effect	29
Heat-conduction-model effect	29
Heat-transfer-area correction effect	29
Coolant tube roughness and curvature effects	29
Combined effects	32
Coolant	33
Wall temperatures	34
Coolant-passage stresses	35
Use of Thermal-Barrier Coating	37
Off-Design Conditions	38
General Remarks	40

CONCLUDING REMARKS 40

APPENDIXES

 A - SYMBOLS 42

 B - STAGNATION PRESSURE STATE 45

 C - COOLANT-PASSAGE STRESS ANALYSIS 48

 D - DETAILS OF DESIGN AND EVALUATION PROGRAMS 53

REFERENCES 90

DIGITAL CODES FOR DESIGN AND EVALUATION OF CONVECTIVELY COOLED ROCKET NOZZLE WITH APPLICATION TO NUCLEAR-TYPE ROCKET

by John E. Rohde, Rudolph A. Duscha, and George Derderian

Lewis Research Center

SUMMARY

The design of the coolant passages of a convectively cooled nozzle is dictated by heat-transfer and flow considerations that are compatible with the overall rocket system and acceptable stresses within the nozzle structure. The method presented for designing this type of nozzle utilizes both a design and an evaluation computer program used in conjunction. These digital computer programs are coded in FORTRAN IV for use on an IBM 7094 computer.

The design program calculates coolant passage dimensions for a specified gas-side wall temperature distribution, and the evaluation program calculates a gas-side wall temperature distribution for specified coolant-passage dimensions. In addition, coolant conditions are calculated, and all heat-transfer and fluid flow results are utilized to calculate coolant-passage tangential and longitudinal stresses.

The programs are set up to utilize a range of heat-transfer correlations, different tube surface roughness conditions, and a tube splice. The evaluation program has the additional capability to handle radial or flat-plate heat conduction across the tube crown and the application of a coating to the gas side of the coolant passage.

Application of these programs is shown for the design and the evaluation of a nuclear-type rocket nozzle operating at chamber conditions of 4000°R and 530 pounds per square inch absolute with hydrogen as both the coolant and the propellant. The wide range of available heat-transfer correlations for both the hot-gas and coolant sides and the conduction model used across the tube crown result in maximum gas-side wall temperatures ranging from 1550°R to 2250°R . The majority of the calculated coolant-passage stresses are well into the plastic range for the material considered (347 stainless steel).

INTRODUCTION

Contemporary designs being developed for high-thrust propulsion systems employ

convergent-divergent nozzles. For liquid-chemical-fueled and nuclear rockets, the nozzle is convectively cooled by the fuel.

The coolant-passage design for this nozzle is dictated by heat-transfer requirements, flow considerations that are compatible with the overall rocket system, and acceptable stresses within the nozzle structure. The final design is the result of many iterations that involve the associated parameters of heat-transfer and flow considerations. The complexity of these calculations and the numerous iterations involved require the use of a high-speed digital computer.

Computer programs to perform these calculations are in use on a limited basis throughout the rocket-nozzle-development industry and at government agencies. However, there is an apparent lack of programs available for general use or being documented in a form suitable for publication.

This report describes two computer programs developed at the Lewis Research Center and discusses their application. The programs are written in FORTRAN IV for use on an IBM 7094 computer. Usage of the programs will accomplish the required calculations necessary for the final design of a convectively cooled rocket nozzle operating at steady-state conditions. One program is employed for the design and the other for the evaluation of this type of nozzle. The report is divided into a discussion of the analytical formulation of the two programs and an application to a given design that also includes determination of the effects of variations in available heat-transfer correlations and heat-conduction model.

The design program utilizes the desired gas wall temperature profile as an input and calculates the coolant-passage dimensions required to match it, while the evaluation program utilizes fixed coolant-passage dimensions as an input and calculates the resulting temperature profile. The preceding calculations are performed by an interrelated series of heat-transfer and fluid-flow equations. The state of the coolant as it progresses through the passage is also calculated. The results of the preceding calculations are used at each specified axial increment to determine the magnitude of the tangential and longitudinal stresses in the coolant-passage structure. The formulation of the coolant-passage stress analysis is described in appendix C by Rene E. Chambellan.

The model chosen for the application is a convectively cooled 347 stainless-steel conical nozzle with a throat diameter of 4.3 inches, a contraction ratio of 12, and an expansion ratio of 8. This model is considered to be a scaled version of a nuclear-rocket nozzle. Because nuclear rockets utilize hydrogen for attainment of high specific impulse, hydrogen was chosen as the propellant and the coolant with equal flow rates of 16.7 pounds per second. Chamber conditions are 4000° R and 530 pounds per square inch absolute, and coolant inlet conditions are 56° R and 1150 pounds per square inch absolute.

Coolant-passage configurations for convectively cooled nozzles have been rectangular, circular, elliptical, and U- or D-shaped, as shown in figure 1. The coolant-passage

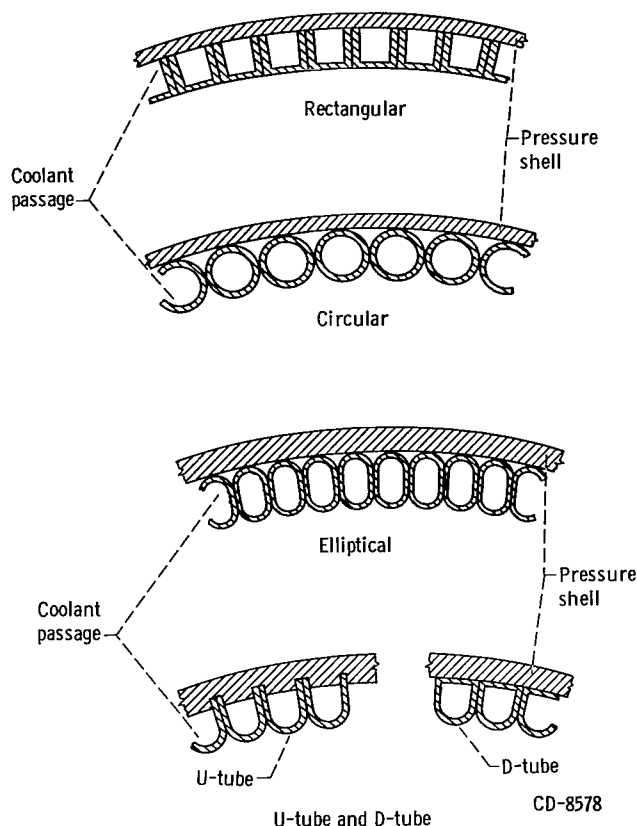


Figure 1. - Coolant-passage configurations for convectively cooled nozzles.

geometry of each of these programs has been restricted specifically to the use of flow areas for U- or D-shaped tubes. This choice of geometry was made because U- or D-shaped tubes are currently widely used in the construction of nuclear-rocket-engine nozzles.

In addition to the final design presented, the use of the available heat-transfer correlations leads to a wide range of predicted values for coolant-passage wall temperatures. These results for a fixed design can be an aid to revising the design to allow a slight amount of conservatism or safety margin. A study of these effects was made based on the design achieved for the previously mentioned conditions, and these results are also presented.

DESCRIPTION OF COMPUTER CODES

Basic Analytical Procedure

The design program and the evaluation program are similar in that the same heat-transfer and pressure-drop equations are used. The basic difference between the programs is that the design program utilizes specified gas-side wall temperatures and determines the required coolant-passage geometry, while the evaluation program uses a given coolant-passage geometry and calculates the gas-side wall temperature.

Design procedure. - The design procedure is similar to that discussed in reference 1 and is as follows:

(1) Specify the input data

- (a) Chamber fluid conditions, hot-gas-expansion data, flow rates, passage-wall thickness, gas-side contour dimensions, coolant inlet conditions, number of tubes, and material and fluid properties

- (b) Gas-side wall temperature

(2) Calculate the hot-gas heat flux into the nozzle-coolant-passage wall

(3) Calculate the coolant-side wall temperature

- (4) Calculate coolant-passage dimensions required to match specified wall temperatures
- (5) Calculate the coolant state
- (6) Iterate items (4) and (5) until convergence is obtained on the coolant state within prescribed limits
- (7) Calculate the coolant-passage wall stresses

Limitations in the form of geometry and flow conditions are imposed on this procedure.

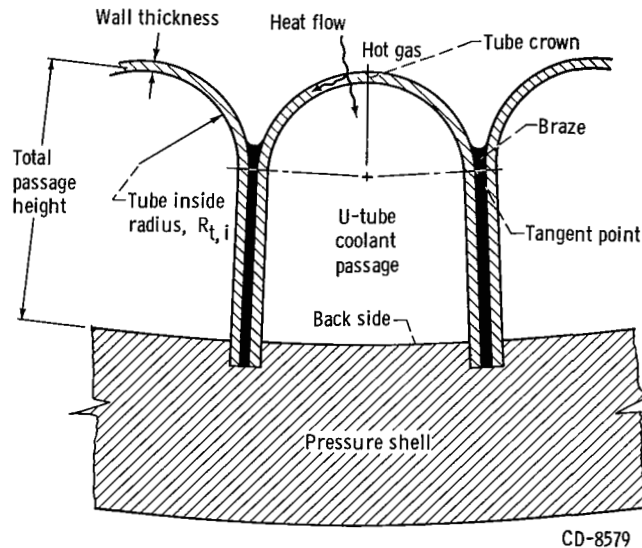


Figure 2. - Description of U-tube coolant passage.

Figure 2 illustrates the geometry of a U-tube coolant passage. The approximate flow area consists of a semicircle of radius $R_{t,i}$ combined with a trapezoid of a height equal to the total passage height minus $R_{t,i}$. (All symbols are defined in appendix A.) The area of the semicircle of radius $R_{t,i}$ is considered as being the minimum allowable passage flow area. If the area required for heat-transfer purposes is smaller than this, the minimum semicircular area and shape are used. The resulting temperatures are calculated by an evaluation procedure within the design program.

A coolant velocity limitation in the form of a maximum allowable Mach number is also set to preclude choked flow and excessive pressure drops. When this velocity limit is reached, the required coolant flow area not to exceed this limit is determined, and the resulting temperatures are calculated by the same evaluation procedure as mentioned previously.

Another limitation related to the maximum allowable Mach number is a limitation on the coolant static pressure. At high coolant velocities, conditions could exist, from one increment along the coolant passage to the next, so that all the coolant pressure could be lost. The reason is that in the established sequence of calculations, pressure drop is calculated prior to the Mach number calculation. Therefore, before the limiting Mach number routine increases the passage flow area, pressure conditions could be obtained that would give unrealistic results. This possibility can be avoided by setting a minimum coolant static pressure as a percentage of inlet pressure.

When this limit is reached, at any station for which passage dimensions are being determined, the prescribed gas-side wall temperature at that station is too low and must be increased. Consideration is first given to the possibility of the calculation being made in the region of the nozzle where wall temperatures are decreasing, usually beyond the

throat in the direction of coolant flow. The temperature is reset equal to a temperature 200°R lower than that existing at the previous station. Calculations are then repeated. If this station were in a region of the nozzle where temperatures would be still increasing at subsequent stations, a minimum pressure could again be reached and a second adjustment of wall temperature would be required. This time the temperature is set equal to that of the previous station. If the minimum pressure is reached a third time, the program will stop and print out the results for each station up to the troublesome one. The previously mentioned temperature adjustment routines in most cases should yield results that are sufficient to allow the calculations to continue for the rest of the nozzle. However, if two adjustments are not adequate, the program is stopped and the existing results are examined. This procedure is used rather than attempting to anticipate and adjust within the program for any further unrealistic input values. If two adjustments of wall temperature are adequate to avoid reaching the minimum pressure, the Mach-number - area-adjustment routine could still cause an additional increase in the temperature, as described previously.

Typically, the nozzle design resulting from the design program is refined by exterior adjustments that are then used as input to the design or evaluation program. These refinements result from a trade-off between heat transfer, pressure losses, material selection, stresses, and fabrication complexity. The predominant refinement of the final result from the design program is the smoothing of the coolant-passage heights. For fabrication purposes, the pressure shell axial profile desired is a smooth continuous curve along the nozzle.

Evaluation procedure. - The evaluation procedure is similar to the design procedure and is as follows:

- (1) Specify the input data
 - (a) Chamber conditions, hot-gas-expansion data, flow rates, passage-wall thicknesses, gas-side contour dimensions, coolant inlet conditions, number of tubes, material and fluid properties
 - (b) Coolant-passage dimensions
- (2) Estimate the hot-gas heat flux into the nozzle coolant-passage wall
- (3) Calculate the gas-side wall temperature
- (4) Calculate the coolant-side wall temperature
- (5) Calculate the coolant state
- (6) Calculate the heat flux being added to the coolant
- (7) Iterate items (2) to (6) until a balance exists between the two heat fluxes within convergence limits
- (8) Calculate the coolant-passage wall stresses

A limitation in the form of a minimum coolant static pressure is imposed on this procedure to avoid complete loss of all the coolant pressure. When this limit is reached,

at any station, an informative message is printed and the evaluation program is restarted with the inlet coolant pressure increased by 50 pounds per square inch. This limitation will usually allow the complete evaluation of a nozzle in one run, which could require several restarts.

Variations of design and evaluation procedures. - Each program has the provision for incorporating the use of tube splices. In regions where the nozzle contour diameter is much greater than that at the throat, the tube radius to thickness ratio could be so large from a stress consideration associated with tube buckling that a tube splice would be required. By doubling the number of tubes, this ratio would then be reduced by a factor of 2, and the potential for tube buckling would be reduced. The programs only consider the use of a bifurcation as being practical from a fabrication viewpoint.

For the nuclear-rocket nozzle, the back or shell side of the coolant passage, which is normally considered a non-heat-transfer surface, does transfer into the coolant the heat generated within the nozzle pressure shell as a result of nuclear heating. Both programs have a provision to account for this heat as an addition to the total amount of heat the coolant absorbs. However, the resulting temperature rise of the shell is not considered in the stress analysis. In addition, both programs have provision to include thermal radiation as an addition to the hot-gas-side heat flux utilized. The radiation heat-flux is specified in the form of an input constant at each nozzle station.

Provision is made in the evaluation program for the utilization of a coating on the gas side of the coolant passage. The program accepts the coating in the form of either a thermal resistance or a specific coating and thickness of coating at each section along the nozzle. The use of a coating is presented in the section Use of Thermal Barrier Coating.

Heat-Transfer Equations Utilized

To accomplish the heat balance through the coolant-passage wall, equations are required for the convective heat-transfer coefficients on both the hot-gas side and the coolant side. References 2 to 9 discuss the extensive amount of analytical and experimental work that has been conducted in the area of heat transfer, which can be utilized for convectively cooled rocket nozzles. The following correlations are a comprehensive collection selected to encompass the range of correlations available. However, the coolant-side correlations have been restricted to the extent that only correlations obtained for hydrogen were considered.

Hot-gas side. - Typical of the hot-gas-side equations is the Bartz equation of reference 2

$$Nu_f = C_g Re_f^{0.8} Pr_f^{0.4} \quad (1)$$

where $C_g = 0.026$ and where the properties are evaluated at a film temperature that is the average of the gas-side wall and the gas-static temperatures.

Reference 3 has shown that this type of correlation is valid if appropriate values of C_g are used with properties evaluated at a reference condition, as described subsequently. The authors of reference 3 indicated that C_g is a function of nozzle area ratio and could vary from their experimental values for other nozzle contours. They also indicated an exponent of 0.3 for the Prandtl number.

The Nusselt equation utilized for the computer programs is

$$Nu_f = C_g Re_f^{0.8} Pr_f^{0.3} \quad (2)$$

The C_g values are supplied as input to the program. Figure 3 shows three distinct

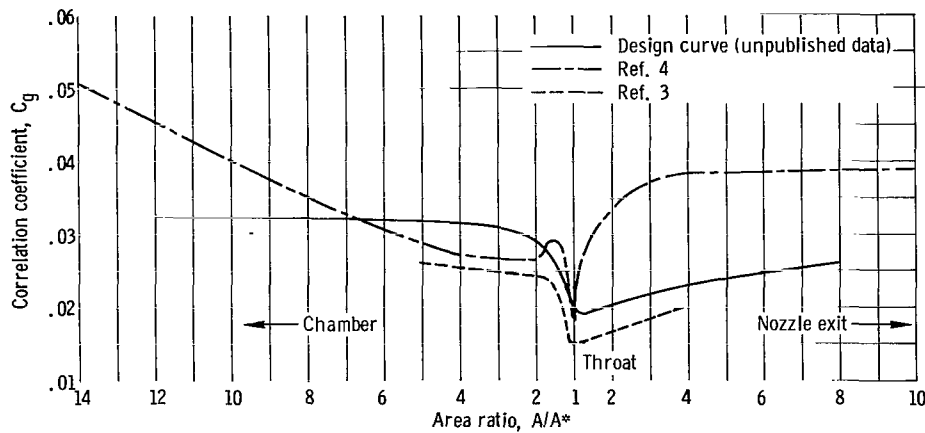


Figure 3. - Various distributions of hot-gas-side correlation constant as function of nozzle area ratio.

curves of C_g as a function of nozzle area ratio. One is from reference 3, another is from reference 4, and the third has been determined from unpublished heat-transfer data and will be referred to hereinafter as the design curve. The curve from reference 4 is based on equation (1) with properties evaluated at a film temperature defined as the average of the gas-side wall and the gas effective temperature, which is discussed in the following paragraph. Both the curve from reference 3 and the design curve are based on equation (2) with fluid properties evaluated at a reference condition, which is also discussed in the following paragraph. Values of C_g should be selected by taking into consideration the experimental conditions for which these values were determined.

Reference 5 discusses the evaluation of properties for high velocity gas flow through the use of a reference enthalpy. If any variation of the hot-gas specific heat is neglected, a reference temperature for fluid properties evaluation of the same form as equation (10-16) in reference 5 can be used as follows

$$T_{\text{ref}} = 0.5 T_{w, g} + 0.28 T_{g, s} + 0.22 T_{\text{eff}} \quad (3)$$

where

$$T_{\text{eff}} = T_{g, s} + R_f (T_{g, \text{tot}} - T_{g, s}) \quad (4)$$

and the turbulent flow recovery factor

$$R_f = \sqrt[3]{Pr_{\text{ref}}}$$

For the range of conditions considered in this report, gas properties have been evaluated at reference temperature as indicated.

The value of effective gas temperature is considered the driving temperature producing the heat transfer across the gas film in the relation

$$\left(\frac{q}{A}\right)_o = h_g (T_{\text{eff}} - T_{w, g}) \quad (5)$$

The resulting equation for the gas-side heat-transfer coefficient, which is used in the programs, is

$$h_g = \frac{C_g k_{g, f}}{D_{H, g}} \left[\left(\frac{\dot{w}}{A_{f\ell}} \right) \frac{D_H \rho_f}{\mu_f \rho_b} \right]_g^{0.8} \left(\frac{c_p \mu}{k} \right)_{g, f}^{0.3}$$

Included in the preceding equation is the film Reynolds number, which is defined as

$$Re_f = \left(\frac{\dot{w}}{A_{f\ell}} \right) \frac{D_H \rho_f}{\mu_f \rho_b}$$

where

$$\frac{\dot{w}}{A_{f\ell}} = \rho_b V_b$$

and where b refers to a static condition. The term ρ_f/ρ_b is used to correct for the value of the bulk density appearing in the $\dot{w}/A_{f\ell}$ term.

Coolant side. - Again, a type of Nusselt relation is used to calculate the heat-transfer coefficient on the coolant side as follows

$$Nu_f = C_\ell Re_f^{0.8} Pr_f^{0.4} C_1 C_2 \quad (6)$$

where C_ℓ can be varied according to axial location or held constant. Properties are evaluated at a coolant film temperature, which is the average of the coolant-side wall and the coolant total temperatures.

The coefficients C_1 and C_2 are optional corrections or modifications. The correction C_1 is that determined in reference 6 for turbulent flow and supercritical hydrogen at pressures to about 800 pounds per square inch absolute. The term accounts for the effects of the extreme variations of the fluid properties across the boundary layer. It is normally applied while using C_ℓ as a constant and equal to 0.0208. The relation for determining C_1 is

$$C_1 = 1.0 + 0.01457 \frac{\nu_w}{\nu_b} \quad (7)$$

The existence of a secondary flow in curved pipes influences the heat-transfer coefficient and friction factor, as shown in references 7 and 8. The term C_2 is a correction for the effect of coolant passage curvature on the heat-transfer process. Although this correction was derived from pressure-drop measurements, its adaptation to heat transfer was made because of the analogy between fluid friction and heat transfer. The following relation is employed that does not consider the effect of angular position as shown in reference 8:

$$C_2 = \left[Re_f \left(\frac{R_{t,i}}{R_c} \right)^2 \right]^{0.05} \quad (8)$$

The original experimental friction factor results of reference 7 were published with the Reynolds number as the bulk Reynolds number. To allow some degree of conservatism, until better heat-transfer results for curvature effects are published, the Reynolds number used for heat transfer in the C_2 term is that based on film conditions.

Reference 9 indicates that, for straight tubes and supercritical hydrogen at pressures of 1000 to 2500 pounds per square inch absolute and turbulent flow, the relation

$$Nu_f = 0.021 Re_f^{0.8} Pr_f^{0.4} \quad (9)$$

is valid. However, it should be noted that equation (9) was derived from data where the wall to bulk temperature ratios ranged from 1.5 to 11.0.

The resulting equation for the coolant-side heat-transfer coefficient, which is used in the programs, is

$$h_{\ell} = \frac{C_{\ell} k_{\ell, f}}{D_{H, \ell}} \left[\left(\frac{\dot{w}}{A_{f \ell}} \right) \frac{D_{H \ell} \rho_f}{\mu_f \rho_b} \right]_{\ell}^{0.8} \left(\frac{c_p \mu}{k} \right)_{\ell, f}^{0.4} C_1 C_2$$

with the option available for using C_1 and/or C_2 . Note that the film Reynolds number for the coolant side is defined exactly the same as the hot-gas film Reynolds number.

Heat-transfer model. - To accomplish a heat balance across the coolant passage wall, a working heat-transfer model with some simplifying assumptions is required. Figure 2 has illustrated the geometry of a U-tube coolant passage. The scalloped gas-side wall configuration is sufficiently complex so that the flow conditions cannot be defined readily in the braze region between the tubes. Previous experience leads to the observation that the top of the tube crown has the highest temperature and that the wall temperature diminishes at points closer to the tube braze. This temperature variation is further augmented by the fin effect of the tube walls, which conducts heat away from the tube crown. This leads to a complex two-dimensional heat-transfer problem in which the heat-transfer coefficients vary around the tube wall on both the inner and outer surfaces. The present state of development in the theory of nozzle design does not warrant a two-dimensional heat-flow analysis, because of its additional complexity.

The objective of the heat-transfer model is to circumvent this complexity and yet obtain a realistic heat balance across the coolant passage wall. This balance is necessary for the determination of the metal wall temperatures and the coolant heat pickup.

Meaningful metal wall temperatures can be obtained by considering the tube crown only, which is the region of maximum temperature. The tube portion exposed to the hot gas can be arbitrarily divided into two parts, according to the predominant mode of heat flow. One portion, the crown, transmits heat in a path essentially radial toward the tube centerline, whereas the remaining portion transmits heat in a skewed direction down toward the heat sink in the braze region where adjacent tubes meet. One-dimensional heat flow in the tube crown region can be considered radial or the area of heat flow for the outside and inside surface can be considered equal, as in the case of a flat plate. The true crown temperature is equal to or less than the maximum possible temperature based on pure radial heat flow, and the flat plate temperature is believed to set a lower limit for encompassing the true temperature. However, if experimental results establish that temperatures well below the flat plate temperatures exist, a complex analysis as described previously could be justified.

The following equations are for one-dimensional radial flow of heat through a cylinder

$$T_{w, g} - T_{w, \ell} = \frac{\left(\frac{q}{A}\right)_o R_{t, o} \ln\left(\frac{R_{t, o}}{R_{t, i}}\right)}{k_t} \quad (10)$$

where $(q/A)_o$ is the heat flux entering the tube and is determined by

$$\left(\frac{q}{A}\right)_o = h_g(T_{\text{eff}} - T_{w, g}) \quad (11)$$

The heat flux leaving the tube on the inside is

$$\left(\frac{q}{A}\right)_i = \left(\frac{q}{A}\right)_o \frac{R_{t, o}}{R_{t, i}} \quad (12)$$

where the difference in the outside and inside areas is accounted for.

The following equations are for the one-dimensional flow of heat through a flat plate of constant area

$$T_{w, g} - T_{w, \ell} = \frac{\left(\frac{q}{A}\right)_o t_w}{k_t} \quad (13)$$

where $(q/A)_o$ is calculated through the use of equation (11) and $(q/A)_i = (q/A)_o$.

There is a significant difference between the temperature produced by the two methods. As shown later in this report in the section Heat-conduction-model effect, the use of the radial heat-transfer equation results in a value of gas wall temperature 200°R greater than that obtained by the use of the flat-plate heat-transfer equation for typical conditions at the nozzle throat. Therefore, the use of the radial equation is more conservative and is used in both programs with the option of flat-plate heat flow being available in the evaluation program.

Another area of concern, in completing the heat balance across the coolant passage wall, is the heat input to the coolant

$$q = \sum_{n=1}^n \left(\frac{q}{A} \right)_{2-d, n} A_{ht, n} \quad (14)$$

where $(q/A)_{2-d, n}$ and $A_{ht, n}$ are the outside heat flux and surface area over the increment considered for a two-dimensional study. This heat flux would be the result of a two-dimensional analysis mentioned earlier as being too complex for use in the programs.

The following equation can be used with the radial or flat-plate one-dimensional equation as a basis

$$q = \left(\frac{q}{A} \right)_{1-d, cr} A_{ht} \quad (15)$$

where the surface area used for heat transfer is

$$A_{ht} = \Delta \ell \pi R_{t, o, av} \epsilon_{c, av}$$

where $\epsilon_{c, av}$ is a heat-transfer-area correction. The value of $\epsilon_{c, av}$ used does not appreciably affect the wall temperature, but it does affect the coolant heat pickup, as shown in the section Heat-transfer-area correction effect. A generally accepted value for $\epsilon_{c, av}$ is 0.8, and this value is used throughout this report, except where noted.

The definition of the heat-transfer-area correction can be made in the following form:

$$\epsilon_c = \frac{\sum_{n=1}^n \left(\frac{q}{A} \right)_{2-d, n} A_{ht, n}}{\sum_{n=1}^n \left(\frac{q}{A} \right)_{1-d, cr} A_{ht, sc}}$$

If the two-dimensional study were performed at each station along the nozzle, a set of values for ϵ_c could be established. By assuming that the established value of ϵ_c at each station will remain constant for slight perturbations of conditions, the use of equation (15) should yield results essentially equal to those of equation (14). This two-dimensional approach is recommended when attempting to match experimental coolant exit temperatures accurately.

Fluid Flow Equations Utilized

Pressure drop. - Two factors, friction pressure drop and momentum pressure drop, comprise the complete coolant pressure drop calculated by the program. Any coolant passage inlet and exit losses are excluded and have to be considered for each separate design.

The friction pressure drop is calculated from

$$\Delta p_{fr} = \frac{2G_{av}^2 f \Delta \ell}{\rho_{s,av} D_{H,av}^5} \quad (16)$$

where G_{av} and $D_{H,av}$ are determined as average values over the increment $\Delta \ell$ as follows:

$$G_{av} = \frac{\dot{w}}{A_{fl,av}} = \frac{2\dot{w}}{A_{fl,1} + A_{fl,2}} \quad (17)$$

$$D_{H,av} = \frac{4A_{fl,av}}{WP_{av}} = \frac{4(A_{fl,1} + A_{fl,2})}{WP_1 + WP_2} \quad (18)$$

The value of $\rho_{s,av}$ is determined from an average static pressure and average static enthalpy over $\Delta \ell$.

For smooth tube conditions, the friction factor is determined by equation (6-8b) of reference 10, which is recommended for extrapolation to high values of Reynolds number. Equation (6-8b) is given as

$$\frac{1}{\sqrt{f}} = 4.0 \log \left(Re_{av} \sqrt{f} \right) - 0.40 \quad (19)$$

For rough tube conditions, the friction factor is determined by the equation

$$\frac{1}{\sqrt{f}} = -4.0 \log \left(\frac{e}{3.7 D_{H,av}} + \frac{1.255}{Re_{av} \sqrt{f}} \right) \quad (20)$$

of reference 11, where e is the tube relative roughness.

These equations are used in the program, and the average Reynolds number is calculated from

$$\text{Re}_{av} = \frac{G_{av} D_{H, av}}{\mu_{av}} \quad (21)$$

where G_{av} , $D_{H, av}$, and μ_{av} are average values over $\Delta\ell$, evaluated as previously discussed.

A pressure drop curvature correction C_3 from reference 7 is applied to the friction factor, similar to the heat-transfer curvature correction C_2 that was applied to the heat-transfer coefficient. The equation

$$C_3 = \left[\text{Re}_{av} \left(\frac{R_{t, i}}{R_c} \right)^2 \right]^{0.05} \quad (22)$$

is used where the Reynolds number is the same one as used for evaluating the friction factor. The term C_3 is applied to the friction factor as follows:

$$f_c = C_3 f$$

with f_c being used in equation (16). The range of validity for C_2 and C_3 is

$$\text{Re} \left(\frac{R_{t, i}}{R_c} \right)^2 \geq 6$$

The momentum pressure drop is calculated from

$$\Delta p_{mom} = \frac{\dot{w}^2}{g A_{fl, av}} \left[\frac{1}{(\rho_s A_{fl})_2} - \frac{1}{(\rho_s A_{fl})_1} \right] \quad (23)$$

where $A_{fl, av}$ is the average flow area over $\Delta\ell$.

Determination of coolant stagnation and static conditions. - The inlet conditions, temperature and pressure, of the coolant are prescribed and are considered as being the stagnation or total temperature and the static pressure. For all practical purposes at the inlet to the coolant passage, total and static conditions are equal because of the low veloci-

ties usually existing there. These criteria have been adopted to facilitate the comparison of test data with analytical results. Generally, the inlet total temperature and static pressure would be measured because the instrumentation required is simpler.

Initially, the static condition is assumed to be equal to the total condition, and iterations are required to arrive at the true conditions. From the relation

$$p_{tot} = p_s + \frac{\rho_b V_b^2}{2g} \quad (24)$$

the total pressure at the inlet is calculated. The density used is evaluated at an average between the static and total conditions, which is assumed to be adequate for the low inlet velocities. The value of p_{tot} and the prescribed value of T_{tot} determine the total condition for obtaining the total enthalpy H_{tot} . By using this value for H_{tot} and the relation

$$H_s = H_{tot} - \frac{V_b^2}{2gJ} \quad (25)$$

a value of static enthalpy H_s is obtained and when combined with the given pressure yields the static condition. The iteration to arrive at an average density finally results in completely known static and total conditions.

The total heat pickup by the coolant between the nozzle stations is based on an average heat flux over the increment and heat-transfer surface area between stations:

$$\Delta H_{tot} = \frac{\left(\frac{q}{A}\right)_{av} A_{ht, av}}{\dot{w}} \quad (26)$$

For the design of a nuclear rocket nozzle where heat is also generated within the nozzle pressure shell, provision is made for including this heat in the coolant enthalpy increase. The heat generation rate in Btu per cubic inch per second is specified as input data. The average value between stations is multiplied by the incremental shell volume, and it is assumed that all this heat enters the coolant. This value is then added to the heat transferred to the coolant from the hot gas. Therefore,

$$H_{tot, 2} = H_{tot, 1} + \Delta H_{tot} + \text{Nuclear heat addition} \quad (27)$$

is the enthalpy of the coolant at station 2. The static condition at station 2 is determined by using this enthalpy in equation (25) and the static pressure calculation described in the section Pressure drop.

The total condition of the coolant will be known when the iteration on total pressure is completed. For large differences between the total and static conditions, the variations of the density term in equation (24) must be known. To avoid the problem of determining the variation between those two conditions, a relation was derived for the variation of total pressure, through the use of the energy equation and defining state equations. The derivation is described in appendix B, and the result is as follows

$$\Delta p_{\text{tot}} = J \rho_{\text{tot, av}} \Delta H_{\text{tot}} \left(1 - \frac{T_{\text{tot, av}}}{T_{\text{s, av}}} \right) - \Delta p_{\text{fr}} \left(\frac{\rho_{\text{tot, av}} T_{\text{tot, av}}}{\rho_{\text{s, av}} T_{\text{s, av}}} \right) \quad (\text{B13})$$

where all averages are arithmetic mean values from station 1 to station 2. It can be seen that, for the low velocity case, where static and total conditions are nearly equal, the change in total pressure is approximately equal to the friction pressure drop, which is to be expected. With this relation for the change in total pressure, the value of total pressure at station 2 is obtained, and the iteration is made by using the new values for total conditions in the Δp_{tot} relation. Thus, the total fluid condition at station 2 is determined.

Coolant-Passage Stress Analysis Utilized

The final design is based on considerations of heat transfer, pressure drop, and stresses developed in the structure. The temperatures of the coolant passage material alone are not necessarily indicative of safe operation; therefore, a stress analysis was incorporated into the programs. The stress calculations are made for each station, after the heat-transfer and pressure-drop routines have determined local temperatures and pressures.

Since it is anticipated that thermal stresses due to the temperature gradients will be very high, the assumption that deformations will be elastic gives a qualitative character to the results. Because of the complexity of a plastic-elastic analysis, one was not included. Use of the stress-strain curves for the materials can give an insight into the degree of yielding that can occur. The calculated stresses can be of value for predicting the relative adequacy of a nozzle design.

The idealized structure for the U-tube thick-shell configuration was assumed to consist of completely circular tubes supported in a bundle by a relatively thick shell, as shown in figure 4. Since the region of interest, the hot gas semicircular tube crown region, is adequately represented by this configuration, it is assumed valid for the purpose intended in the programs.

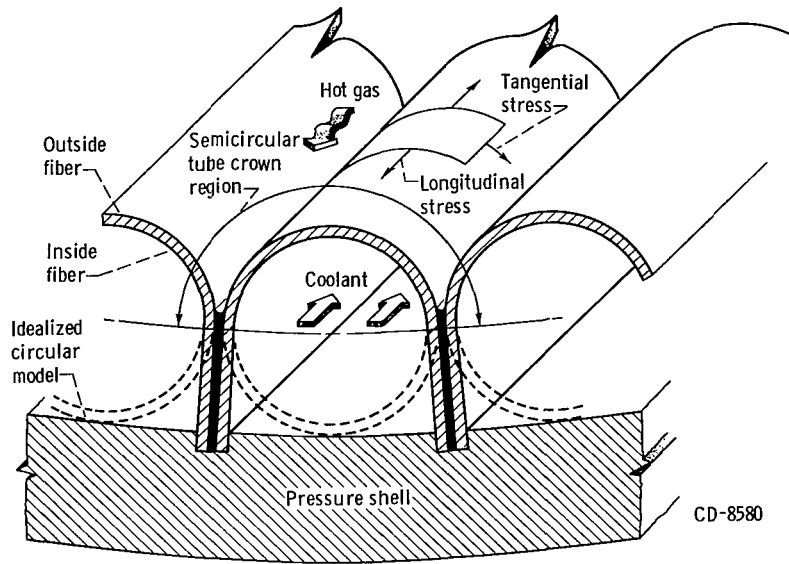


Figure 4. - Tube and shell idealized model for stress calculations showing orientation of stresses.

In general, the supporting conical shell is thick compared with the tube walls, which means that it will be much stiffer than the tubes. Therefore, the tubes will give negligible resistance to deformation of the shell, and the tubes will deform as the shell dictates. No distinction is made for the fact that the flow passage diameter (which is the diameter of the tube crown in the U-tube configuration) varies along the nozzle length. Local conditions arising from bending of the shell at the throat and knuckle are neglected. The method used to analyze the nozzle stresses is discussed in appendix C, where the equations used in the analysis are presented.

The three pertinent calculated stresses shown in figure 4 are the total tangential stress at the inner and outer fibers of the tube crown and the average tube longitudinal stress. The tangential stresses consist of both bending and the membrane stresses at the crown. The longitudinal stress is caused by the net longitudinal strain in the tubes, due primarily to the large temperature difference within the material from the hot-gas side to the cold-shell side and the pressure forces acting on the shell.

Another important structural consideration is the possible occurrence of buckling of the tube crown due to longitudinal stress. Since no adequate buckling analysis exists for this configuration, no attempt has been made to perform such an analysis for these programs. However, an analytical approach for similar situations is presented in reference 12. This reference delineates that the longitudinal stress and the ratio of tube crown radius to tube thickness are important parameters with regard to tube buckling, and both should be maintained at as low a value as possible to prevent buckling.

The specific details of the use of both the design and the evaluation codes are described in appendix D.

APPLICATION OF THE CODES TO A NUCLEAR-ROCKET-TYPE NOZZLE

Design Procedure

In the situation where a completely new nozzle design is required, various parameters would be known and fixed, a range could exist for some, and others would be open for examination for effect. In the case of designing a nozzle for a nuclear rocket, the hot-gas conditions, that is, flow rate, and reactor exit temperature and pressure, would be set. For either flight or reactor test conditions, an exit area ratio would be established also. By knowing these values, an inside contour for the nozzle is determined for either a conical or bell-shaped nozzle. The convergence region could be a subject for examination, such as determining the effect of convergence angle on the heat-transfer and stress results. Usually there are governing factors such as overall length and the interface design between the reactor pressure vessel and nozzle pressure shell; therefore, it will be assumed that the complete gas-side contour and fluid condition would be set.

On the coolant side, an exit temperature and pressure requirement would exist to allow a matching of system conditions. The coolant inlet temperature would be established according to supply conditions. The inlet pressure would be a variable up to a maximum value equal to the feed systems limitations. Therefore, two criteria associated with the coolant to be achieved by the design would be a fixed minimum temperature rise and a pressure drop not exceeding the maximum allowable. The coolant flow rate for a nuclear nozzle would be essentially equal to the hot-gas flow rate. A slight deviation could exist to allow for a small percentage of bleed off from the main coolant supply to cool other parts of the system.

The major parameter to be specified as input is the hot-gas-side wall temperature distribution. The actual distribution desired is difficult to specify until some initial results have been obtained and the effect of these temperatures on the overall design determined. As a start, a suitable approach is to specify a relatively low constant gas-side wall temperature and a Mach number limit of 0.3. The Mach number, pressure, and minimum area limitations would then cause the program to recalculate new temperatures for the region where the low temperatures are unobtainable. A higher constant temperature and a Mach number limit of 0.3 could be specified and a new design obtained. The results of these two designs should reasonably bracket the final design desired. Typically, the gas-side wall temperatures and related heat fluxes reach a peak near the throat and then drop to lower values in the regions fore and aft of the throat.

Nozzle conditions. - A scaled down configuration of a nuclear-rocket nozzle was chosen as the model for the example presented herein. Chamber conditions were set at 4000°R and 530 pounds per square inch absolute, and coolant inlet conditions were set at 56°R and 1150 pounds per square inch absolute. A throat diameter of 4.3 inches was established. Hydrogen was the coolant and the propellant with equal flow rates of 16.7 pounds per second being used. Figure 5 shows the gas-side contour, axial station division of the nozzle and lists the basic dimensions.

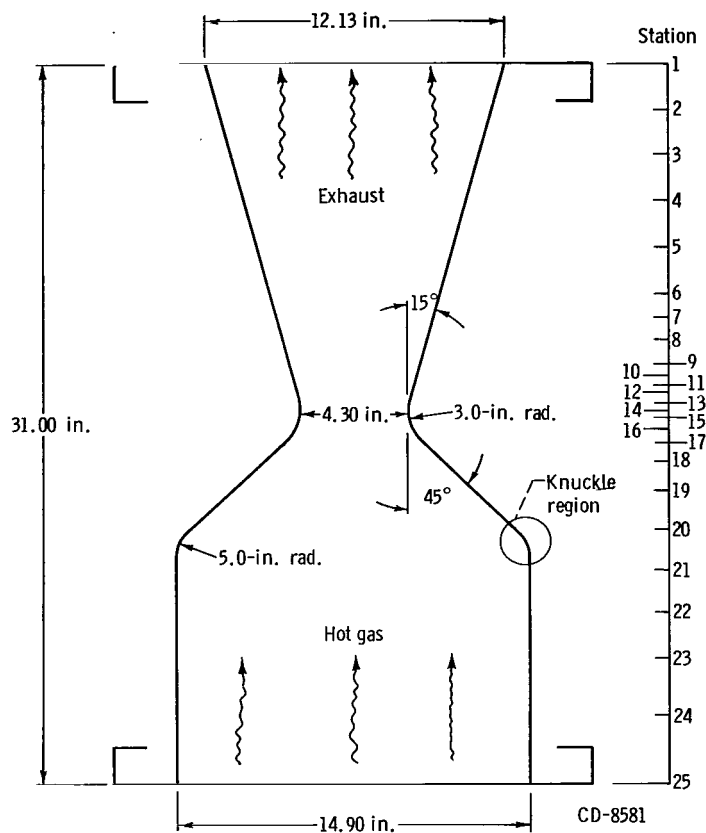


Figure 5. - Nozzle gas-side contour and station location.

The coolant passage material selected was 347 stainless steel with properties as shown in figure 6. The initial selection of the number of tubes is made by selecting probable minimum values of tube wall thickness and tube crown radius that can be fabricated readily. A thickness of 0.012 inch and a radius of $1/16$ inch were assumed to be reasonable values based on existing fabrication information. By using these values, the throat diameter of 4.3 inches, and a gap thickness for shim and braze material between tubes of 0.010 inch, the number of tubes determined as an initial number for which to obtain results was 90. The use of other numbers of tubes is discussed later.

The following assumptions were made to obtain the results for the design discussion

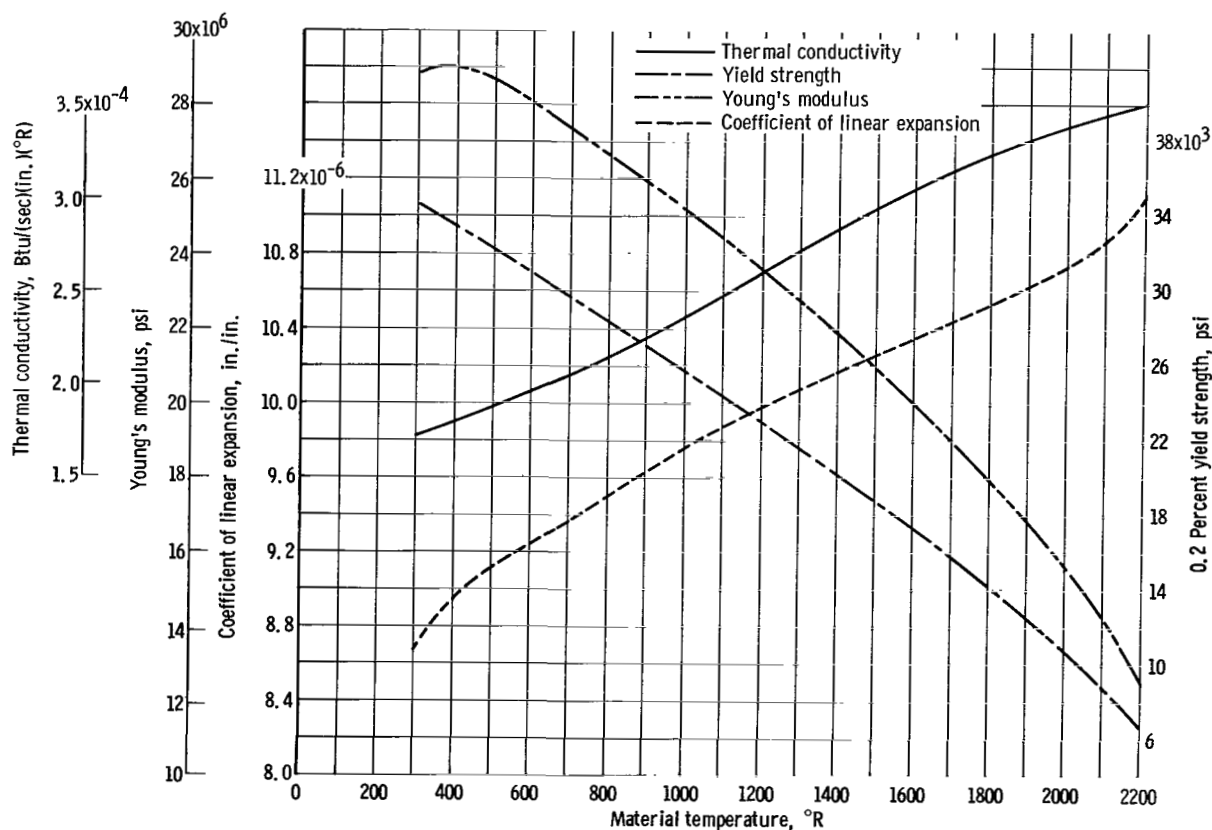


Figure 6. - Properties of 347 stainless steel as function of material temperature from curve fits of data.

that follows. On the gas side, equation (2) was used in conjunction with the design C_g curve of figure 3 (p. 7), with fluid properties being evaluated at reference temperature of equation (3). On the coolant side, because of the high coolant pressure range, equation (9) was used.

The program calculations were made at each of the 25 axial stations into which the nozzle was divided, as shown in figure 5. Because the calculations assume a linear relation in each variable from one station to the next, the lengths between stations are not uniform. In regions where small changes in variables occur, relatively large distances were chosen. In the region near the throat where variables are rapidly changing, increments were chosen small enough so that the assumption of linear changes would still be valid and not lead to erroneous results.

Temperatures and heights of coolant passages. - A temperature of 1300° R and another of 1700° R were chosen as the initial constant values of gas-side wall temperatures for two design runs. Figure 7 shows the resulting temperature distributions produced by the program limitation features. The constant temperature of 1300° R was achieved up to station 8. At station 9, the Mach number limit of 0.3 was exceeded, so that the passage area was increased to just produce this flow condition. This resulted in a wall tem-

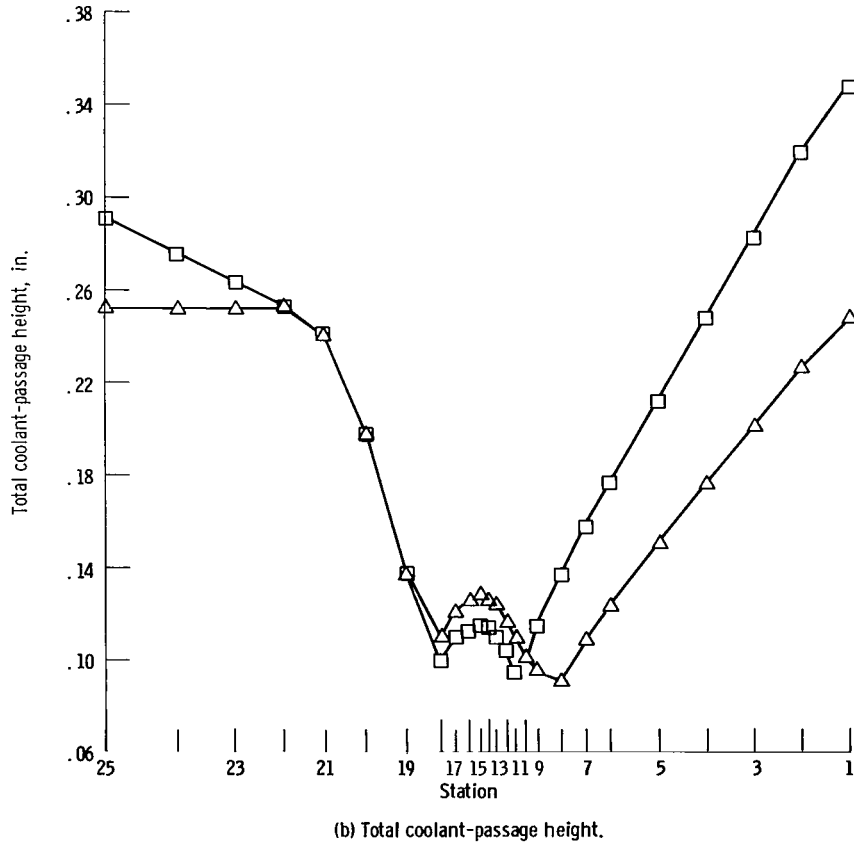
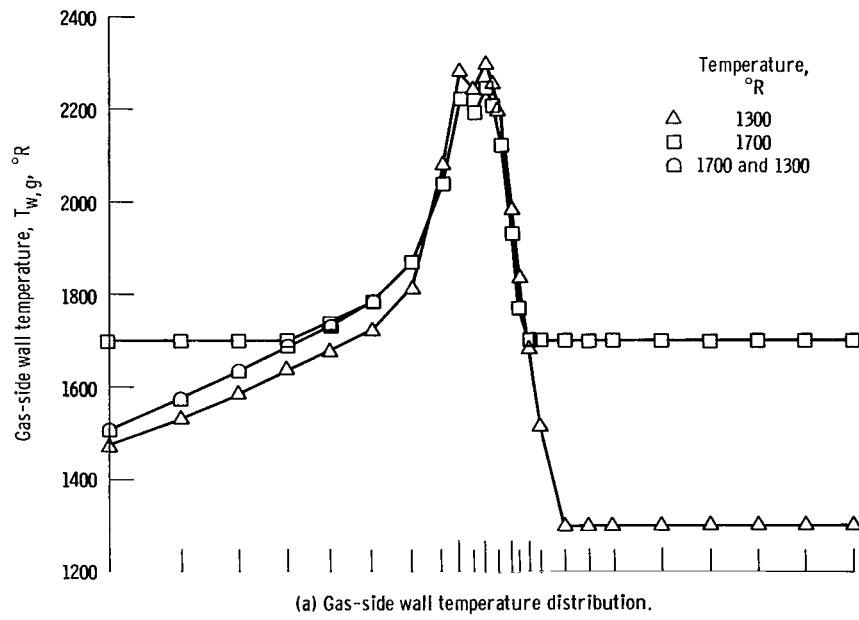


Figure 7. - Effect of gas-side wall temperature input on results of design program.

perature of 1514°R . This Mach number limitation was the governing factor at each successive station up to and including station 18. The required increase in flow area resulted in the calculated temperatures, as shown in figure 7(a). At station 19, the area required to produce 1300°R was smaller than the limiting semicircular minimum area. The use of the minimum area resulted in a temperature of 1809°R . This minimum area limitation was the governing factor at each successive station up to and including the final one and also resulted in temperatures higher than the specified input value of 1300°R .

For the next computer run, the constant temperature of 1700°R was maintained up to station 10. At station 11, the Mach number limit again prevailed and continued to produce temperatures in excess of 1700°R up to station 18. For stations 19 to 21, the minimum area limitation governed and also produced temperatures greater than 1700°R . Conditions for stations 22 to 25 permitted the attainment of the specified 1700°R .

The third temperature distribution, shown in figure 7(a), is that resulting from an input of 1700°R for the first 20 stations and 1300°R for the remaining five. Therefore, the results for the first 20 stations are identical to those for a constant input of 1700°R for the entire nozzle. At station 19, the minimum area limitation governed and prevailed for the rest of the remaining stations resulting in a temperature distribution similar to that for a constant input of 1300°R but higher by about 50°R at each station.

TABLE I. - COOLANT TEMPERATURE RISE AND PRESSURE
DROP FOR THREE TEMPERATURE DISTRIBUTIONS

Total coolant conditions	Temperature input, $^{\circ}\text{R}$		
	1300	1700	1700 and 1300
Temperature rise, ΔT , $^{\circ}\text{R}$	94.3	86.4	87.8
Pressure drop, Δp , psi	180.3	158.1	160.5

Table I gives the coolant temperature rise and pressure drop for each run. The 1300°R case produces the highest coolant temperature rise due to the cooler wall temperatures and resulting greater heat flux. This case also has the greatest pressure drop due predominantly to the smaller tube flow areas required to produce the cooler temperatures. The combined 1700° and 1300°R case with wall temperatures appreciably cooler than those of the 1700°R case at the last three stations produced no appreciable increase in coolant pressure drop over the 1700°R case.

Figure 7(b) shows the axial distribution of total passage heights for each case. The combined 1700° and 1300°R case heights are the same as those of the 1700°R case up to station 21 and then are the same as those of the 1300°R case for the rest of the length. From the results indicated in figure 7 and table I, it is apparent that in the cylindrical part, upstream from the convergent region, the use of minimum areas at stations 21 to 25

(indicated by the constant value of total height) yields the most acceptable results. In the throat region from stations 8 to 18 either case results in irregular coolant passage heights.

Starting with the results from the design procedure, the first step is the smoothing of the coolant passage heights from one station to another. These heights combined with the fixed gas-side wall diameters determine the inside shell contour. This contour must be selected to produce a smooth transition from one section to another without any discontinuities and must also be based on matching the preliminary design coolant passage heights as closely as possible. The selected shell contour with resulting coolant passage heights is then checked through the use of the evaluation program, to determine if un-

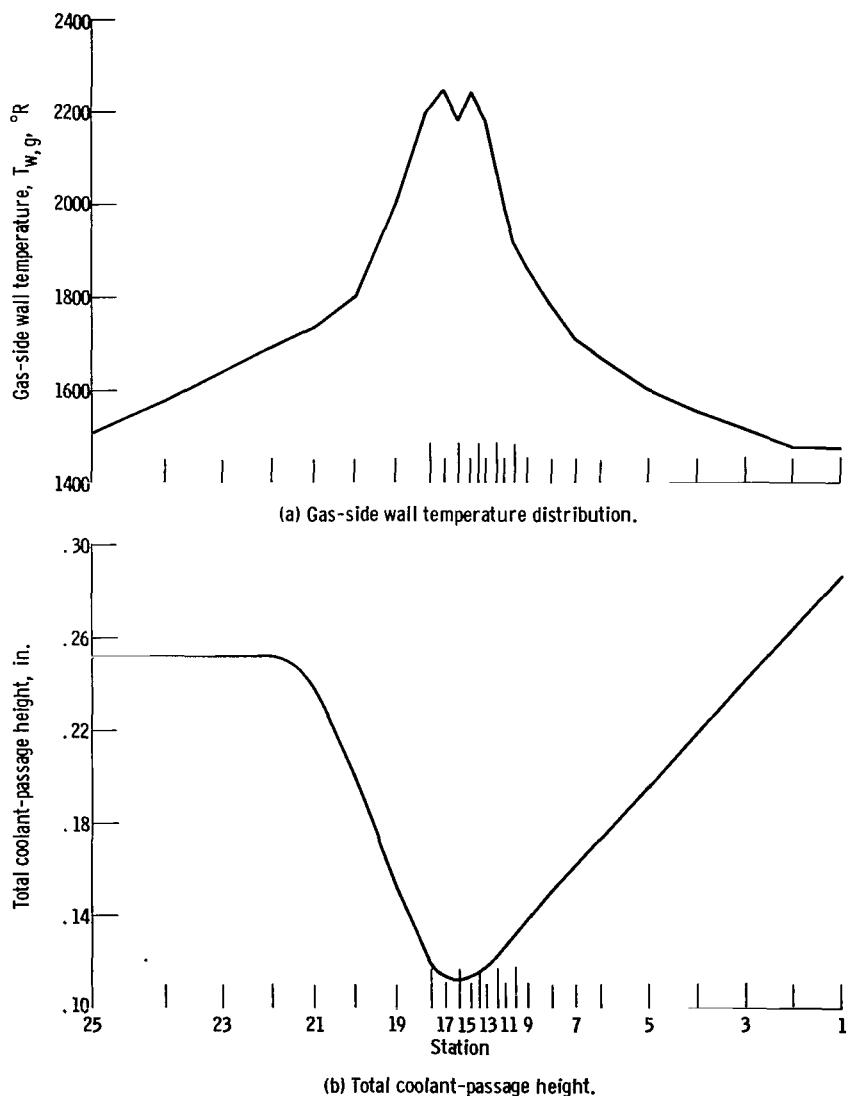


Figure 8. - Final results obtained through use of design and evaluation programs. Case 1.

acceptable material temperatures, coolant exit temperature, or coolant pressure losses are produced. This procedure is repeated until an acceptable shell contour is obtained.

The final coolant passage conditions resulting from the aforementioned procedure are referred to as those of case 1 and are shown in figure 8. Figure 8(a) shows the final hot-gas wall temperature distribution and figure 8(b) shows the total passage height variation along the nozzle. The coolant temperature rise is 87.4°R and the pressure drop is 116.8 pounds per square inch. The gas-side wall temperature varies from approximately 1500°R at both the divergent and convergent regions to 2250°R in the throat region. The design Mach number limit of 0.3 could be increased to allow smaller passage areas that would reduce this calculated temperature of 2250°R . However, this would also result in an increased pressure drop thereby possibly requiring an increase in coolant inlet pressure.

This design was accepted as is, because conditions in the coolant passage of a nozzle are such that this should be conservative and actual temperatures should be lower. The correlations used on the coolant side did not include any curvature effect at the throat or any effect of coolant property variation due to the extremes existing between the wall temperature and the coolant temperature. Later it will be shown how the variations available produce a range of predicted temperatures.

Coolant-passage stresses. - Figure 9 shows the stresses for these cases. It can be seen that basically they follow the contour and temperature distribution profiles. In all cases the maximum values for each specific stress are nearly identical. By referring to the yield strength curve of figure 6 (p. 20), it is apparent that almost all resultant calculated stresses are in the plastic region. Therefore, conventional engineering criteria, based on yield strength, for predicting failure cannot be used. As the design becomes more nearly fixed, the conditions are severe enough to demand a detailed analysis of what really can be expected from a structural aspect. The predominant factor causing the high values of stress is the large difference in temperature from the hot-gas side to the cold shell. For the conditions being considered, it is difficult to reduce the large stresses through geometry modifications alone. However, if a thermal-barrier type of coating were put on a given design, this difference in temperature would be reduced markedly with a corresponding decrease in stresses and coolant exit temperature. The results of putting a coating on this design is discussed in the section Use of Thermal Barrier Coating.

Variation in number of coolant tubes. - When the final temperature distribution of figure 8(a) was achieved, it was used for two more sets of design calculations, one for 80 tubes and the other for 100 tubes. The 100-tube case results in comparable values for temperature rise and pressure drop of 86.7°R and 126.6 pounds per square inch, respectively. Although the gas-side wall temperature distribution achieved was identical to the 90-tube case, the minimum tube radius at the throat of 0.0525 inch appears to be approaching a fabrication limitation. The 80-tube case results in higher temperatures in

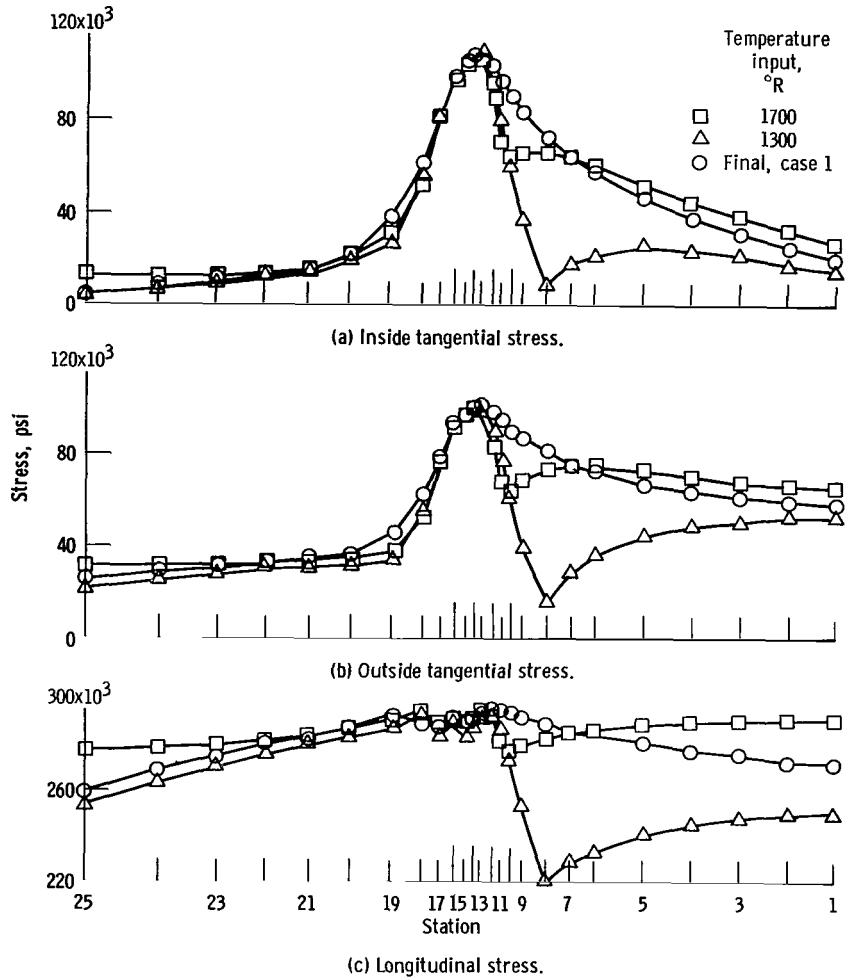


Figure 9. - Coolant-passage stresses as influenced by gas-side wall temperature input for design program.

TABLE II. - GAS-SIDE WALL TEMPERATURE FOR DIFFERENT NUMBER OF TUBES

Station	Temperature, °R	
	90 Tubes	80 Tubes
19	2000	2005
20	1800	1923
21	1734	1885
22	1692	1846
23	1638	1795
24	1578	1735
25	1509	1664

the cylindrical region because the minimum area restriction for the wider tubes results in larger flow areas than those of the 90-tube case. Table II shows the comparison of these temperatures for stations 19 to 25. Only the 80-tube- and 90-tube-case temperatures are shown, because as noted previously, those for the 100-tube case were identical to those of the 90-tube case. The higher temperatures of the 80-tube case are not desired. Therefore, of the three different numbers of tubes, the value of 90 appears to be an adequate choice.

Effect of Assumptions on the Design

This section illustrates how the evaluation program is used to determine the possible variations in predicted conditions during steady-state operation for a fixed design. These variations are produced by varying the correlations used and assumptions made during the design phase. If any of these variations produce an excessive wall temperature, pressure drop, or temperature rise, the results must be analyzed with the possibility of re-design or the addition of a coating. If the decision is made to redesign, the nozzle is sent back to the design program with the assumptions that proved to be troublesome being incorporated into the design for conservatism.

In the sections Heat-Transfer Equations Utilized and Fluid-Flow Equations Utilized, the following variations were presented:

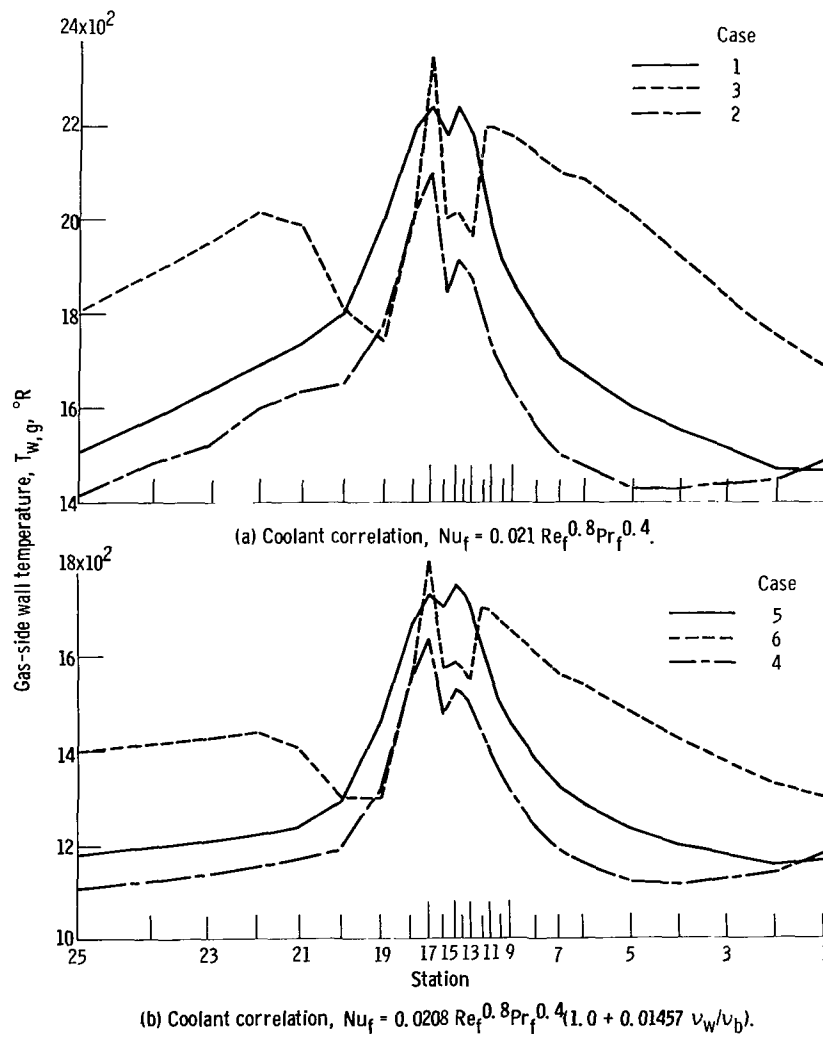


Figure 10. - Effect of gas-side correlation on gas-side wall temperatures.

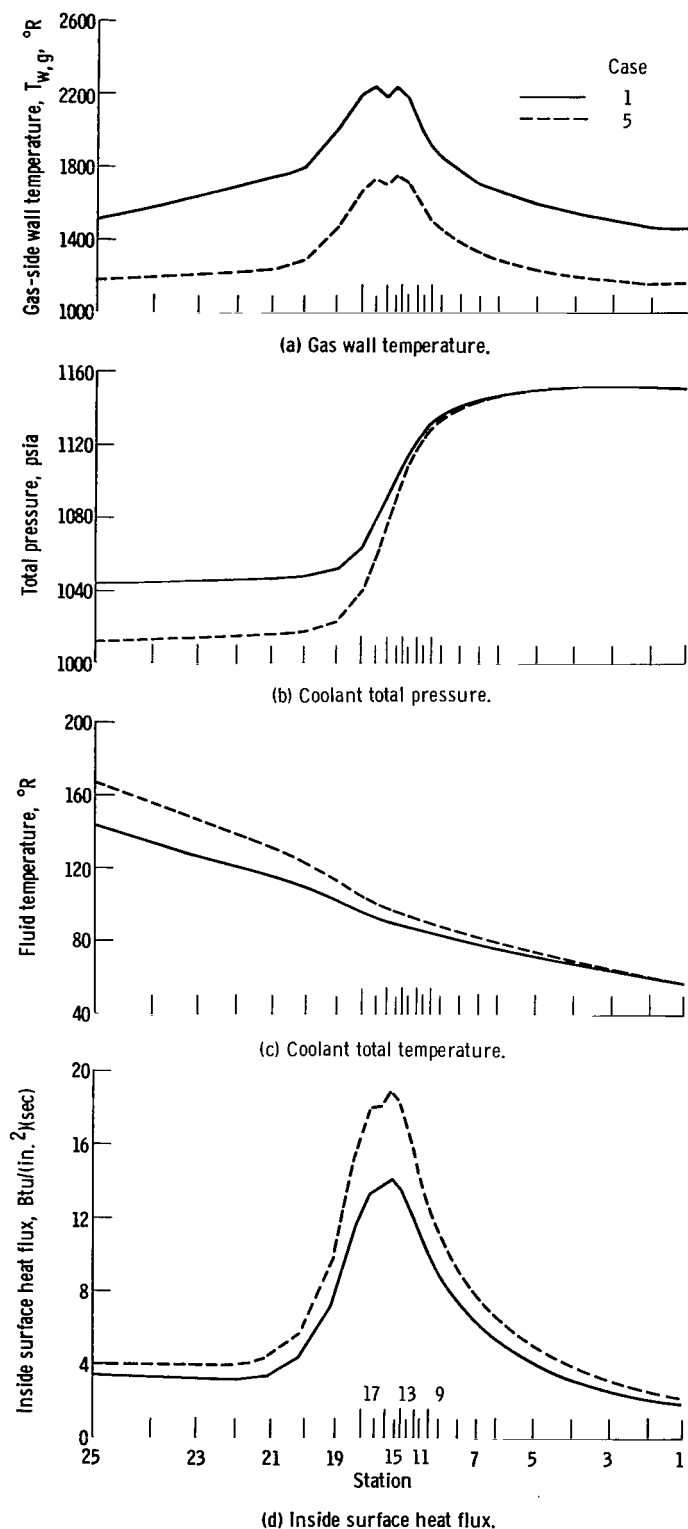


Figure 11. - Typical variations produced by use of different heat-transfer correlations on coolant side.

- (1) Three curves of C_g values with two hot-gas heat-transfer correlations
- (2) Two coolant heat-transfer correlations
- (3) A curvature correction on the coolant-side heat-transfer correlation C_2
- (4) Two modes of heat conduction through the tube crown
- (5) A heat-transfer-area correction for the heat added to the coolant
- (6) Two types of wall-surface conditions for friction pressure losses
- (7) A curvature correction on the friction factor C_3

Heat-transfer-correlation effects. -

Figures 10 and 11 show the effect produced by the variations of items (1) and (2). The case numbers in the figure are listed in table III with some of the significant resulting differences.

Figures 10(a) and (b) show the effect on the gas-side wall temperatures produced by varying the hot-gas-side correlation while using identical coolant-side correlations, respectively, as indicated in the figures. The hot-gas-side correlation and/or C_g distribution that is selected can be seen to have an appreciable effect on the wall temperature. An overall deviation of about 200°R exists between the maximum temperatures of the three curves of each figure.

Figure 11(a) is a replot of the temperature distributions of cases 1 and 5.

TABLE III. - HEAT-TRANSFER CORRELATIONS AND RESULTS FOR CASES EVALUATED

Case	Gas-side equation	C_g	Gas film temperature	Coolant equation	Exit total temperature, °R	Exit total pressure, psia
1	$Nu_f = C_g Re_f^{0.8} Pr_f^{0.3}$	Design	$T_f = T_{ref}$	$Nu_f = 0.021 Re_f^{0.8} Pr_f^{0.4}$	143.4	1043
2	$Nu_f = C_g Re_f^{0.8} Pr_f^{0.3}$	Ref. 3	$T_f = T_{ref}$	$Nu_f = 0.021 Re_f^{0.8} Pr_f^{0.4}$	137.3	1050
^a 3	$Nu_f = C_g Re_f^{0.8} Pr_f^{0.4}$	Ref. 4	$T_f = (T_{eff} + T_{w,g})/2$	$Nu_f = 0.021 Re_f^{0.8} Pr_f^{0.4}$	150.6	1037
4	$Nu_f = C_g Re_f^{0.8} Pr_f^{0.3}$	Ref. 3	$T_f = T_{ref}$	$Nu_f = 0.0208 Re_f^{0.8} Pr_f^{0.4} C_1$	155.7	1029
5	$Nu_f = C_g Re_f^{0.8} Pr_f^{0.3}$	Design	$T_f = T_{ref}$	$Nu_f = 0.0208 Re_f^{0.8} Pr_f^{0.4} C_1$	166.9	1012
^a 6	$Nu_f = C_g Re_f^{0.8} Pr_f^{0.4}$	Ref. 4	$T_f = (T_{eff} + T_{w,g})/2$	$Nu_f = 0.0208 Re_f^{0.8} Pr_f^{0.4} C_1$	181.3	993

^aSee appendix D for program revisions necessary to run cases 3, 6, and 7.

This figure is a comparison of the effect of identical hot-gas-side correlations and indicates that the effect of the different coolant-side correlations on wall temperature for these conditions is more significant. The deviation between maximum temperatures is about 500° R and is also the same for the other two pairs of curves shown in figures 10(a) and (b).

Figures 11(b) and (c) show a comparison of the coolant total pressure and temperature distribution, respectively, for the same two cases, 1 and 5. These figures and table III indicate that the combination of hot-gas-side and coolant-side correlations has a significant effect on coolant conditions. For example, between the combination of cases 2 and 6, the coolant exit temperature varies from 137° to 181° R and the coolant exit pressure varies from 1050 to 993 pounds per square inch absolute.

The resulting variation of inside surface heat fluxes for cases 1 and 5 is shown in figure 11(d). The maximum heat flux varies from 14.0 to 18.8 Btu per square inch per second in the throat region and drops to approximately 4 and 2 Btu per square inch per second in the convergent and divergent sections, respectively. Although not shown, the outside surface heat fluxes vary considerably from the inside surface heat fluxes for the case of radial heat flow. For example, the maximum heat fluxes near the throat vary from 11.7 to 14.0 Btu per square inch per second and 15.7 to 18.8 Btu per square inch per second for the outside and inside heat fluxes of cases 1 and 5, respectively.

These variations indicate that the use of the design assumptions of case 1, design C_g curve, and the coolant correlation of reference 9, produce high wall temperatures on the average but relatively low coolant heat pickup. The remaining comparisons of items (3) to (7) are made by using the design assumptions of case 1 as the standard case.

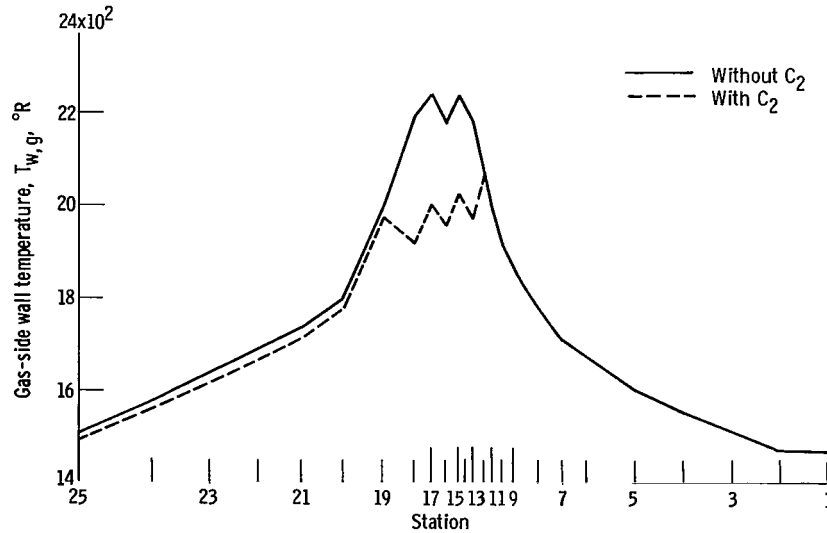


Figure 12. - Gas-side wall temperature variations produced by curvature effect on heat transfer. Case 1.

Curvature heat-transfer-correction effect. - Figure 12 shows the variations produced in the wall temperature by the C_2 correction in the localized regions of axial gas wall curvature. The heat-transfer enhancement due to curvature in the throat region has reduced the wall temperatures about 250°R . However, as mentioned previously the angular effect is not considered in this correction, and that is why this correction does not produce a smooth gas wall temperature distribution.

Heat-conduction-model effect. - Figure 13 shows the differences that exist if the heat-transfer calculations are based on either one-dimensional radial heat flow across the tube crown utilizing cylindrical geometry or normal heat flow utilizing flat-plate geometry. Figure 13(a) shows a reduction of approximately 200°R in maximum gas-side wall temperatures due to the use of flat-plate heat-conduction equations across the crown of the tube. Figures 13(b) and (c) show the resulting differences in coolant total pressure and temperature as being relatively small.

Heat-transfer-area correction effect. - Figure 14(a) shows the effect on the coolant heat pickup produced by a variation from 0.75 to 0.90 in the area correction ϵ_c . This variation produces a significant increase in the coolant exit temperature of 21°R while producing only a 125°R variation in wall temperatures in the chamber region, as shown in figure 14(b).

Coolant tube roughness and curvature effects. - Figure 15 shows the singular and combined effects of roughness and axial gas wall curvature on the coolant pressure. For the nozzle under analysis the rough tubes produced a decrease in exit pressure of 53 pounds per square inch and the curvature reduced the exit pressure by 18 pounds per square inch. The value of tube relative roughness e used was 0.00006 inch, the value for

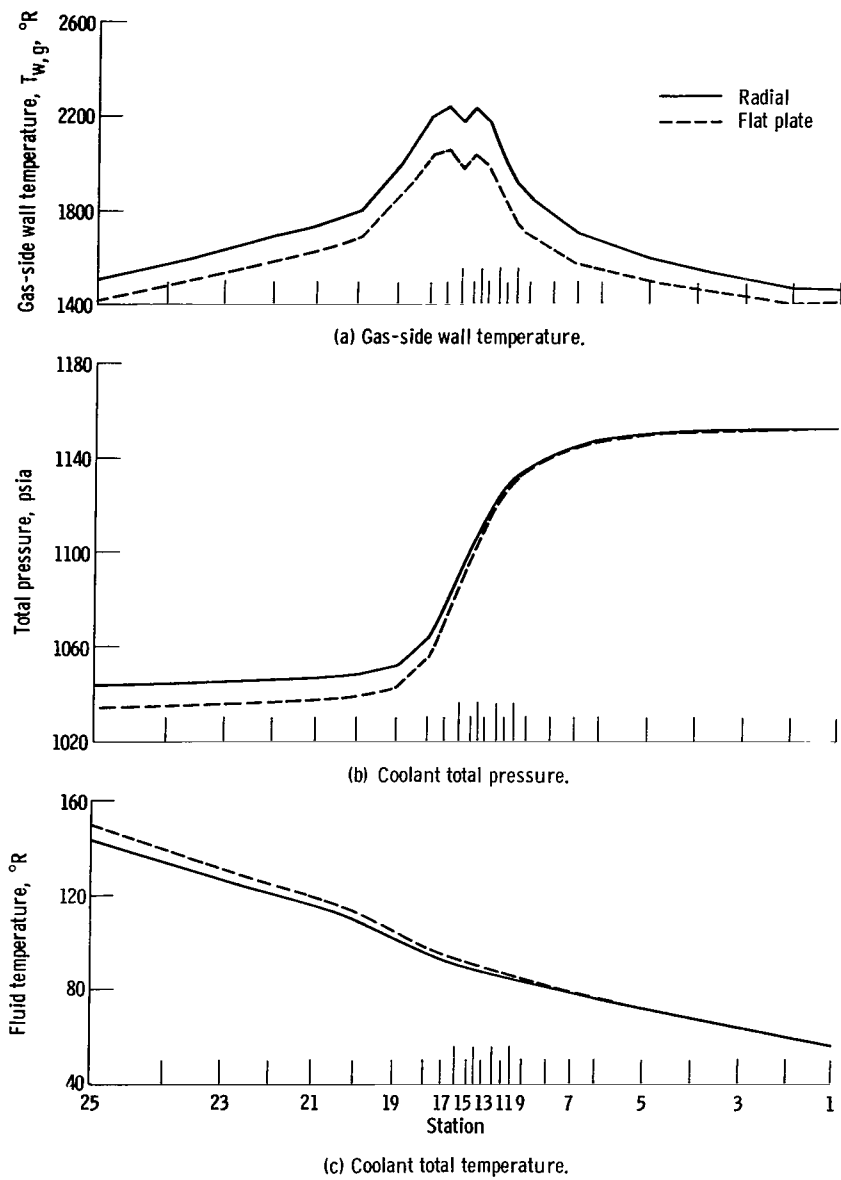


Figure 13, - Comparison of variations produced by use of radial or flat plate heat conduction through tube crown. Case 1.

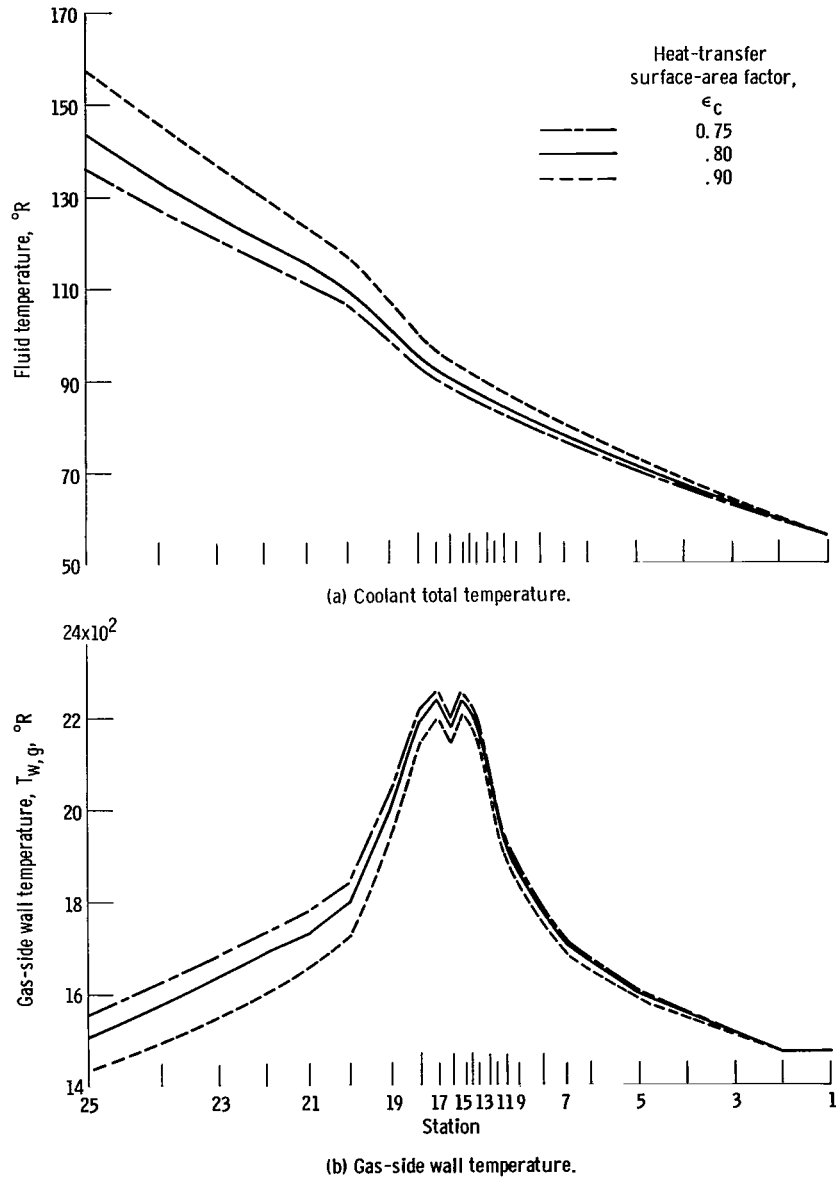


Figure 14. - Variations produced in case 1 by changing value for area correction.

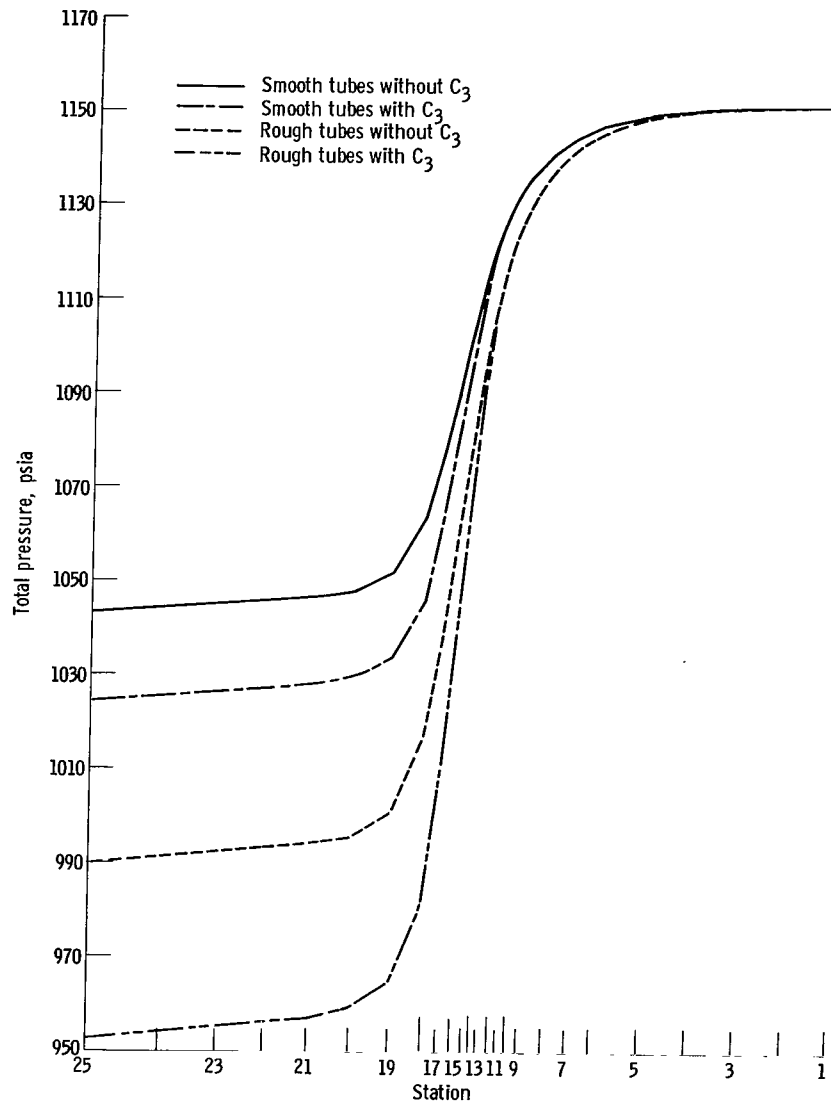


Figure 15. - Effects produced on total pressure by tube roughness and curvature. Case 1.

commercially drawn tubes.

Combined effects. - As an additional check, the nozzle design is evaluated with the assumptions that will produce the maximum coolant heat pickup and pressure loss in the coolant passage, the lowest possible wall temperatures reasoned to exist in the nozzle, and the anticipated range of coolant passage stress values.

Coolant: To achieve the maximum coolant heat pickup and pressure loss in the coolant passage the following assumptions were made:

- (1) Flat-plate heat conduction applies
- (2) A fluid-properties variation correction on the convective heat-transfer coefficient C_1 applies

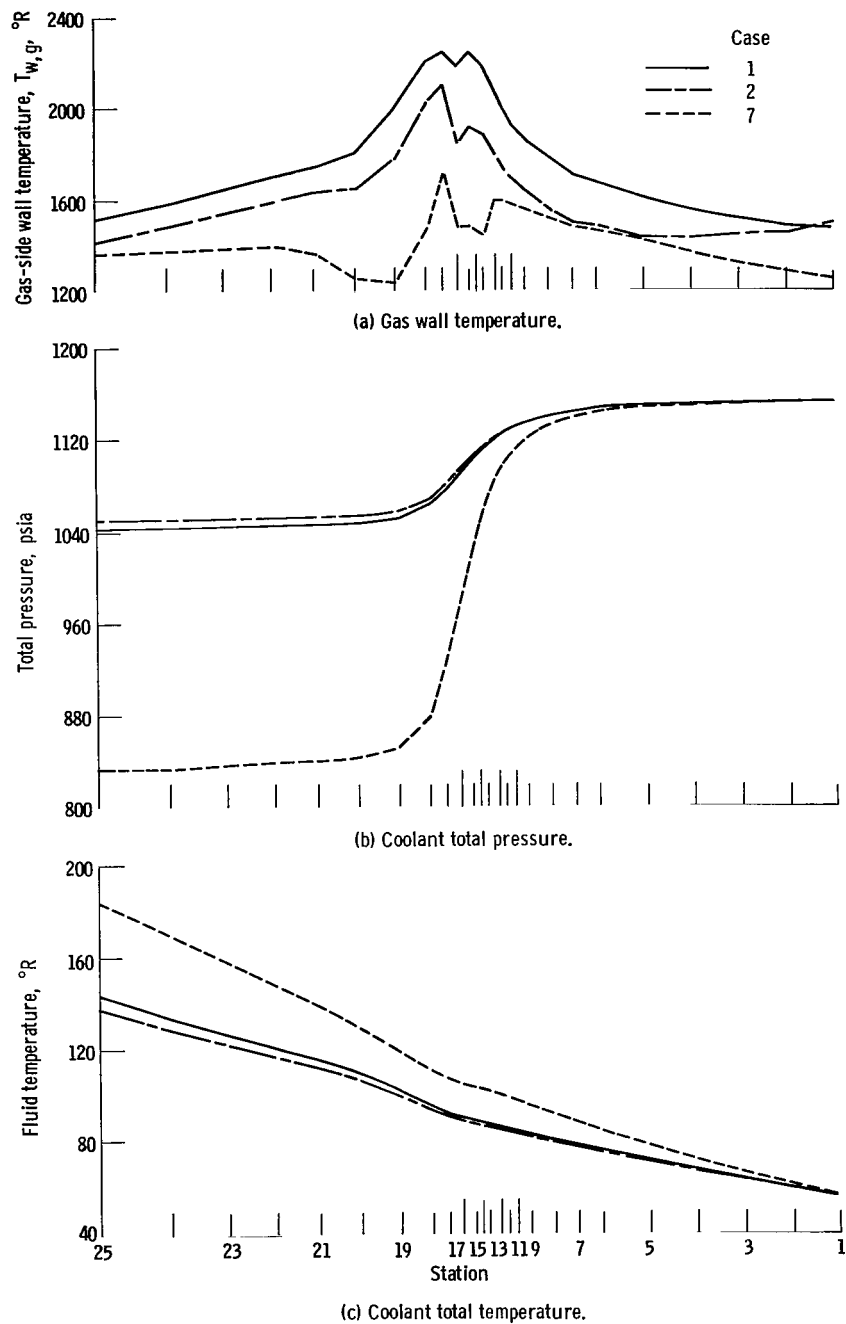


Figure 16. - Comparison of design values with minimum and maximum heat pickup and pressure loss cases.

- (3) The maximum C_g curve applies
- (4) The tubes are rough
- (5) A curvature correction on the friction factor C_3 applies

These assumptions will be referred to as case 7.

Figure 16(a) shows the significant drop in wall temperatures by comparing the resulting gas-side wall temperatures, case 7, against the designed values, case 1. As can be seen from figures 16(b) and (c), respectively, the bulk coolant temperature has increased by 41°R and the exit pressure has decreased by 210 pounds per square inch. However, to see the most significant effect, comparisons of the coolant velocity in each case must be made as shown in figure 17. This comparison gives an indication that the coolant flow may be in danger of choking. The maximum velocity has increased from 760 to 1100 feet per second and the maximum Mach number has increased from 0.3 to 0.5. In addition, this trend can be further augmented by increasing the area correction above 0.8.

Also, shown in figure 16 are the curves for minimum heat pickup and pressure drop, case 2. This case results in relatively negligible deviations of coolant conditions from the design, case 1, but produces an anticipated range of coolant conditions when combined with the maximum heat pickup and pressure drop curve, case 7.

Wall temperatures: To achieve the minimum wall temperatures thought to exist in the nozzle, the following assumptions were made:

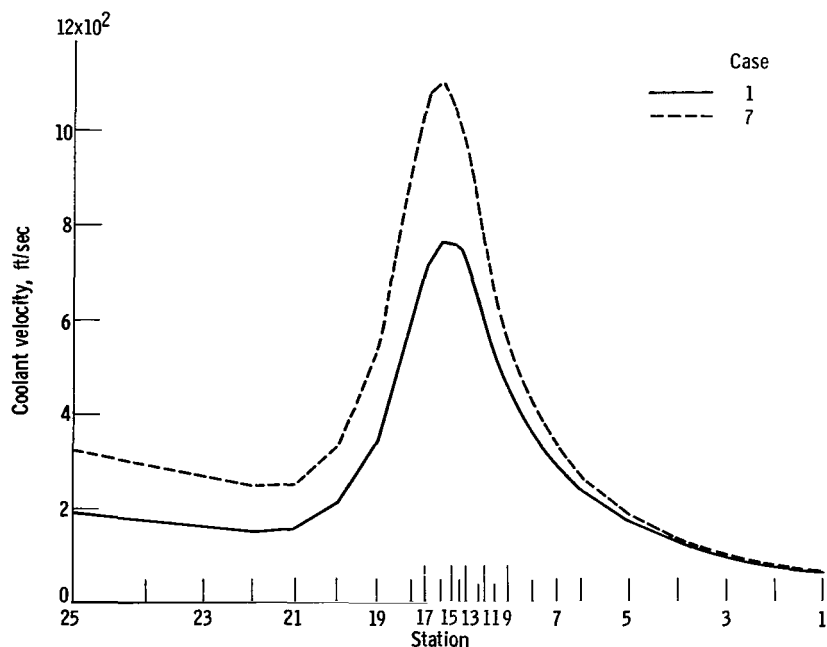


Figure 17. - Effect produced by maximum heat pickup and pressure loss on coolant velocity.

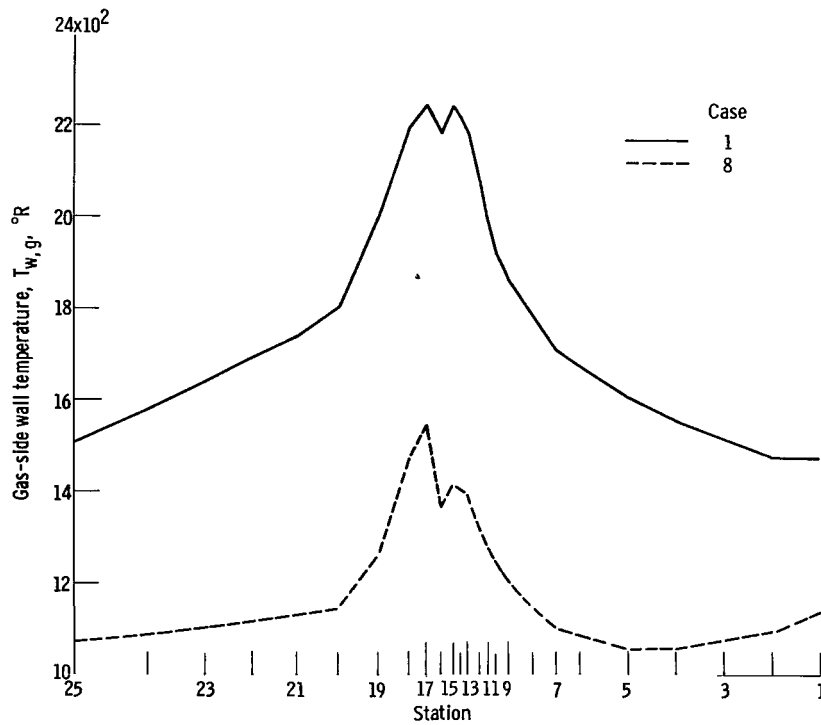


Figure 18. - Comparison of design gas-side wall temperatures with expected minimum gas-side wall temperatures.

- (1) Flat-plate heat conduction applies
- (2) A fluid-properties variation correction on the convective heat-transfer coefficient C_1 applies
- (3) The minimum C_g curve applies

These assumptions will be referred to as case 8.

The resulting wall temperatures of case 8 are shown in figure 18 and, when combined with the temperatures of case 1, produce a range of anticipated wall temperatures. This range includes a variation from 1550° to 2250° R in the predicted maximum gas wall temperature. However, this range does not include the effects of coolant passage curvature on heat transfer that would further reduce the maximum wall temperature.

Coolant passage stresses: As the coolant passage stresses are primarily a function of wall temperatures, the stress comparison will be made by using the maximum wall temperature range of cases 1 and 8. Figure 19 shows the anticipated range of stresses produced by the uncertainty in the heat-transfer analysis. It should be noted that a considerable drop in the magnitude of the stresses is produced by the lower material temperature of case 8.

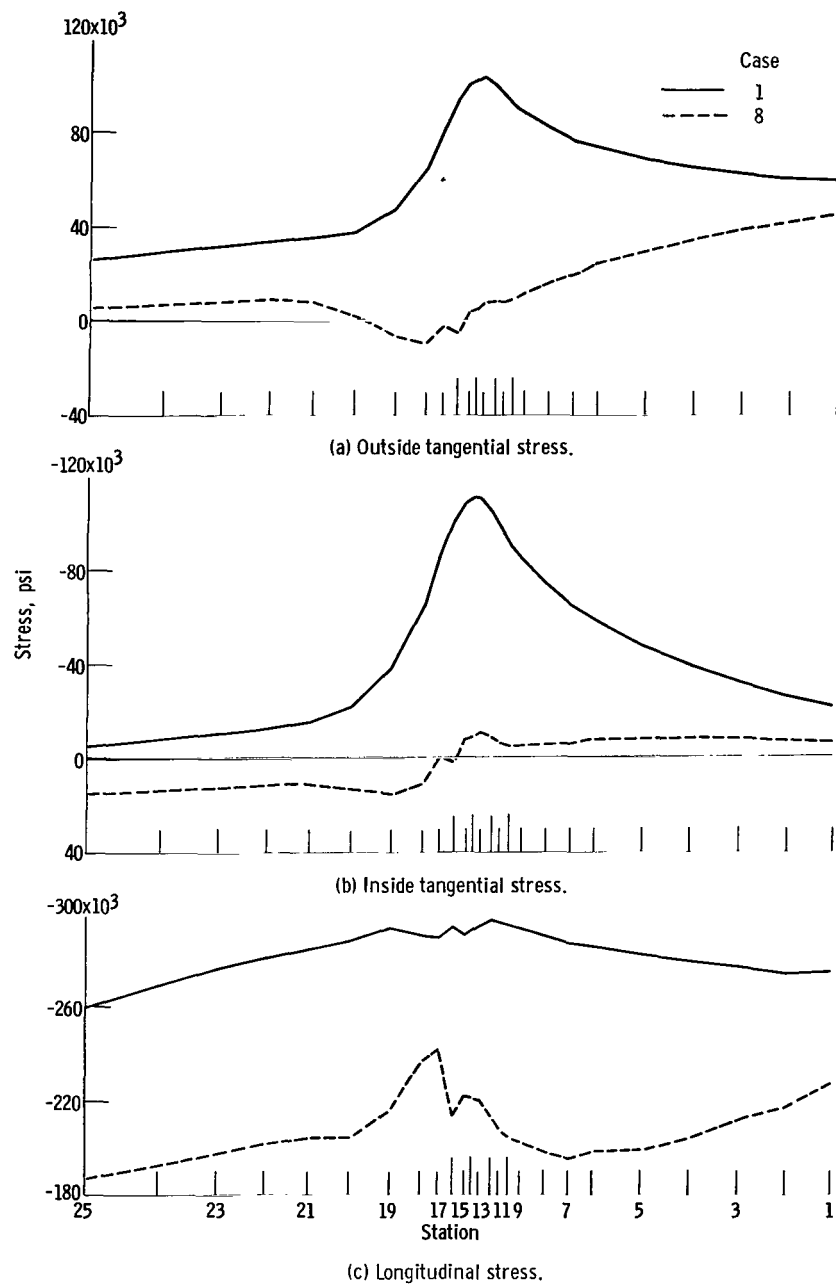


Figure 19. - Variations in tube stresses produced by heat-transfer correlations.

Use of Thermal-Barrier Coating

The evaluation program has the provision for the addition of a coating to the gas side of the coolant passages. This coating would be added to an existing nozzle for uprating it or to a design with excessively high wall temperatures. Figures 20 and 21 show the effects of two different thermal resistances on the designed nozzle. Figure 20 shows the marked decrease in the metal wall temperature and the marked increase in the gas-side coating wall temperatures. Figure 21 shows the decrease in all the tube wall stresses produced by the thermal resistance. However, the stress analysis presented in this report does not consider the coating. Although the tube stresses are reduced, the stresses in the coating and mismatch due to relative thermal expansion between tube and coating may still be excessive and would require further analysis.

Figures 19 and 21 show that the variation in the predicted wall temperatures produced a greater reduction in the stresses than the thermal resistance. However, it may

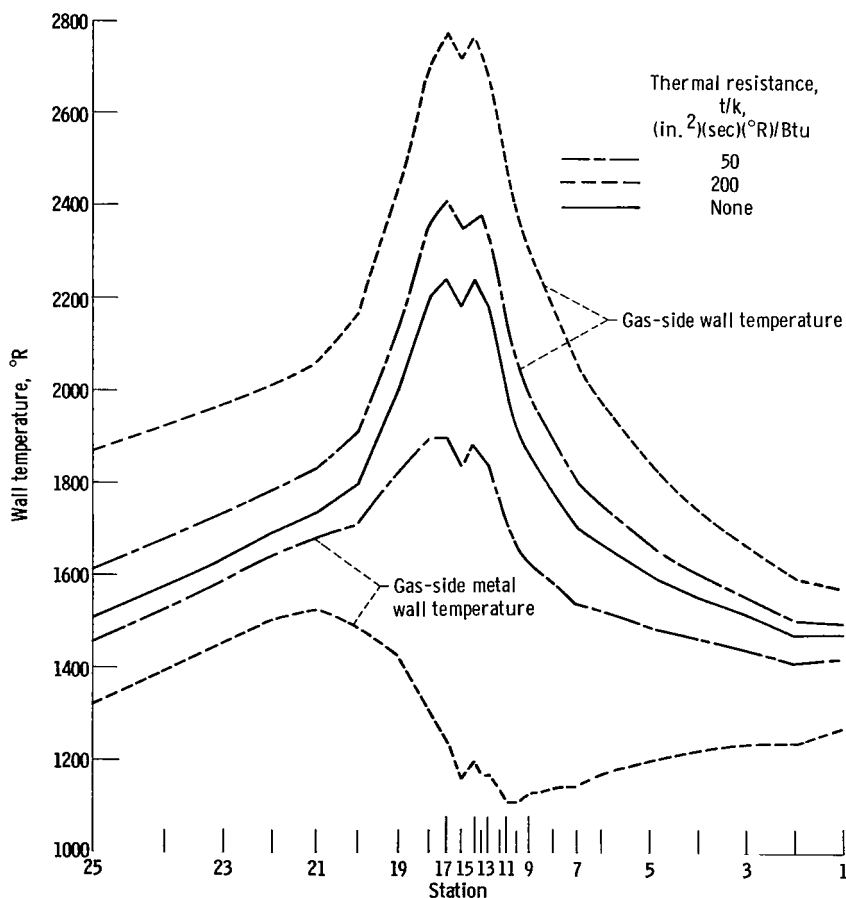


Figure 20. - Gas wall and gas-side metal wall temperature profiles produced by addition of thermal barrier to designed nozzle for case 1.

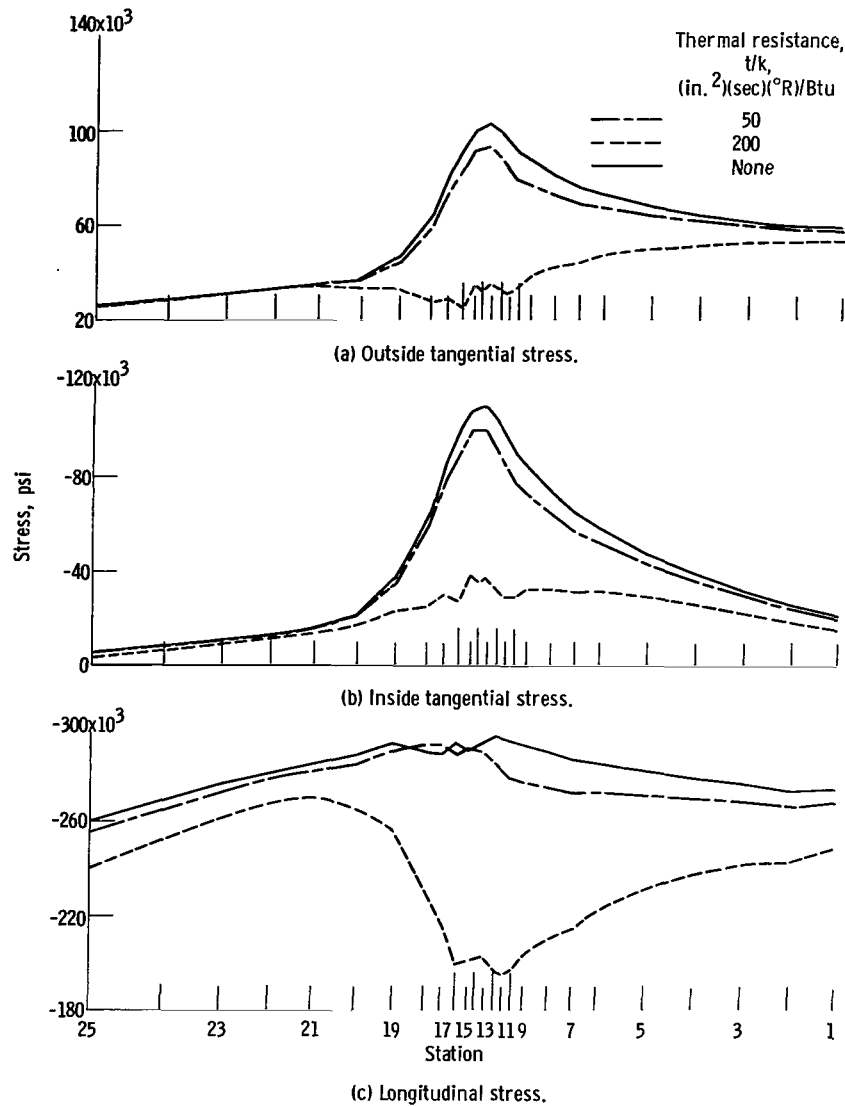
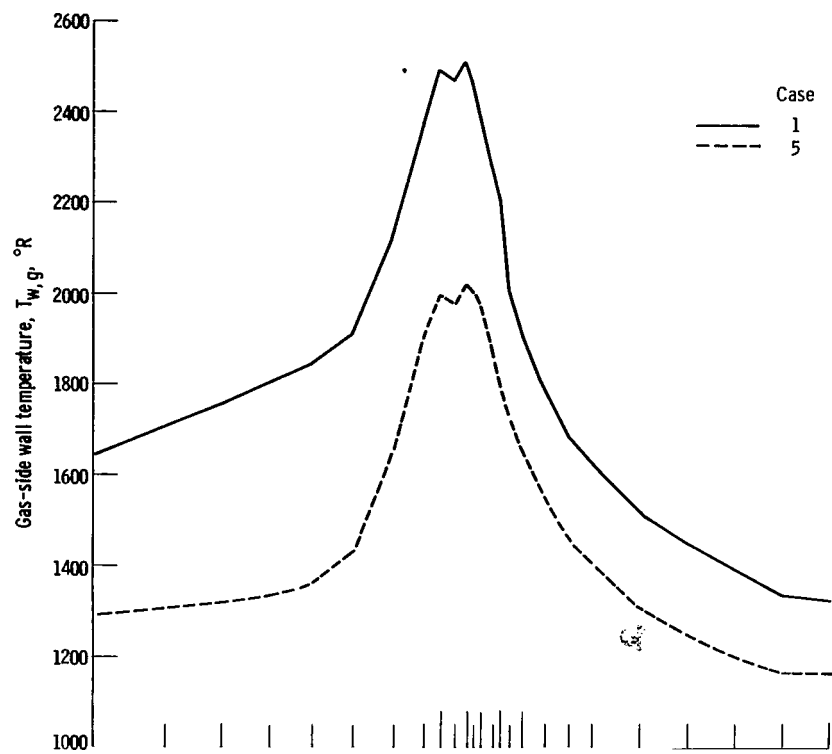


Figure 21. - Tube stress variation produced by addition of thermal barrier to designed nozzle for case 1.

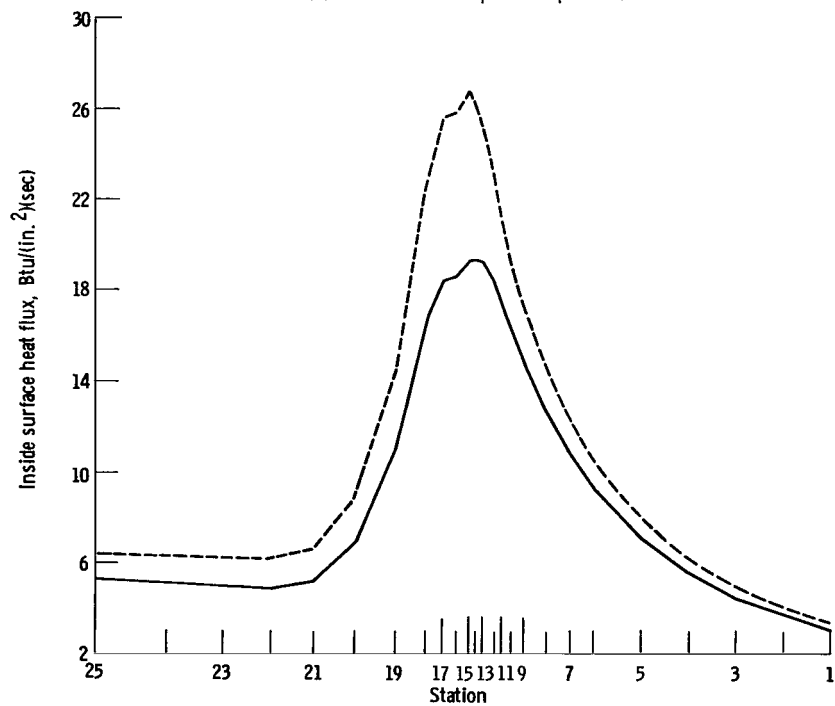
be observed that the temperature reduction caused by the thermal resistance would also be superimposed on the reduction due to the use of the assumptions that produced variations in the predicted wall temperatures.

Off-Design Conditions

The evaluation program can also be used to determine the conditions that exist at off-design points and the maximum extent to which a nozzle could be uprated based on some given criterion of failure. Figure 22(a) shows the high wall temperatures that result when the nozzle chamber pressure is increased to 1000 pounds per square inch



(a) Gas-side wall temperature profiles.



(b) Inside surface heat flux.

Figure 22. - Results for uprated conditions of designed nozzle. Chamber pressure, 1000 pounds per square inch absolute.

absolute from the design value of 530 pounds per square inch absolute and the coolant inlet pressure is increased to 1500 from 1150 pounds per square inch absolute. The spread of 500° R between the wall temperatures of the two uprated cases indicates potential failure of the nozzle if the correlations of case 1 were to apply. Figure 22(b) shows the range of inside surface heat fluxes that result from the uprating of conditions.

General Remarks

The previous discussion has been written in a general manner to give an insight into the approach to be used in obtaining a nozzle design. Each specific design has its own requirements that have to be obtained through a complete analysis whereby many parameters such as tube number, tube thickness, tube material, coolant inlet pressure, and possibly coolant inlet temperature and flow rate would be varied. For the purposes of this report, a detailed discussion describing all of the permutations possible leading to a final design was not deemed necessary.

CONCLUDING REMARKS

The large number of perturbations leading to any given final design for a nozzle coolant passage substantiates the requirement for the use of a design and evaluation program in conjunction, as shown in this report. Each program complements the other and together they produce the design, initial evaluation, and final resulting evaluation of feasible convectively cooled U- or D-tube nozzles with hydrogen as both the coolant and the propellant.

The programs are set up to allow the option as to the heat-transfer correlations utilized, the condition of tube roughness employed, and the use of a tube splice. Additional options of radial or flat plate heat conduction across the tube crown and adding a coating to the gas side of the coolant passage exist in the evaluation program.

The design program is used to determine a feasible nozzle coolant passage by using certain basic assumptions, fabrication limits, and a physical limit. The fabrication limits used were wall thickness of 0.012 inch and a minimum inside coolant tube radius of 1/16 inch. The physical limit used was a Mach number limit of 0.3 on the coolant flow. These limits were combined with reasonable wall temperatures and minimum coolant pressure loss requirements to produce a realistic design.

The results presented are for a U-tube nozzle with a throat diameter of 4.3 inches, a contraction ratio of 12, an expansion ratio of 8, and a total length of 31 inches. The nozzle is to operate at a chamber condition of 4000° R and 530 pounds per square inch

absolute and coolant inlet condition of 56° R and 1150 pounds per square inch absolute with hydrogen as both the coolant and the propellant.

The final contour determined by the design program for the nozzle coolant passage was smoothed, and the effects of varying the basic assumptions were then checked by the use of the evaluation program. These variations include the following items:

- (1) Three curves of C_g values with two hot-gas heat-transfer correlations
- (2) Two coolant heat-transfer correlations
- (3) A curvature correction on the coolant-side heat-transfer correlation
- (4) Two modes of heat conduction through the tube crown
- (5) A heat-transfer-area correction for the heat added to the coolant
- (6) Two types of wall-surface conditions for friction pressure losses
- (7) A curvature correction on the friction factor

The variations of the hot-gas and coolant-heat-transfer correlations employed produced an overall predicted maximum gas-side wall temperature variation of 200° and 500° R, respectively. The two modes of heat conduction across the coolant tube crown, radial and flat plate conduction, produced a predicted maximum gas-side wall temperature variation of 200° R. Gas wall axial curvature produced localized regions near the throat with 250° R variations in the predicted gas wall temperatures. The combined effects produced a variation in the predicted maximum gas-side wall temperature from 1550° to 2250° R.

The variations in the heat-transfer correlations also produced a significant variation of 44° R in the coolant exit temperature and 57 pounds per square inch in the exit pressure. The effect of using a tube roughness equal to commercially drawn tubes resulted in an increase in pressure drop of 53 pounds per square inch, over the original pressure drop of 117 pounds per square inch for smooth tubes.

In general, calculated tangential and longitudinal stresses for the coolant passage wall are well into the plastic region. Therefore, their usefulness for predicting failure is doubtful, but they can be used to evaluate various designs on a relative basis.

In addition, the scope of the final evaluation can include the following: variations in operating conditions such as uprating the nozzle; use of coatings; analyzing nozzle failures; and matching experimental nozzle test data to determine the validity and applicability of correlations and assumptions. Examples of the uprating and coating addition were presented for the chosen application.

Lewis Research Center,
National Aeronautics and Space Administration,
Cleveland, Ohio, August 8, 1966,
122-29-07-07-22.

APPENDIX A

SYMBOLS

A	area	J	mechanical equivalent of heat
A*	nozzle-throat area	k	thermal conductivity
C	numerical coefficient	L	cone slant height from previous station
C ₁	convective heat-transfer coefficient correction for fluid-properties variation	$\Delta \ell$	linear distance along coolant-passage wall between stations
C ₂	convective heat-transfer-coefficient correction for tube curvature	M	bending moment acting on tube crown
C ₃	friction-factor correction for tube curvature	N	membrane force per unit length in circumferential direction
c _p	specific heat at constant pressure	NS	membrane force per unit length in longitudinal direction
D	diameter	N _t	number of coolant tubes
E	Young's modulus	Nu	Nusselt number
e	relative roughness of surface	Pr	Prandtl number
f	friction factor for straight tubes	p	pressure
f _c	friction factor for curved tubes	Δp_{fr}	friction static-pressure drop between stations
G	mass flow per unit cross-sectional area	Δp_{mom}	momentum static-pressure drop between stations
g	gravitational conversion factor	q	local heat flow rate
H	enthalpy	R	radius
ΔH	enthalpy increase between nozzle stations	R _c	radius of curvature
h	convective heat-transfer coefficient	R _f	recovery factor
		Re	Reynolds number
		S	cone slant height from present station

s	entropy	fl	flow
T	temperature	g	gas
t	thickness	H	hydraulic
V	velocity	h	hoop
W	deflection force acting on tube	ht	heat transfer
WP	wetted perimeter	i	inside
\dot{w}	mass weight of flow	int	internal
α	coefficient of thermal expansion	l	liquid or coolant
δ	tube deflection	long	longitudinal
ϵ	strain	M	meridional
ϵ_c	heat-transfer surface-area correction factor	m	mean
μ	dynamic viscosity	max	maximum
ν	kinematic viscosity	met	average between inside and outside metal-wall temperatures
ν_p	Poisson's ratio	n	division of cross section into n nodes for two-dimensional heat-conduction study; also n^{th} node
ρ	density	o	outside
σ	stress	p	pressure
ϕ	angle between nozzle side wall and nozzle axis	ref	reference
Subscripts:		s	static
A	axial	sc	semicircular
av	average	sh	shell
b	bulk	T	temperature
bend	bending	t	tube
com	combined	tan	tangential
cr	tube crown	tot	total or stagnation
d	deflection	w	wall
e	external	y	yield
eff	effective	1	previous station
f	film		

2 present station

1-d one dimensional

2-d two dimensional

θ circumferential

8

APPENDIX B

STAGNATION PRESSURE STATE

For a constant density fluid, the following relation for stagnation pressure is adequate:

$$p_{\text{tot}} = p_s + \frac{\rho V^2}{2g} \quad (\text{B1})$$

However, when the density varies with both temperature and pressure, the evaluation of the proper density value to use becomes involved. To circumvent this problem, a different approach to stagnation pressure determination was used.

The variation of stagnation pressure in a fluid process can be obtained from the energy equation. The process of attaining the stagnation state is isentropic, and, therefore,

$$ds_{\text{tot}} = ds_s \quad (\text{B2})$$

From the definition of entropy, the relation that exists is

$$ds_{\text{tot}} = \frac{1}{T_{\text{tot}}} \left(dH_{\text{tot}} - \frac{dp_{\text{tot}}}{J\rho_{\text{tot}}} \right) \quad (\text{B3})$$

where T_{tot} and ρ_{tot} are an average between stagnation conditions from one station to the next over which Δp_{tot} is being determined. This change in entropy is equal to the sum of the external entropy change ds_e due to external heat transfer and the internal irreversible entropy change ds_{int} due to frictional losses.

The external entropy change is calculated from

$$ds_e = \frac{dq}{\dot{w}T_s} \quad (\text{B4})$$

where by definition

$$\frac{dq}{\dot{w}} = dH_{\text{tot}} \quad (\text{B5})$$

is the increase of coolant total enthalpy between stations.

The internal entropy change is determined from the pressure-energy equation of reference 11

$$dp_s + \frac{\rho_s V_b dV_b}{g} + J\rho_s T_s ds_{\text{int}} = 0 \quad (\text{B6})$$

and the differential momentum equation

$$dp_s + \frac{2\rho_s V_b^2 \Delta\ell}{gD_H} + \frac{\rho_s V_b dV_b}{g} = 0 \quad (\text{B7})$$

from the same reference.

Subtracting equation (B7) from equation (B6) yields

$$J\rho_s T_s ds_{\text{int}} = \frac{2\rho_s V_b^2 \Delta\ell}{gD_H} \quad (\text{B8})$$

which results in

$$ds_{\text{int}} = \frac{2V_b^2 \Delta\ell}{JgD_H T_s} \quad (\text{B9})$$

where T_s is an average value over the increment $\Delta\ell$.

Using these results in equation (B3) further yields

$$\frac{1}{T_{\text{tot}}} \left(dH_{\text{tot}} - \frac{dp_{\text{tot}}}{J\rho_{\text{tot}}} \right) = \frac{dH_{\text{tot}}}{T_s} + \frac{2V_b^2 \Delta\ell}{JgD_H T_s} \quad (\text{B10})$$

which reduces to

$$dp_{\text{tot}} = J\rho_{\text{tot}} dH_{\text{tot}} \left(1 - \frac{T_{\text{tot}}}{T_s} \right) - \frac{2V_b^2 \Delta\ell \rho_{\text{tot}} T_{\text{tot}}}{gD_H T_s} \quad (\text{B11})$$

where all values of ρ_{tot} , D_H , T_{tot} , T_s , and V_b are averages over the increment $\Delta\ell$.

Substituting the equation for friction pressure drop

$$\Delta p_{fr} = \frac{2G_{av}^2 f \Delta \ell}{\rho_{s,av} D_{H,av} g} = \frac{2\rho_{s,av} V_{b,av}^2 f \Delta \ell}{g D_{H,av}} \quad (B12)$$

into equation (B11) yields

$$\Delta p_{tot} = J \rho_{tot,av} \Delta H_{tot} \left(1 - \frac{T_{tot,av}}{T_{s,av}} \right) - \Delta p_{fr} \left(\frac{\rho_{tot,av} T_{tot,av}}{\rho_{s,av} T_{s,av}} \right) \quad (B13)$$

By establishing a value of p_{tot} at the first station, as discussed in the text of this report, successive values of p_{tot} are determined by use of equation (B13).

APPENDIX C

COOLANT-PASSAGE STRESS ANALYSIS

by Rene E. Chambellan

To perform the desired analysis without creating a statically indeterminate problem, the following simplifying assumptions were made:

- (1) All materials remain elastic. (In an actual situation it is anticipated that localized regions would yield, due particularly to high thermal stresses.)
- (2) Bending of the pressure shell is not considered. (This is a very localized effect in the throat and knuckle regions.)
- (3) The shell is much stiffer than the tubes and the tubes therefore will deform as the shell, thus offering negligible resistance to shell deformations.
- (4) The tube radius is constant along the length of the pressure shell cone considered.
- (5) The material is the same for the shell and tubes.
- (6) The complete nozzle is uniformly cooled down to the bulk coolant temperature at startup.
- (7) No residual stresses remain from the fabrication processes.
- (8) Nuclear heating of the pressure shell is neglected.

In addition, the nozzle pressure shell is divided into conical sections compatible with the heat-transfer and fluid-flow sections. The analysis is repeated at each section and the results that influence the next section are carried over.

Shell

The hot-gas pressure forces produce the membrane forces per unit length NS and N , shown in figure 23, in the shell structure. These forces are defined by equations (C1) and (C2) which are revised equations from reference 13 (p. 112):

$$NS_2 = -p_{g, av} \left(\frac{L^2 - S^2}{2S} \right) \tan \varphi_2 + NS_1 \left(\frac{L}{S} \right) \cos(\varphi_2 - \varphi_1) \quad (C1)$$

$$N_2 = p_{g, 2} S \tan \varphi_2 \quad (C2)$$

The last term in equation (C1) is the reaction of the previous section acting on the section under analysis.

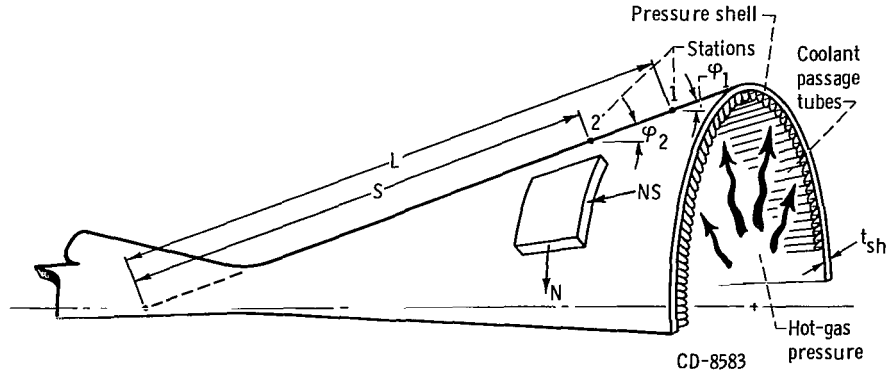


Figure 23. - Nozzle pressure shell membrane forces. Cone slant height from previous station, L; cone slant height from present location, S; membrane force in longitudinal direction, NS; membrane force in circumferential direction, N; shell thickness, t_{sh} .

The resulting shell strains are

$$\epsilon_{M, 2} = \frac{1}{E_{sh} t_{sh, 2}} (NS_2 - \nu_p N_2) \quad (C3)$$

$$\epsilon_{h, 2} = \frac{1}{E_{sh} t_{sh, 2}} (N_2 - \nu_p NS_2) \quad (C4)$$

No thermal strains appear in the shell with respect to the tube wall because the tubes and the shell are cooled down to the bulk coolant temperature uniformly, and then the tubes are heated relative to the shell with the nuclear heating of the pressure shell being neglected.

Tubes

The tubes are first considered to act as if they were not restrained, and then the shell restraint with the resulting stresses is added. The tubes are forced to match the strain that the shell restraint dictates.

The pressure difference across the tube crown produces a membrane stress of

$$\sigma_p = \frac{(p_\ell - p_g) R_t}{t_w} \quad (C5)$$

The temperature gradient, assumed linear, through the tube crown produces a biaxial stress at the surfaces as follows:

$$\sigma_T = \mp \frac{E_t \alpha (T_{w,g} - T_{w,\ell})}{2(1 - \nu_p)} \quad (C6)$$

where compression exists at the outer surface and tension at the inner surface as denoted by the minus and plus signs, respectively (see ref. 14, p. 337).

The tube axial and tangential strains due to pressure and heating (see fig. 24) are

$$\epsilon_A = - \frac{\nu_p (p_\ell - p_g) R_t}{E_t t_w} + \alpha_{av} (T_{met} - T_\ell) \quad (C7)$$

$$\epsilon_\theta = \frac{(p_\ell - p_g) R_t}{E_t t_w} + \alpha_{av} (T_{met} - T_\ell) \quad (C8)$$

The crown tube temperature T_{met} is used to obtain the average tube growth.

By considering the net restraint on the tube produced by the shell, the longitudinal strain in the tube is

$$\epsilon_{long} = \epsilon_M - \epsilon_A \quad (C9)$$

The stress produced by this strain is

$$\sigma_{long} = E_t \epsilon_{long}$$

The total longitudinal stress is composed of the combination of this stress plus the bending stress due to the temperature gradient through the tube wall

$$\sigma_{long, com} = \sigma_{long} + \sigma_T = E_t \epsilon_{long} \mp \frac{E_t \alpha (T_{w,g} - T_{w,\ell})}{2(1 - \nu_p)}$$

The tangential deflection of the tube produced by the shell restraint is

$$\delta_\theta = \left[\epsilon_\theta - \nu_p (\epsilon_M - \epsilon_A) \right] 2R_t - \frac{\pi}{N_t} (D_{sh} - 2R_t) \epsilon_h \quad (C10)$$

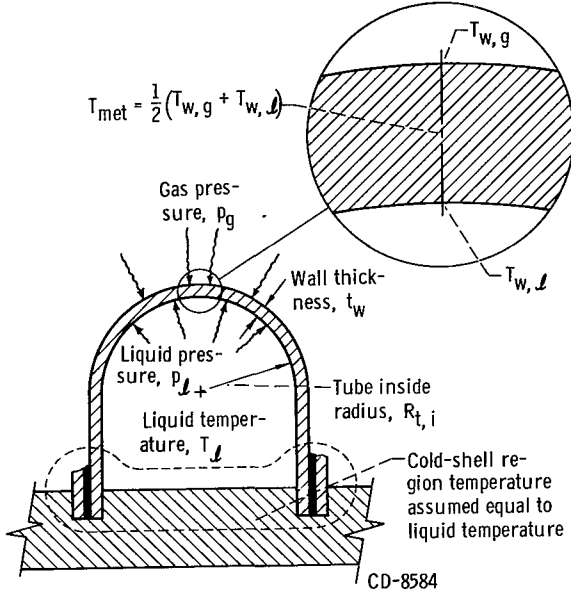


Figure 24. - Stress model for tube axial and tangential strain due to pressure and temperature.

From reference 14 (p. 156) case 1, the required forces and resulting moment acting on the tube to produce this deflection are

$$W = \frac{\delta_{\theta} E_t t_w^3}{1.788 R_t^3 (1 - \nu_p^2)} \quad (C11)$$

and

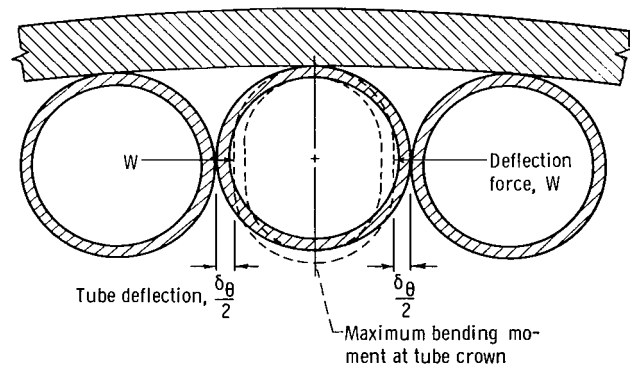
$$M_{\max} = 0.3183 W R_t \quad (C12)$$

with the maximum moment occurring at the tube crown (see fig. 25). Also, from reference 14, the resulting circumferential bending stress at the tube crown is

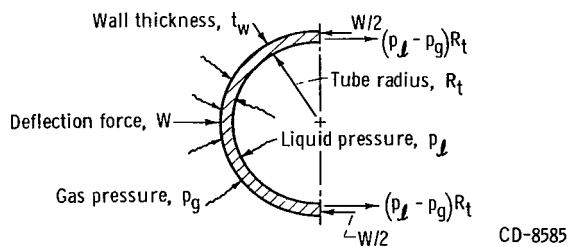
$$\sigma_{\text{bend}} = \pm 6 \frac{M_{\max}}{t_w^2} \quad (C13)$$

which is tension at the outer surface and compression at the inner surface.

The membrane stress at the tube crown from figure 25 is



(a) Bending moment.



(b) Membrane forces.

Figure 25. - Deflection force resulting in bending and membrane stresses.

$$\sigma_M = \sigma_p + \sigma_d = \frac{(p_l - p_g) R_t}{t_w} - \frac{W}{2 t_w}$$

or

$$\sigma_M = \frac{(p_l - p_g) R_t}{t_w}$$

$$- \frac{\delta_{\theta} E_t t_w^2}{3.576 R_t^3 (1 - \nu_p^2)} \quad (C14)$$

The total tangential stress at the tube crown is then the sum of the bending stress due to the tube deflection, the thermal stress due to the temperature

gradient through the tube crown, and the membrane stress due to pressure and tube deflection:

$$\sigma_{\text{tan}} = \sigma_{\text{b}} + \sigma_{\text{T}} + \sigma_{\text{M}} \quad (\text{C15})$$

$$\sigma_{\text{tan}} = \pm \frac{1.068 E_t \delta_{\theta} t_w}{R_t^2 (1 - \nu_p^2)} \mp \frac{E_t \alpha (T_{w,g} - T_{w,\ell})}{2(1 - \nu_p)} + \frac{(p_{\ell} - p_g) R_t}{t_w} - \frac{0.2796 E_t \delta_{\theta} t_w^2}{R_t^3 (1 - \nu_p^2)} \quad (\text{C16})$$

The material properties E_{sh} , E_t , ν_p , and α used in these equations are required at the appropriate temperatures. E_{sh} and ν_p are supplied as input and should be values for the shell and both shell and tube, respectively, at an average temperature in the nozzle. E_t is evaluated at the average metal-wall temperature, and α is evaluated at the average temperature of the associated temperature differences.

APPENDIX D

DETAILS OF DESIGN AND EVALUATION PROGRAMS

The two programs presented in this report are written in FORTRAN IV for use on an IBM 7094 Model 2 utilizing the IBSYS (International Business System) system. The programs have an average run time of 0.5 to 2.0 minutes, largely dependent on the number of sections into which the nozzle is divided. The input and output formats utilized by both programs are the same except for minor variations as explained later in this section.

The basic equations utilized in both programs are the same with internal variations in procedure and variable names. However, the major variables used throughout the programs are consistent between both programs.

Data Input

The basic means of data input is through the use of the NAMELIST statement using the title STUFF. The variable names and definitions are shown in tables IV and V for the array and single valued variables, respectively. One significant factor that must be observed in the input of data for a variable in an array, is that the first element of the array must contain a zero. The only exception to this rule is for the input of the variable X into a double array, here no leading zero is used. The first element of the variable array is used as a computational location and the other elements are moved into this location as they are needed for computations.

The material properties k , α , E , and σ_y as a function of temperature are input in the form of coefficients to a polynomial ranging to the ninth degree and located in the KMET subroutine. The coefficients of the polynomials were obtained by a least-squares method of curve fitting applied to data from reference 15 and to unpublished data. The resulting coefficients are those shown in table VI with the resulting curves being those previously shown in figure 6 (p. 20). For the coefficients presented in table VI, the temperature range of applicability is from 300° to 2200° R. These limits are input in the form of TEMP1 and TEMP2, respectively, with TEMP3 being an upper limit on the temperature for the thermal conductivity of a coating material. In the event one of these limits is exceeded, the limiting temperature value is used to determine the properties.

The hydrogen fluid thermodynamic and transport properties used in both programs are obtained from a FORTRAN IV version of the subroutine described in reference 16. The properties subroutine is called from a library within the Lewis Computer System and would have to be added as a subroutine on other systems. The hydrogen composition used in the programs is specified as input data in the form of the variable COMP.

TABLE IV. - ARRAY VARIABLES FOR NAMELIST STUFF

FORTTRAN symbol	Definition	Units
ANWEB	Number of coolant tubes at station	-----
AREACR ^a	Area correction, ϵ_c	-----
AREAL ^b	Coolant flow area per tube	sq in.
AX	Axial length from datum plane to station	in.
COEFG	Hot-gas correlation coefficient	-----
COEFL	Coolant correlation coefficient	-----
CT	Convergence tolerance used	see table VII
DHG	Engine diameter to gas side of metal wall at tube crown	in.
PGS	Hot-gas static pressure at station	psia
PHI	Angle gas wall makes with nozzle centerline	deg
QGEN	Nuclear heating rates in shell	Btu/(in. ³)(sec)
QRAD	Radiation heat flux entering gas wall	Btu/(in. ²)(sec)
RC	Radius of gas-wall curvature in axial direction	in.
ROUGH ^a	Tube-wall roughness on coolant side	in.
SHELTH	Average pressure shell wall thickness	in.
TESTC ^c	Coating test, negative for no coating, positive for given coating, and zero for thermal barrier	-----
TGS	Hot-gas static temperature at station	^o R
TKCER ^c	Coating thickness or thermal resistance	in. or (in. ²)(sec)(^o R)/Btu
TW	Metal-wall thickness	in.
TWG ^b	Hot-gas-side metal-wall temperature	^o R
X	Coefficients for material properties polynomial	-----

^aAREACR and ROUGH are used as a single value in the design program, and a value is specified at each station in the evaluation program.

^bAREAL is used only in the evaluation program input, and TWG is used only in the design program input.

^cTESTC and TKCER are used only as input to the evaluation program.

TABLE V. - SINGLE VALUED VARIABLES FOR NAMELIST STUFF

FORTTRAN symbol	Definition	Units
AKR ^a	Estimate used in determining recovery factor	-----
AMU	Average Poisson ratio of material	-----
BRAZ	Thickness of braze material	in.
C1 ^b	Option on use of C1 correlation	-----
C2 ^b	Option on use of C2 correlation	-----
C3 ^b	Option on use of C3 correlation	-----
COMP	Fraction of ortho-hydrogen present in composition	-----
DEN	Average density of tube and shell material	lb/in. ³
DIAM	Hot-gas-side nozzle-throat diameter	in.
ES	Average Young's modulus of shell at its operating temperature	psi
F1 ^c	Estimate used in determining friction factor	-----
NUMB	Number of sections nozzle is divided into	-----
PLIN	Coolant inlet static pressure	psia
QEST ^{d, e}	Estimate used in determining convection heat flux	Btu/(in. ²)(sec)
TCER ^{d, f}	Initial estimate of average coating temperature	°R
TEMP1	Lower limit of temperature range on material properties	°R
TEMP3 ^d	Upper limit of temperature range on material properties	°R
TEMP3	Upper limit of temperature range on coating properties	°R
TLIN	Coolant inlet total temperature	°R
TMET1 ^{d, g}	Initial estimate of average metal-wall temperature ^δ	°R
TWGE ^{d, h}	Initial estimate of hot-gas-side metal-wall temperature	°R
WG	Hot-gas mass flow rate	lb/sec
WL	Coolant mass flow rate	lb/sec
YM ^b	Mach number limit	-----

^aSuggested initial estimate for use in evaluation program, 0.9.^bUsed only in design program.^cSuggested initial estimate for use in evaluation program, 0.003.^dUsed only in evaluation program.^eSuggested initial estimate, 1.0.^fSuggested initial estimate, 1500.0.^gSuggested initial estimate, 750.0.^hSuggested initial estimate, 1000.0.

TABLE VI. - POLYNOMIAL COEFFICIENTS FOR
PROPERTY CURVES OF 347 STAINLESS STEEL

KMET ^a	Thermal conductivity	Yield strength	Young's modulus	Thermal expansion
A	1.456672	37.72398	20.60063	5.05081
B	1.131624	-9.03007	62.24962	25.84439
C	-1.341449	-5.64351	-168.24084	-71.93478
D	1.912256	3.49807	214.93276	111.25141
E	-.951701	-.90454	-155.08070	-98.19083
F	.155014	0	62.56724	49.60798
G	0	0	-12.96823	-13.37053
H	0	0	1.03951	1.49251
I	0	0	0	0
J	0	0	0	0
Scale fac- tor, SF	1.0×10^{-4}	1.0×10^3	1.0×10^6	1.0×10^{-6}

^aKMET = (A + BT + CT² + . . . + JT⁹)SF, where T is the temperature in °R divided by 1000. This division and the scaling factor are taken care of internally within the programs.

The major input data difference between the two programs is that the design program uses the hot-gas-side metal-wall temperature as input, and the evaluation program uses the exact coolant passage area as input. Other differences are that the design program accepts only single values of area correction ϵ_c and tube roughness as input while the evaluation program accepts values at each individual station; the means of obtaining different options as to the use of the C_1 , C_2 , C_3 , and rough or smooth tube conditions varies as shown in table VII; the evaluation has the flexibility of handling both the radial and flat plate cases of heat conduction across the tube crown and a choice must be specified as input data. One other difference exists in the input of data; that difference being that the evaluation program utilizes realistic initial estimates of certain parameters at the first station, as shown at the end of table V.

Data Output

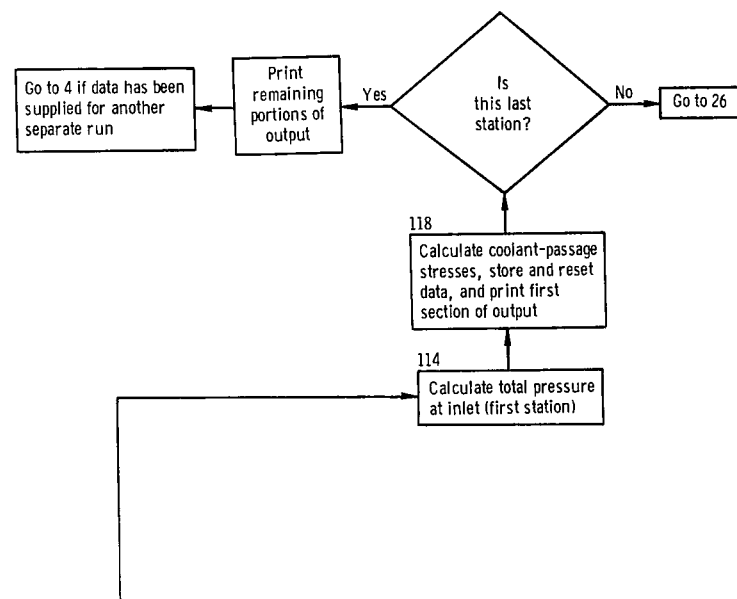
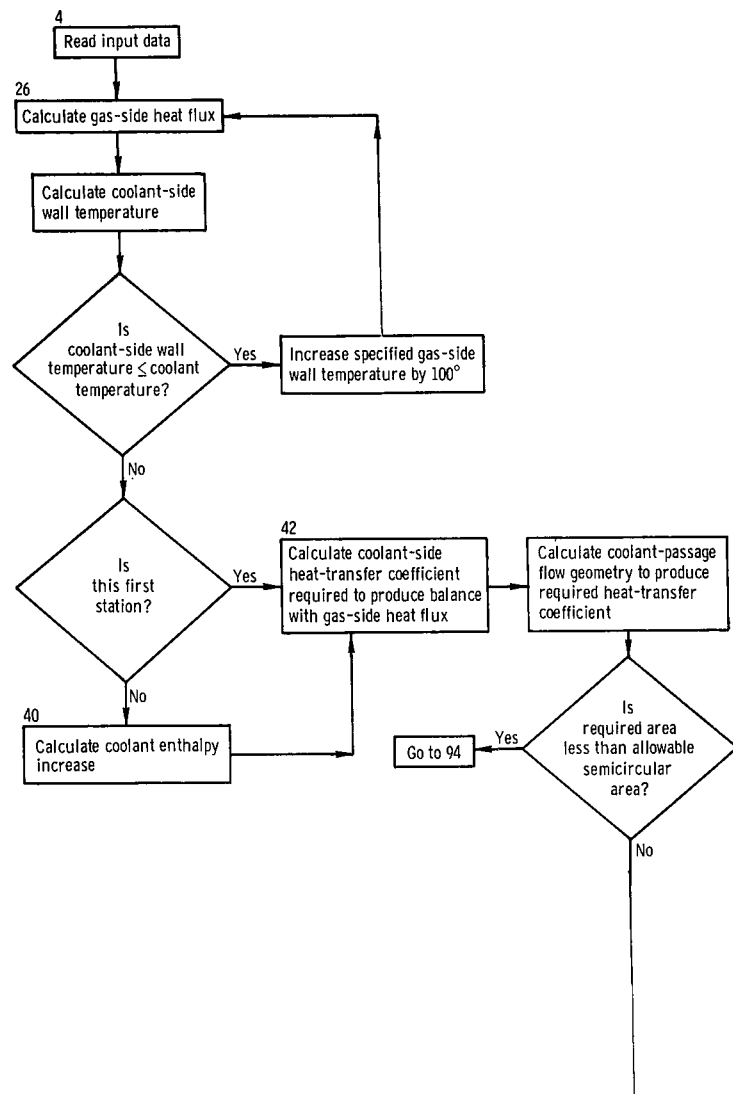
The basic output format is shown at the end of this appendix for case 1 (p. 65). The input data is printed out for the purpose of maintaining run records and checking. The definitions of the output variables that are not self-explanatory are shown in table VIII. In addition to the output shown additional write-outs are possible to note the use of a tube splice, in the event the materials properties temperature range is exceeded, in the event the coolant flow chokes or an iteration loop does not converge.

TABLE VII. - PROGRAM OPTIONS

Evaluation logicals	
LESTC1	True for use of C_1
LESTC2	True for use of C_2
LESTC3	True for use of C_3
LESTC4	True for assumption of smooth tubes
LESTC5	True for assumption of radial heat conduction
Design program reads under NAMELIST	
C1	0.0 or 1.0; 1.0 for use of C_1
C2	0.0 or 1.0; 1.0 for use of C_2
C3	0.0 or 1.0; 1.0 for use of C_3
ROUGH	0.0 or value; 0.0 for use of smooth tubes

TABLE VIII. - OUTPUT PARAMETERS

Output headings	Definition
Q/A OUT	Heat flux entering outside surface of tube crown, $\text{Btu}/(\text{in.}^2)(\text{sec})$
Q/A IN	Heat flux leaving inside surface of tube crown, $\text{Btu}/(\text{in.}^2)(\text{sec})$
T. REF.	Temperature utilized in determining hot-gas properties, $^{\circ}\text{R}$
T. COAT. G	Temperature on hot-gas side of coating or thermal barrier, $^{\circ}\text{R}$
T. MET. G	Temperature on hot-gas side of metal wall, $^{\circ}\text{R}$
T. MET. L	Temperature on coolant side of metal wall, $^{\circ}\text{R}$
Q/SECTION	Total heat added to coolant between stations, Btu/sec
Q/A NUC	Heat flux passing through shell wall, $\text{Btu}/(\text{in.}^2)(\text{sec})$
HYD. DIA	Coolant passage hydraulic diameter, in.
WALL AREA	Total heat-transfer surface area, in.^2
YIELD STRENGTH	Yield strength at average metal-wall temperature, psi
COEF. OF LIN. EXP	Coefficient of linear expansion at average temperature between metal wall and shell, $\text{in.}/\text{in.}$
YOUNG'S MODULUS	Young's modulus at average metal-wall temperature, psi



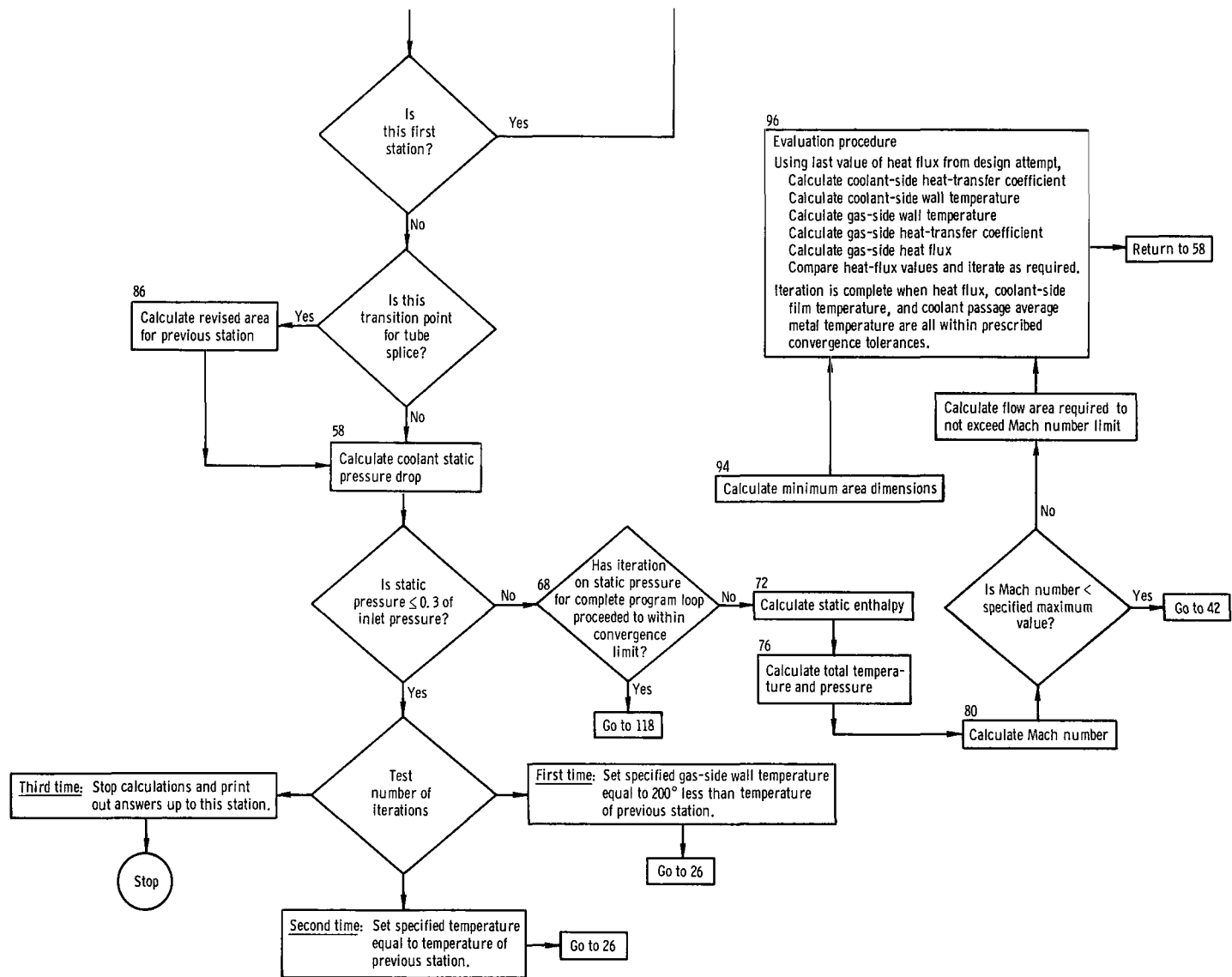
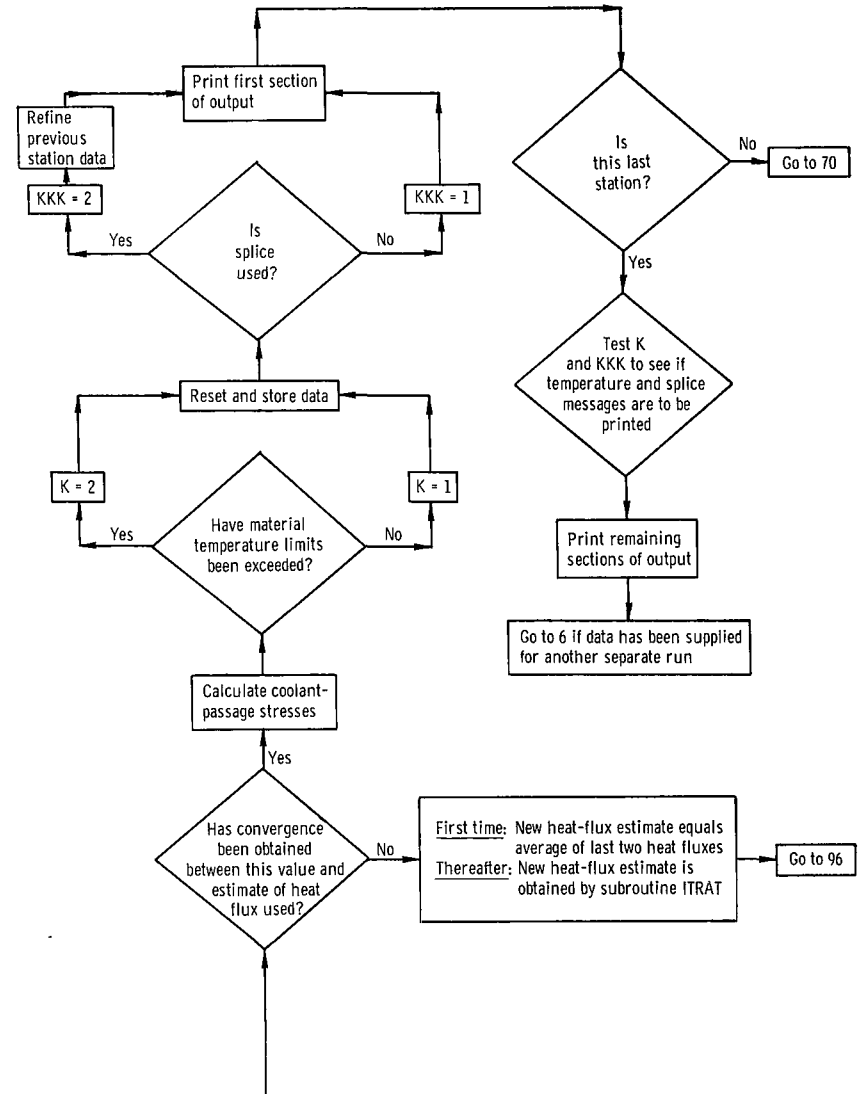
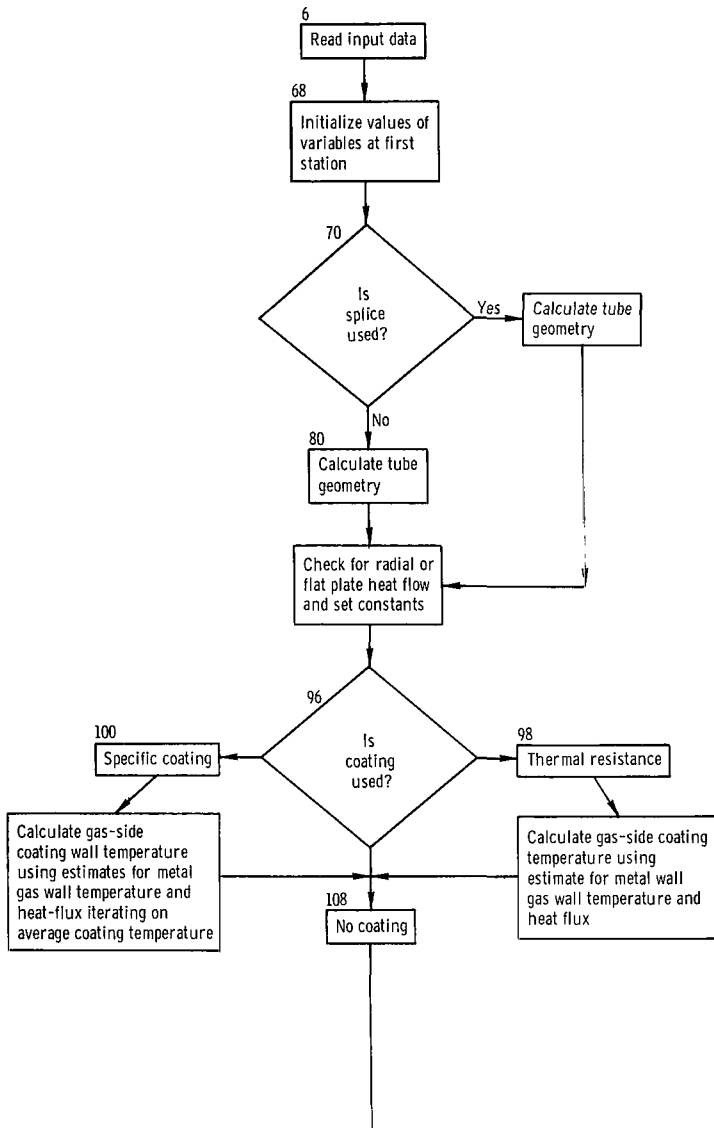


Figure 26. - Design program flow diagram. (Numbers correspond to FORTRAN statement numbers.)



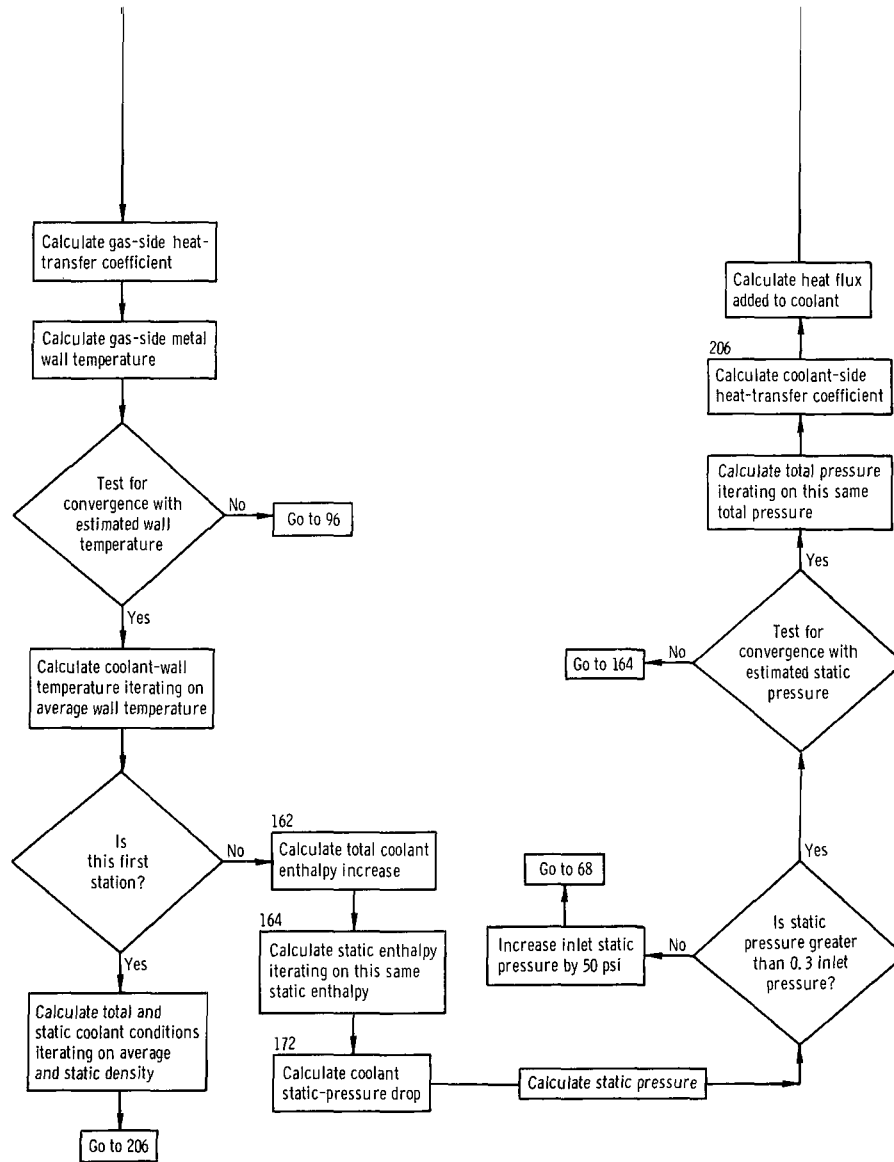


Figure 27. - Evaluation program flow diagram. (Numbers correspond to FORTRAN statement numbers.)

Program Details

The main programs utilize the basic equations set forth in the text of this report. The FORTRAN IV coding of the design (pp. 70 to 79) and evaluation (pp. 80 to 89) programs is included. The basic flow diagrams of both the design and evaluation program are shown in figures 26 and 27, respectively. The iterative procedures contained in these programs require specified convergence tolerances for solution. These convergence tolerances are defined in table IX and are used as fixed internal values as shown unless changed by specified input values. Internal limits are also specified as to the maximum number of iterations required for convergence. The design program accepts the final value if convergence has not been reached and proceeds with the calculations. The evaluation program, however, stops and prints an appropriate write-out and the answers calculated to that point. The evaluation program also employs a straight line iteration subroutine called ITRAT to determine the next estimate during some of the iteration.

TABLE IX. - INTERNAL CONVERGENCE TOLERANCES UNLESS CHANGED

FORTTRAN symbol	Definition	Value	Units
CT(1)	Used to solve equations (19) and (20) for friction factors	3.0×10^{-6}	-----
CT(2)	Used to determine the coolant-passage height and also width in design program	2.0×10^{-4}	in.
CT(3)	Used to determine average metal temperature, average coating temperature in evaluation program, and hot-gas film temperature in design program	1	$^{\circ}\text{R}$
CT(4)	Used to determine static coolant pressure and also total coolant pressure in evaluation program	0.1	psi
CT(5)	Used to determine hot-gas recovery factor	1.0×10^{-3}	-----
CT(6)	Used to determine static coolant enthalpy	1.0×10^{-4}	Percent difference
CT(7)	Used to determine heat-flux balance across tube wall	1.0×10^{-3} 1.0×10^{-3}	$^{\text{a}}\text{Btu}/(\text{in.}^2)(\text{sec})$ $^{\text{b}}\text{Percent difference}$
CT(8)	Used to determine total coolant temperature in design program and gas-side metal-wall temperature in evaluation program	0.1	$^{\circ}\text{R}$
CT(9)	Used to determine coolant state at first section in evaluation program	1.0×10^{-4}	Percent difference

^aEvaluation program.

^bDesign program.

The programs are set up to handle counterflow of the coolant and hot gas, but could be revised or used for parallel flow of the coolant and hot gas. The revision would require a minor variation in the output of data and a change in the sequence of stress calculations to allow the integration of the hot-gas pressure forces acting on the shell to proceed from the hot-gas exit end back toward the chamber. Because the heat-transfer and fluid-flow calculations are not interrelated to the stress calculations, the program can be used for parallel flow if the resulting stress values are not considered.

As mentioned previously in this report, both programs have the provision for incorporating a tube splice in the form of a bifurcation. For the purpose of analysis, a station is chosen at the point of the tube splice. The number of tubes specified at the transition station is that number of tubes which exists between the preceding station and the transition station (see fig. 28). In addition, the length between stations, where the transition occurs, should be as small as possible while including all the region of uncertain tube geometry.

Two internal program variations that exist are associated with the average density used to calculate the coolant inlet total pressure and the method of handling the calculation

of pressure drop over the transition increment for the situation where a tube splice exists. The design program uses the static density instead of an average density for calculating total pressure at the first station (eq. (24)). The pressure-drop calculations use the areas at both the preceding and present stations. Over the spliced-tube transition section, the flow from two tubes enters one tube or vice versa depending on where the splice is located. Therefore, the change in flow area from one station to the next is not actually the change in area from that of one tube before the splice to that of one tube after the splice. A revision of the previous area is made in each program to account for this change in the number of tubes. The design program assumes that, at the splice joint, the area and radius of one small U-tube equals one-half the area and radius of one large U-tube, and dimensional revisions for the pressure-drop

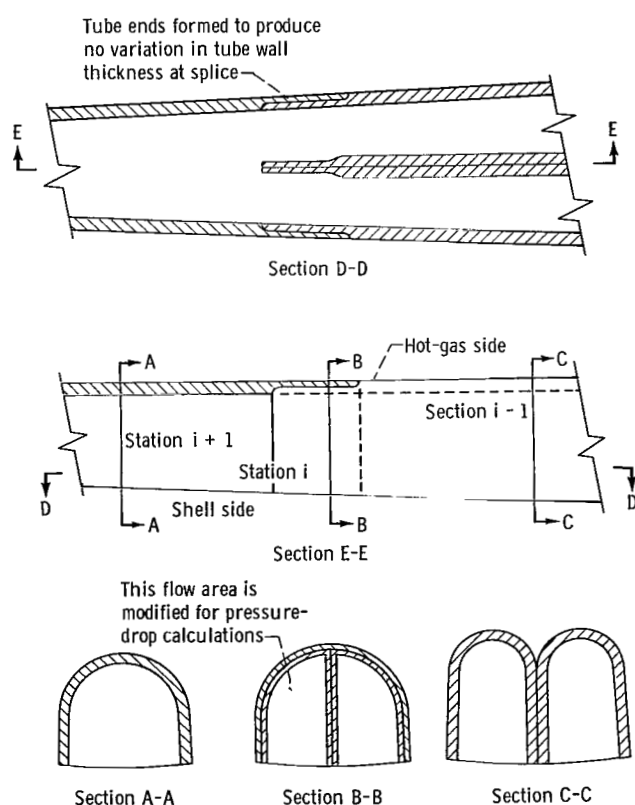


Figure 28. - Tube splice transition section showing geometry before, at, and after bifurcation.

calculations are made accordingly. The evaluation program assumes that the area, radius, and geometrical configuration are as shown in figure 28. This is more nearly the actual condition where two small tube ends would be formed into a back-to-back symmetrical configuration to fit into one large U-tube.

The evaluation program has one option for restart, that option being on the conditions which could result in choked coolant flow. This option is exercised when the static coolant pressure drops to 0.3 of the inlet coolant pressure. The option causes a written message of output to be printed, increases the coolant inlet pressure by 50 pounds per square inch, and restarts the evaluation run at the first station. The design program has no program restarts, but does contain other coolant and geometry limits as explained in the section Basic Analytical Procedure.

As explained in the section Design Procedure, care should be exercised in subdividing the nozzle into sections, because excessively large sections can lead to errors in the pressure calculations, trouble in excessive iterating of the pressure calculation, and the overlooking of a nozzle hot spot. Also, using large section lengths in the convergent section, where the slope of the heat flux curve is steep, can lead to a problem in the evaluation program. The problem occurs in the heat-flux iteration that uses the value of heat flux from the last station as an estimate to start calculations at the next station. A sharp drop in heat flux results in the use of an excessively large heat-flux estimate that produces unrealistic temperatures in the program. Traps are present in the program to work this condition out, but if conditions become excessive the iteration limits could be exceeded.

The programs are set up so that cases can be executed in sequential order by simply stacking the input data back to back. Variations of input data for the same nozzle can be obtained by simply reading in only the input values that vary and the logicals in the evaluation program. Each program uses the last value of friction factor and recovery factor calculated for a given case for input to the succeeding case unless their input values are also repeated. These calculated values are just as adequate as the input estimates used initially and need not be repeated. For the design program, if the input values for gas-wall temperature are not achieved and new values are calculated, these values will be used as input to the succeeding case unless the original values are again specified as input.

Cases 3, 6, and 7 were run by using the reference 4 correlation on the hot-gas side with internal program revisions in statements 110, 112, and 122. The existing statements in the evaluation program were replaced by

$$110 \text{ TGF} = (\text{TGE} + \text{TGCER})/2.0$$

$$112 \text{ TGF} = (\text{TGE} + \text{TWGE})/2.0$$

$$122 \text{ PRGEX} = \text{PRGF} ** 0.4$$

BASIC OUTPUT FORMAT

FLUID PROPERTY LIBRARY WITH A COMPOSITION OF 96.8 PERCENT PARA-, AND 3.2 PERCENT ORTHO- HYDROGEN, 11/1/61

\$CONST

```
CT = 3.0000000E-06, 2.0000000E-04, 1.0000000E 00, 1.0000000E-01, 1.0000000E-03, 1.0000000E-04,
      1.0000000E-03, 1.0000000E-01, 1.0000000E-04,

X = 1.4566720E 00, 1.1316240E 00, -1.3414490E 00, 1.9122560E 00, -9.5170100E-01, 1.5501400E-01,
      0., 0., 0., 0., 0., -9.0301000E 00,
      -5.6435000E 00, 3.4981000E 00, -9.0450000E-01, 0., 0., 0.,
      0., 0., 2.0500600E 01, 6.2249600E 01, -1.6824080E 02, 2.1493280E 02,
      -1.5508070E 02, 6.2567200E 01, -1.2968200E 01, 1.0395000E 00, 0., 0.,
      5.0508000E 00, 2.5844400E 01, -7.1934800E 01, 1.125140E 02, -9.8190799E 01, 4.9607999E 01,
      -1.3370500E 01, 1.4925000E 00, 0., 0., 0., 0.,
      0., 0., 0., 0., 0., 0.,
      0., 0., 0., 0., 0., 0.,

TESTC = 0., -5.0000000E-01, -5.0000000E-01, -5.0000000E-01, -5.0000000E-01, -5.0000000E-01,
      -5.0000000E-01, -5.0000000E-01, -5.0000000E-01, -5.0000000E-01, -5.0000000E-01, -5.0000000E-01,
      -5.0000000E-01, -5.0000000E-01, -5.0000000E-01, -5.0000000E-01, -5.0000000E-01, -5.0000000E-01,
      -5.0000000E-01, -5.0000000E-01, 0., 0., 0., 0.,
      0., 0., 0., 0., 0., 0.,
      0., 0., 0., 0., 0., 0.,
      0., 0., 0., 0., 0., 0.,

TEMP1 = 3.0000000E 02, TEMP2 = 2.2000000E 03, TEMP3 = 0., QEST = 1.0000000E 00, TCER = 1.5000000E 03,
TWGE = 1.0000000E 03, TMET1 = 7.5000000E 02, FI = 3.0000000E-03, AKR = 8.9999999E-01,
```

\$ END

SEC.NO.	AXIAL LENGTH (IN.)	ENG.DIAM. (IN.)	NO.TUBES	ANGLE PHI (DEG.)	TUBE THICK. (IN.)	AREA PER.TUBE (SQ.IN.)	STAT.GAS TEMP (DEG. R)	STAT.GAS PRESS (PSIA)
1	0.	12.1260	90.0	15.000	0.0120	0.0980	1225.0	5.90
2	2.0000	11.0540	90.0	15.000	0.0120	0.0815	1325.0	7.80
3	4.0000	9.9820	90.0	15.000	0.0120	0.0671	1445.0	10.60
4	6.0000	8.9100	90.0	15.000	0.0120	0.0539	1600.0	15.90
5	8.0000	7.8380	90.0	15.000	0.0120	0.0419	1795.0	24.50
6	10.0000	6.7680	90.0	15.000	0.0120	0.0317	2040.0	40.00
7	11.0000	6.2300	90.0	15.000	0.0120	0.0268	2200.0	50.00
8	12.0000	5.6940	90.0	15.000	0.0120	0.0227	2400.0	68.00
9	13.0000	5.1580	90.0	15.000	0.0120	0.0187	2635.0	96.00
10	13.5000	4.8900	90.0	15.000	0.0120	0.0167	2800.0	120.00
11	13.9000	4.6760	90.0	15.000	0.0120	0.0153	2940.0	148.00
12	14.2240	4.5040	90.0	15.000	0.0120	0.0142	3100.0	184.00
13	14.7000	4.3300	90.0	5.750	0.0120	0.0130	3325.0	240.00
14	15.0000	4.3000	90.0	0.	0.0120	0.0125	3458.0	287.00
15	15.3000	4.3300	90.0	5.750	0.0120	0.0125	3598.0	323.00
16	15.8000	4.5180	90.0	15.480	0.0120	0.0128	3643.0	353.00
17	16.4000	4.9920	90.0	27.800	0.0120	0.0142	3852.0	448.00
18	17.1210	6.0580	90.0	45.000	0.0120	0.0182	3942.0	500.00
19	18.4000	8.6160	90.0	45.000	0.0120	0.0335	3987.0	522.00
20	20.0760	11.9680	90.0	45.000	0.0120	0.0620	3996.0	528.00
21	21.8000	14.2160	90.0	21.300	0.0120	0.0900	3998.0	528.00
22	23.6120	14.8960	90.0	0.	0.0120	0.1000	3998.0	530.00
23	25.6000	14.8960	90.0	0.	0.0120	0.1000	3999.0	530.00
24	28.0000	14.8960	90.0	0.	0.0120	0.1000	4000.0	530.00
25	31.0000	14.8960	90.0	0.	0.0120	0.1000	4000.0	530.00

SEC.NO.	GAS COEF.	COOL.COEF.	AREA CORR.	ROUGHNESS (IN.)	RAD.OF CJRV (IN.)	Q RAD. BTU.PER. SQ.IN-SEC	NUC.HEAT BTU.PER. CU.IN-SEC	SHELL.THICK. (IN.)	COAT.THK.OR RES. (IN) OR SQ.IN-SEC-R PER.BTU.
1	0.0260	0.0210	0.8000	0.600E-04	0.1000E 08	0.	0.	0.750	0.
2	0.0247	0.0210	0.8000	0.600E-04	0.1000E 08	0.	0.	0.750	0.
3	0.0240	0.0210	0.8000	0.600E-04	0.1000E 08	0.	0.	0.750	0.
4	0.0230	0.0210	0.8000	0.600E-04	0.1000E 08	0.	0.	0.750	0.
5	0.0220	0.0210	0.8000	0.600E-04	0.1000E 08	0.	0.	0.750	0.
6	0.0209	0.0210	0.8000	0.600E-04	0.1000E 08	0.	0.	0.750	0.
7	0.0203	0.0210	0.8000	0.600E-04	0.1000E 08	0.	0.	0.750	0.
8	0.0198	0.0210	0.8000	0.600E-04	0.1000E 08	0.	0.	0.750	0.
9	0.0193	0.0210	0.8000	0.600E-04	0.1000E 08	0.	0.	0.750	0.
10	0.0191	0.0210	0.8000	0.600E-04	0.1000E 08	0.	0.	0.750	0.
11	0.0192	0.0210	0.8000	0.600E-04	0.1000E 08	0.	0.	0.750	0.
12	0.0194	0.0210	0.8000	0.600E-04	0.1000E 08	0.	0.	0.750	0.
13	0.0200	0.0210	0.8000	0.600E-04	0.3000E 01	0.	0.	0.750	0.
14	0.0202	0.0210	0.8000	0.600E-04	0.3000E 01	0.	0.	0.750	0.
15	0.0204	0.0210	0.8000	0.600E-04	0.3000E 01	0.	0.	0.750	0.
16	0.0207	0.0210	0.8000	0.600E-04	0.3000E 01	0.	0.	0.750	0.
17	0.0242	0.0210	0.8000	0.600E-04	0.3000E 01	0.	0.	0.750	0.
18	0.0288	0.0210	0.8000	0.600E-04	0.3000E 01	0.	0.	0.750	0.
19	0.0316	0.0210	0.8000	0.600E-04	0.1000E 08	0.	0.	0.750	0.
20	0.0321	0.0210	0.8000	0.600E-04	0.1000E 08	0.	0.	0.750	0.
21	0.0322	0.0210	0.8000	0.600E-04	-0.5000E 01	0.	0.	0.750	0.
22	0.0323	0.0210	0.8000	0.600E-04	-0.5000E 01	0.	0.	0.750	0.
23	0.0323	0.0210	0.8000	0.600E-04	-0.1000E 08	0.	0.	0.750	0.
24	0.0323	0.0210	0.8000	0.600E-04	-0.1000E 08	0.	0.	0.750	0.
25	0.0323	0.0210	0.8000	0.600E-04	-0.1000E 08	0.	0.	0.750	0.

AVG.METAL DENSITY= 0.280 LBS/CU.IN SHELL YOUNG'S MODULUS= 0.300E 08 PSI POISSON'S RATIO= 0.290 BRAZE THICK= 0.0100 (IN.)
PROPELLANT FLOW RATE 16.6650 LBS/SEC COOLANT FLOW RATE 16.6650 LBS/SEC
CHAMBER TEMPERATURE 4000.0 DEG.R ENTRANCE COOLANT TEMP. 56.00 DEG.R
CHAMBER PRESSURE 530.0 PSIA ENTRANCE COOLANT PRESS 1150.0 PSIA

THROAT DIAMETER 4.3000 (IN.)
TOTAL NOZZLE LENGTH 31.0000 (IN.)
CONVERGENT AREA RATIO A/A* 12.0006
DIVERGENT AREA RATIO A/A* 7.9524

C-1 IS NOT USED
C-2 IS NOT USED
C-3 IS NOT USED
TUBE IS ASSUMED SMOOTH
ASSUMED RADIAL HEAT CONDUCTION

SEC.NO.	Q/A OUT (BTU./SQ.IN.-SEC.)	Q/A IN	EFF.GAS T (DEG.R)	T.REF. (DEG.R)	T.COAT.G (DEG.R)	T.MET.G (DEG.R)	T.MET.L (DEG.R)	LIQ.T. TOTAL (DEG.R)	LIQ.P. STATIC (PSIA)	LIQ.VEL FT/SEC	MACH NO
1	1.62	1.72	3644.	1880.	0.	1471.	1401.	56.0	1150.	63.	0.016
2	1.93	2.05	3658.	1912.	0.	1472.	1389.	59.6	1149.	78.	0.020
3	2.34	2.52	3676.	1970.	0.	1514.	1414.	63.3	1147.	98.	0.026
4	2.91	3.15	3699.	2038.	0.	1553.	1429.	67.2	1144.	126.	0.035
5	3.72	4.08	3726.	2123.	0.	1601.	1444.	71.3	1138.	170.	0.049
6	4.87	5.43	3759.	2233.	0.	1669.	1465.	75.7	1126.	237.	0.072
7	5.69	6.40	3780.	2301.	0.	1707.	1469.	78.0	1114.	289.	0.091
8	6.68	7.61	3806.	2400.	0.	1780.	1504.	80.4	1097.	353.	0.114
9	7.96	9.22	3836.	2512.	0.	1861.	1535.	82.9	1068.	446.	0.149
10	8.79	10.28	3856.	2591.	0.	1917.	1559.	84.1	1044.	511.	0.174
11	9.54	11.24	3873.	2669.	0.	1987.	1604.	85.2	1020.	569.	0.198
12	10.24	12.15	3893.	2758.	0.	2067.	1660.	86.1	996.	625.	0.221
13	11.17	13.36	3920.	2883.	0.	2180.	1744.	87.4	958.	703.	0.256
14	11.56	13.85	3936.	2940.	0.	2211.	1762.	88.2	935.	745.	0.276
15	11.71	14.01	3953.	2996.	0.	2239.	1786.	89.0	925.	758.	0.284
16	11.55	13.71	3958.	2981.	0.	2180.	1730.	90.5	917.	762.	0.290
17	11.38	13.26	3983.	3075.	0.	2241.	1808.	92.4	932.	710.	0.273
18	10.06	11.38	3993.	3079.	0.	2193.	1815.	95.3	971.	578.	0.223
19	6.64	7.22	3998.	2996.	0.	2000.	1748.	101.6	1018.	345.	0.133
20	4.19	4.44	4000.	2899.	0.	1830.	1637.	109.4	1033.	210.	0.081
21	3.19	3.35	4000.	2867.	0.	1736.	1611.	115.3	1037.	156.	0.061
22	3.01	3.15	4000.	2845.	0.	1692.	1572.	120.3	1037.	150.	0.058
23	3.09	3.24	4000.	2819.	0.	1638.	1513.	126.1	1036.	161.	0.062
24	3.19	3.34	4000.	2789.	0.	1578.	1445.	133.4	1035.	174.	0.066
25	3.30	3.46	4000.	2754.	0.	1509.	1368.	143.4	1033.	192.	0.072

SEC.NO.	FRI.P.DROP (PSI)	MOM.P.DROP (PSI)	FRI.FACT	HGF (BTU/SQ.IN.SEC.DEG.R)	HLF	C1	C2	C3	Q/SECTION BTU/SEC	Q/A NUC BTU/SQ.IN.SEC
1	0.	0.	0.	0.00075	0.00128	1.000	1.000	1.000	0.	0.
2	0.18	0.96	0.00296	0.00088	0.00155	1.000	1.000	1.000	169.6	0.
3	0.28	1.54	0.00286	0.00108	0.00186	1.000	1.000	1.000	184.9	0.
4	0.47	2.72	0.00277	0.00136	0.00231	1.000	1.000	1.000	203.6	0.
5	0.84	5.23	0.00267	0.00175	0.00297	1.000	1.000	1.000	226.7	0.
6	1.64	10.45	0.00256	0.00233	0.00390	1.000	1.000	1.000	254.9	0.
7	1.47	10.22	0.00248	0.00274	0.00460	1.000	1.000	1.000	138.8	0.
8	2.25	14.89	0.00242	0.00330	0.00535	1.000	1.000	1.000	148.4	0.
9	3.55	25.81	0.00236	0.00403	0.00635	1.000	1.000	1.000	159.1	0.
10	2.65	21.16	0.00232	0.00454	0.00697	1.000	1.000	1.000	83.9	0.
11	2.75	20.98	0.00229	0.00506	0.00740	1.000	1.000	1.000	69.7	0.
12	2.75	21.69	0.00226	0.00561	0.00772	1.000	1.000	1.000	58.3	0.
13	4.93	33.00	0.00223	0.00641	0.00806	1.000	1.000	1.000	87.4	0.
14	3.65	19.13	0.00221	0.00670	0.00827	1.000	1.000	1.000	56.2	0.
15	3.88	6.05	0.00220	0.00683	0.00826	1.000	1.000	1.000	57.6	0.
16	6.52	1.81	0.00219	0.00650	0.00836	1.000	1.000	1.000	100.1	0.
17	7.28	-22.30	0.00219	0.00654	0.00773	1.000	1.000	1.000	134.9	0.
18	6.81	-46.68	0.00222	0.00559	0.00662	1.000	1.000	1.000	204.4	0.
19	4.79	-51.85	0.00228	0.00332	0.00439	1.000	1.000	1.000	431.0	0.
20	1.61	-16.38	0.00238	0.00190	0.00291	1.000	1.000	1.000	519.7	0.
21	0.51	-4.03	0.00247	0.00141	0.00224	1.000	1.000	1.000	395.0	0.
22	0.29	-0.37	0.00251	0.00130	0.00217	1.000	1.000	1.000	333.1	0.
23	0.29	0.61	0.00252	0.00131	0.00234	1.000	1.000	1.000	362.6	0.
24	0.38	0.78	0.00252	0.00132	0.00255	1.000	1.000	1.000	450.9	0.
25	0.52	1.02	0.00252	0.00133	0.00283	1.000	1.000	1.000	582.4	0.

SEC.NO.	SHELL RAD (IN.)	TUBE RADIUS (IN.)	TUBE HEIGHT (IN.)	TUBE WIDTH (IN.)	HYD.DIA (IN.)	WALL AREA (SQ.IN)	TOTAL TUBE HEIGHT (IN.)
1	6.3503	0.2018	0.0836	0.4093	0.3238	0.	0.2855
2	5.7915	0.1825	0.0794	0.3703	0.2957	95.6227	0.2619
3	5.2345	0.1631	0.0769	0.3314	0.2690	86.5540	0.2401
4	4.6768	0.1438	0.0739	0.2925	0.2417	77.4854	0.2177
5	4.1184	0.1244	0.0700	0.2535	0.2137	68.4168	0.1944
6	3.5624	0.1051	0.0676	0.2147	0.1865	59.3492	0.1727
7	3.2814	0.0954	0.0649	0.1951	0.1717	26.2841	0.1602
8	3.0035	0.0857	0.0644	0.1757	0.1583	24.0062	0.1501
9	2.7243	0.0760	0.0625	0.1562	0.1439	21.7390	0.1385
10	2.5838	0.0712	0.0606	0.1464	0.1360	10.0193	0.1318
11	2.4725	0.0673	0.0600	0.1386	0.1302	7.6068	0.1272
12	2.3828	0.0642	0.0593	0.1324	0.1255	5.8940	0.1235
13	2.2949	0.0611	0.0574	0.1262	0.1201	8.1701	0.1185
14	2.2773	0.0606	0.0547	0.1250	0.1177	4.9495	0.1153
15	2.2909	0.0611	0.0535	0.1259	0.1177	4.9495	0.1146
16	2.3790	0.0644	0.0481	0.1321	0.1189	8.6043	0.1126
17	2.6065	0.0727	0.0401	0.1480	0.1244	11.7589	0.1129
18	3.1218	0.0913	0.0279	0.1839	0.1383	19.0667	0.1192
19	4.4237	0.1371	0.0145	0.2748	0.1824	51.6203	0.1516
20	6.1336	0.1970	0.0026	0.3942	0.2435	95.9936	0.1996
21	7.3422	0.2393	0.0001	0.4786	0.2925	107.1460	0.2394
22	7.7124	0.2522	0.0002	0.5044	0.3084	107.4853	0.2524
23	7.7124	0.2522	0.0002	0.5044	0.3084	118.8072	0.2524
24	7.7124	0.2522	0.0002	0.5044	0.3084	143.4292	0.2524
25	7.7124	0.2522	0.0002	0.5044	0.3084	179.2865	0.2524

SEC.NO.	LIQ.T. STATIC (DEG.R)	LIQ.P. TOTAL PSIA	LIQ.ENTHALPY STATIC BTU/LB	LIQ.ENTHALPY TOTAL BTU/LB	LIQ.DENSITY STATIC LBS/CU.IN	LIQ.DENSITY TOTAL	RE GAS FILM	PR GAS FILM	RE LIQ BULK	RE LIQ FILM	PR LIQ FILM
1	56.0	1152.	-14.52	-14.44	0.00250	0.00250	0.983E 06	0.662	0.835E 06	0.652E 05	0.665
2	59.5	1152.	-4.39	-4.26	0.00243	0.00243	0.113E 07	0.664	0.101E 07	0.744E 05	0.666
3	63.2	1151.	6.64	6.83	0.00235	0.00235	0.130E 07	0.666	0.122E 07	0.822E 05	0.665
4	67.1	1151.	18.73	19.05	0.00226	0.00227	0.153E 07	0.669	0.151E 07	0.932E 05	0.664
5	71.2	1149.	32.08	32.65	0.00217	0.00217	0.182E 07	0.672	0.190E 07	0.108E 06	0.664
6	75.4	1147.	46.83	47.95	0.00206	0.00206	0.220E 07	0.675	0.245E 07	0.126E 06	0.663
7	77.5	1145.	54.61	56.27	0.00199	0.00200	0.246E 07	0.676	0.284E 07	0.140E 06	0.663
8	79.7	1141.	62.69	65.18	0.00193	0.00194	0.273E 07	0.679	0.330E 07	0.149E 06	0.662
9	81.7	1135.	70.76	74.73	0.00185	0.00187	0.307E 07	0.681	0.390E 07	0.161E 06	0.661
10	82.5	1131.	74.56	79.76	0.00181	0.00183	0.327E 07	0.682	0.430E 07	0.167E 06	0.660
11	83.2	1127.	77.48	83.95	0.00177	0.00180	0.342E 07	0.682	0.464E 07	0.166E 06	0.659
12	83.6	1122.	79.66	87.45	0.00174	0.00178	0.355E 07	0.684	0.497E 07	0.163E 06	0.657
13	84.1	1114.	82.83	92.69	0.00169	0.00174	0.368E 07	0.686	0.543E 07	0.156E 06	0.655
14	84.5	1108.	84.98	96.07	0.00166	0.00171	0.373E 07	0.687	0.570E 07	0.156E 06	0.654
15	85.1	1101.	88.05	99.52	0.00163	0.00169	0.373E 07	0.687	0.583E 07	0.153E 06	0.653
16	86.4	1090.	93.93	105.53	0.00158	0.00164	0.365E 07	0.687	0.595E 07	0.162E 06	0.655
17	88.8	1077.	103.56	113.62	0.00153	0.00158	0.331E 07	0.687	0.580E 07	0.149E 06	0.653
18	92.8	1063.	119.21	125.89	0.00147	0.00150	0.279E 07	0.687	0.520E 07	0.140E 06	0.652
19	100.6	1052.	149.37	151.75	0.00133	0.00135	0.207E 07	0.687	0.395E 07	0.122E 06	0.654
20	109.1	1048.	182.06	182.94	0.00119	0.00120	0.158E 07	0.686	0.299E 07	0.110E 06	0.657
21	115.0	1047.	206.15	206.64	0.00110	0.00110	0.135E 07	0.685	0.252E 07	0.101E 06	0.658
22	120.1	1046.	226.18	226.63	0.00103	0.00103	0.131E 07	0.685	0.241E 07	0.105E 06	0.659
23	125.8	1045.	247.87	248.39	0.00096	0.00096	0.133E 07	0.685	0.242E 07	0.119E 06	0.660
24	133.2	1044.	274.84	275.45	0.00088	0.00089	0.135E 07	0.684	0.241E 07	0.137E 06	0.662
25	143.1	1043.	309.66	310.39	0.00080	0.00081	0.138E 07	0.683	0.237E 07	0.161E 06	0.665

SEC.NO.	R OVER T	TUBE DELTA (IN.)	LONG.AV (PSI)	LONG.OUT (PSI)	TUBE WALL LONG.IN (PSI)	STRESSES TANG.OUT (PSI)	TANG.IN (PSI)	AVG.METAL TEMP. DEG.R	YIELD STRENGTH (PSI)	COEF.OF LIN.EXP (IN/IN)	YOUNG'S MODULUS (PSI)
1	17.321	0.00732	-273851.	-284587.	-263114.	59315.	-21223.	1436.	19633.	0.942E-05	0.215E 08
2	15.707	0.00657	-273220.	-286084.	-260357.	59890.	-25903.	1431.	19707.	0.942E-05	0.215E 08
3	14.094	0.00600	-276385.	-291718.	-261051.	61932.	-32218.	1464.	19234.	0.945E-05	0.212E 08
4	12.480	0.00539	-278821.	-297555.	-260087.	64453.	-39261.	1491.	18835.	0.947E-05	0.210E 08
5	10.866	0.00477	-281402.	-304927.	-257877.	67844.	-47563.	1523.	18379.	0.949E-05	0.207E 08
6	9.256	0.00417	-284791.	-314841.	-254742.	73070.	-58390.	1567.	17717.	0.952E-05	0.203E 08
7	8.446	0.00385	-286279.	-320967.	-251466.	76058.	-64598.	1588.	17406.	0.954E-05	0.200E 08
8	7.639	0.00360	-289577.	-329011.	-250144.	81451.	-73752.	1642.	16587.	0.957E-05	0.195E 08
9	6.833	0.00334	-292348.	-337811.	-246884.	87639.	-84439.	1698.	15721.	0.961E-05	0.189E 08
10	6.429	0.00322	-293877.	-342824.	-244930.	91402.	-90935.	1738.	15089.	0.964E-05	0.185E 08
11	6.107	0.00317	-295302.	-346331.	-244272.	95835.	-97862.	1796.	14162.	0.968E-05	0.179E 08
12	5.848	0.00316	-295679.	-347840.	-243517.	99968.	-104288.	1863.	13032.	0.972E-05	0.172E 08
13	5.593	0.00320	-293013.	-345649.	-240377.	103391.	-110294.	1962.	11305.	0.978E-05	0.160E 08
14	5.549	0.00322	-291591.	-344917.	-238264.	102445.	-110326.	1987.	10844.	0.980E-05	0.157E 08
15	5.593	0.00329	-289706.	-342433.	-236978.	100567.	-108559.	2013.	10369.	0.981E-05	0.154E 08
16	5.869	0.00333	-293152.	-347717.	-238586.	93558.	-100466.	1955.	11429.	0.978E-05	0.161E 08
17	6.562	0.00388	-288292.	-338302.	-238282.	81036.	-85316.	2025.	10141.	0.982E-05	0.152E 08
18	8.107	0.00472	-289334.	-333764.	-244904.	64166.	-63915.	2004.	10530.	0.981E-05	0.155E 08
19	11.921	0.00642	-292652.	-324789.	-260515.	47028.	-38479.	1874.	12842.	0.974E-05	0.171E 08
20	16.920	0.00822	-287748.	-310297.	-265199.	37446.	-21965.	1718.	15406.	0.964E-05	0.187E 08
21	20.441	0.00964	-283927.	-301594.	-266260.	35228.	-15531.	1674.	16107.	0.962E-05	0.192E 08
22	21.517	0.00984	-280547.	-297727.	-263368.	33727.	-12899.	1632.	16747.	0.959E-05	0.196E 08
23	21.517	0.00940	-275641.	-294053.	-257230.	31788.	-10982.	1575.	17596.	0.956E-05	0.202E 08
24	21.517	0.00890	-268949.	-288860.	-249039.	29329.	-8549.	1511.	18543.	0.952E-05	0.208E 08
25	21.517	0.00833	-259808.	-281557.	-238060.	26181.	-5437.	1438.	19602.	0.948E-05	0.215E 08

TOTAL COOLANT HEAT PICKUP = 5413.36 BTU/SEC

TOTAL NOZZLE WALL AREA = 1344.24 SQ.IN.

TOTAL NOZZLE WEIGHT = 254.02 LBS

TOTAL COOLANT TEMP.DELTA = 87.40 DEG.R

TOTAL COOLANT PRESS.DELTA = 116.72 PSI

TITLE

RESULTS

FUTURE REVISIONS

DESIGN PROGRAM

```

C      DESIGN PROGRAM FOR CONNECTIVELY COUPLED NOZZLES
C
COMMON UCOM,QLTQS,TGE,TGF,TWGG,TWL,TL,PL,VLSF,EML,AL,DF,DM,FF,HGF,
1      HLF,C11,C22,C33,QL,QN,RO,RT,HCP,WCP,UHL,WALT,TOTHT,TL5,PT,
2      HLS,HLT,RS2,RTL,XG,PG,RLU,RL,PF,RUVT,DELT,SIGLON,SIGLUD,
3      SIGLOI,SIGOUT,SIGIN,TMET,SIGALM,ALPHA1,E
4      /INPUT/AX(50),DHG(50),ANWEB(50),PHI(50),TW(50),TWG(50),
5      TGS(50),PGS(50),CUEFG(50),CUEFL(50),RC(50),QRAD(50),
6      QGEN(50),SHELTH(50)
COMMON/INPUT/DEN,SEC,G,PI,PGS1,CPH,AMU,ES,WGHT,N,R1
COMMON/STATE1/SS(50)/STATE2/U(3)

DIMENSION LINE(2),LIST(60),PRINT(60)
DIMENSION SEE(50,39),DZ(50,20),NAME(20),C(100),OUT(5)
DIMENSION C1(8)
EQUIVALENCE (C,QCOM)
EQUIVALENCE (RF,RHOLF)
EQUIVALENCE (DPMOM,DM), (DF,DPER), (DP,DPTOT), (R3,RHOLB)
EQUIVALENCE (MCAL,H(10))
EQUIVALENCE (RL,RLF), (RG,RGF), (PF,PKLF), (PG,PKG6F)
EQUIVALENCE (RS2,RHOLS)
EQUIVALENCE (PLT,PT), (TL,TS)
EQUIVALENCE (DZ,AX)
COMMON/ST/H(10)/MET/TEMP1,TEMP2,X(10,4),XZ(50)

EQUIVALENCE (H(2),CP), (H(3),AM), (H(4),AK), (H(5),SVVL), (H(7),R)

NAMELIST/CONJ/CT,X,TEMP1,TEMP2,F1,AKR,ROUGH,AREACR,C1,C2,C3,YM
NAMELIST/TUFF/TW,DHG,AX,TGS,PGS,ANWEB,TWG,CUEFL,CUEFG,RL,PHI,
1      ISHELTH,QGEN,QRAD,CT,WG,WL,PLIN,TLIN,AMU,BRAZ,DFN,KTH,YM,TOT,
2      AKR,TEMP1,TEMP2,NTRIAL,AREACR,C1,C2,C3,LIST,LTOP,F1,ROUGH,
3      X,DIAM,ES,NUMB,COMP
DATA CT/3.3E-6,5.0072,1.0,2.1,3.001,2.001,2.001,2.001,2.001,2.001/

REAL KMET

C      1=KMET 2=SIG, 3=EEL, 4=APLHA

G2=2.*32.174*12.
PI=3.1415927
G=.5
RAJ=57.29578
AG=6*G2
XJ=778.161*12.
LTOP=60
DO 1 K=1,60
1 LIST(K)=K
DO 2 K=1,578
2 AX(K)=.0
KTH=0
NTRIAL=20
4 READ (5,3TUFF)
TL=TLIN
PL=PLIN
U(2)=LUMP
NXX=NUMB*1
TLNG=ABS(AX(NXX)-AX(2))
AROUN=UMG(NXX)**2/DIAM**2
ARUIV=UMG(2)**2/DIAM**2
WRITE (6,6)
6 FORMAT(1H1)
CALL CUUL(0.0,0.0,3)
WRITE (6,CONST)
NPL=0

```

```

      WRITE (6,8)
8  FORMAT(1H1///1X,8HSEC.VO. ,3X,12HAXIAL LENGTH,4X,9HENG.DIAM.,5X,
1  8HNU.TUBES,3X,9HANGLE PHI,4X,11HTUBE THICK.,6X,7HT.MET.G,
2  6X,13HSTAT.GAS TEMP,4X,14HSTAT.GAS PRESS//16X,5H(IN.),9X,
35H(IN.),20X,6H(DEG.),8X,5H(IN.),9X,8H(DEG. R),11X,8H(DEG. R),9X,
46H(P.SIA)///)
      DO 16 J=2,NXX
      JJ=J-1
10  WRITE (6,12) JJ,(DZ(J,I), I=1,8)
12  FORMAT(2X,13,F16.4,F15.4,F12.1,F13.3,F14.4,F15.0,F19.1,F16.2)
      WRITE (6,14)
14  FORMAT(1H1///1X,9H SEC.VO. ,2X,9HGAS COEF.,2X,10HCOOL.CUEF.,1X,
11HKOOL.OF CURV,3X,6HQ RAD.,6X,8HNUC.HEAT,5X,12HHELL THICK.//
237X,5H(IN.),6X,7HBTU PER,5X,7HBTU PER,9X,5H(IN.)/
348X,9HSEC.IN-SEC,3X,9HCJ.IN-SEC///)
      DO 16 J=2,NXX
      JJ=J-1
16  WRITE (6,18) JJ,(DZ(J,I), I=9,14)
18  FORMAT(3X,13,2X,2F11.4,E14.4,F11.3,2F13.3)
      WRITE (6,20) DEN,ES,AMJ,dRAZ
20  FORMAT(///1X,19HAVG.METAL DENSITY=F6.3,2X,9HLBS/CU.IN,3X,
1  22HSHELL YOUNG'S MODULUS=E10.3,2X,3HPSI,3X,16HPOISSON'S RAT
210=F6.3,3X,12HRAZE THICK=F7.4,2X,5H(IN.))
      WRITE (6,22) WG,WL,TGS(NXX),TL,PGS(NXX),PL,DIAM,TLENG,ARCON,
1ARUIV
22  FORMAT(1H1//9X,21HPRDPELLANT FLOW RATE ,F9.4,2X,7HLBS/SEC,23X,
1  17HCOOLANT FLOW RATE,4X,F9.4,2X,7HLBS/SEC//9X,19HCHAMBER TEM
2PERATURE,3X,F8.1,2X,6HDEG.R ,24X,22HENTRANCE COOLANT TEMP.,
3F8.2,2X,6HDEG.R //9X,16HCHAMBER PRESSURE,6X,F8.1,2X,6HPSIA ,
424X,22HENTRANCE COOLANT PRESS,F8.1,2X,6HPSIA ///43X,15HTHROAT DIA
5METER,13X,F9.4,2X,5H(IN.)/43X,19HTOTAL NOZZLE LENGTH,8X,F10.4,2X,
65H(IN.)/43X,26HCONVERGENT AREA RATIO A/A*,3X,F8.4,743X,25H DIVERGEN
71 AREA RATIO A/A*,4X,F8.4//)
      MT=NTRIAL
      DM=C.O
      UF=C.O
      DP=C.O
      QTUT=C.O
      ATUT=C.O
      WGH=C.O
C      PROGRAM MAIN LOOP
      DO 128 N=1,NUMB
      NSEX=NUMB
      DO 24 L=1,14
      J=N+KTH+1
24  DZ(1,L)=DZ(J,L)
      CPH=LUS(PHI/RAO)
      RE=G*UHG
      RZ=0.0
      NPL=J
      KA=0

```

```

C      CALC. OF GAS SIDE HEAT FLUX
26 DO 28 M=1,MT
   TGE=TGS*AKR*(TGT-TGS)
   TGF=G*TWG*.28*TGS*.22*TGE
   F=2.*T**BRAZ
   QG1=QG2
   QGZ=QGEN*SHELTN
   QH=QGZ
   QZ=G*(QG1+QG2)
   CALL LOUL (TGS,PGS,4)
   RHUGS=R
   CALL LOUL (TGF,PGS,4)
   RHUGF=R
   RG=HL/.785/DHG/AM*RHOGF/RHUGS
   AMU=AM
   NCT=1
   R=RG**.8
   AKG=AK
   CPH=CP
   PU=CP*AM/AK
   AKRX=AKR
   AKR=PG**3333
   IF (ABS(AKRX-AKR).LE.CT(5)) GO TO 30
28 CONTINUE
30 P=PG**3
   HGF=LUEFG*AKR*P/DHG
   QG=HGF*(TGE-TWG)
   QGUM= QG+Q RA0

C      CALC. OF COOLANT SIDE WALL TEMPERATURE
   TMET=TWG
   P2=PI/ANWEB
   RT=(P2*(RE+TW*CPH)-F/2.)/(1.-P2*CPH)
   RTD=RT+TW
   RAUTN=KIU*ALOG(RTD/RT)
   A=QGUM*RAUTN
   DO 32 K=1,MT
   TK=KML1(1,TMET)
   TWL=TWG-A/TK
   IF (TWL-TL) 32,32,34
32 TWG=TWG+100.
   GO TO 26
34 T=TMET
   TMET=G*(TWG+TWL)
   IF (ABS(T-TMET).LT.CT(3)) GO TO 38
36 CONTINUE
38 C2C=1.
   WLI=WL/ANWEB
   RZ=(RT/RC)**2
   RI=RL+CPH*(RT+TW)
   HCP=2.*RT
   KD=1
   H4=PI*KI*RT
   IF (N.GI.1) GO TO 40
   HLP=HLP
   GO TO 42

```

```

C      CALC. OF COOLANT ENTHALPY INCREASE
43 DD=(U1-DHG)/2.
   DX=AX1-AX
   SEC=SQRT(DD*DD+DX*DX)
   WALL=(RT1*ANWFB1/ANWEB+R1+TW1+TW)*PI*SEC*G*AREACR
   WALT=WALL*ANWFB
   ASW=G*(ANWEB1/ANWEB+DHG/U1+1.)*SEC*WCP
   QG=Q2*ASW/WLT
   QA=G*(QCUH+Q1)*WALL/WLT+QG
   QL=QA*WLT*ANWEB
   HLT=HLT1+QA

```

```

C      COOLANT SIDE CALCULATIONS

```

```

42 NCT=1
   DU 112 NH=1,MT
   K91=J
   IF(NH.G1.1) GO TO 44
   CALL CUOL (TL,PL,4)
   RB=R
   AB=AM/R
   GO TU 46
44 CALL CUOL (HL1,PLT,-3)
   TL=SS(7)
   IF(NH.EQ.1) HLS=HL1+QA
   CALL CUOL (HLS,PL,-3)
   TLS=SS(7)
   CALL CUOL (TLS,PL,4)
   RB=R
   AB=AM/R
   KLB=WLT/AL*DH1/AM
45 CALL CUOL (TWL,PL,4)
   AW=AM/K
   HLF=QCUH*RTD/RT/(TWL-TL)
   QLIQ=QCUH*RTD/RT
   TLF=TLF
   TLF=G*(TWL+TL)
   CALL CUOL (TLF,PL,4)
   KF=R
   AML=AM
   CPL=CP
   AKL=AK
   PF=CP*AM/AK
   S=WLT/AM*R/RB
   C11=1.+0.1457*AW/AB*C1
   C22=1.
   IF(NH.NH.EQ.1) GO TU 48
   RL=WLT/AL*DH1/AM*R*DLF/RHULB
   IF(RL.C2.EQ.0.7) GO TU 48
   IF(RL.K2.LT.0.67) GO TO 48
   IF(RL.LT.0.5) C22=1.
   IF(RL.GT.0.5) C22=(RL.K2)**0.05
48 CC=C11*C22
   CSC=CUEFL*AK/HLF*5**0.8*LC*PF**0.4*1.516

```

```

C          GEOMETRY CALCULATIONS
DO 54 J=1,NTRIAL
H1=2.*RT+WCP
H2=CSC/H1
H3=P1*RT+WCP
H5=H4/H1

DO 50 K=1,NTRIAL
HX=HCP
WP=H3+C.*HCP
HCP=H2*WP**0.2-H5
IF(HCP.LE.0.0) GO TO 94
IF(ABS(HX-HCP).LT.GT(2)) GO TO 52
50 CONTINUE
52 RU=R1+CPH*HCP
WX=WCP
WCP=2.*P2*RU-F
IF(ABS(WX-WCP).LT.GT(2)) GO TO 56
54 CONTINUE
56 AL=G*(H4+HCP*H1)
UHL=4.*AL/WP
IF(N.EQ.1) GO TO 114

C          CALC. OF STATIC PRESSURE DROP
IF (KA.EQ.0) GO TO 86
58 AV=G*(AL1+AL)
WPV=G*(WP1+WP)
OV=4.*AV/WPV
GV=WT/AV
TV=G*(TLS+TLS1)
PV=G*(PL+PL1)
CALL COUL(TV,PV,4)
R=GV*OV/AM
C33=1.
IF(R*.03.EQ.0.0) GO TO 60
IF(R*.02.LT.0.0) GO TO 60
C33=(R*.02)**0.75
62 F2=F1
IF(RUOH.EQ.0.0) GO TO 62
FF=(1.0/(-4.0*ALOG10(RJUH/OV/3.7+1.255/R/F1**0.5)))**2
GO TO 64
62 FF=(1.0/(4.0*ALOG10(F1**0.5*R)-0.40))**2
64 F1=FF
IF (ABS(F2-FF).GT.GT(1)) GO TO 60
FF=FF*.33
T=2.*GV*GV*SEC*FF/AG /OV
A1=1./AL1/RS1
A2=1./AL
A=WT*WT/AG/AV

DO 74 J=1,MT
DO 70 K=1,MT
CALL COUL (HLS,PL,-3)
RS2=R
VLS=WT1/RS2/AL
RV=G*(RS1+RS2)
JM=A*(A2/RS2-A1)
UF=T/RV
UP=UF+DM
PLX=PL
PL=PL1-UP
IF(PL.GT..3*SEE(1,8)) GO TO 68
PL=PL1
TWG=TWG1-200.
NPL=NPL+1
IF (NPL.GT.1) GO TO 66
GO TO 26
66 TWG=TWG1
IF (NPL.GT.2) GO TO 13,
GO TO 26
68 IF (ABS(PLX-PL).LT.GT(4)) GO TO (72,118),NCT

```

```

C          EXIT POINT FOR FINAL CONVERGENCE
      NCT=1
      PLX=PL
79  CONTINUE
72  HLS=HLS
      HLS=HLT-VLS**2/G2/XJ
      HTOL=ABS(HLX*CT(6))
      IF(ABS(HLX-HLS).LE.HTOL) GJ TO 76
74  CONTINUE

C          CALC. OF TOTAL PRESSURE AND TEMPERATURE
75  CALL COOL (HLS,PL,-3)
      TLS=SS(7)
      SVL=SVVL
      EML=VLS/SVL
      TV=G*(TLS+TLS1)
      PV=G*(PL+PL1)
      CALL COOL(TV,PV,4)
      RSA=R
      DO 78 L=1,MT
      TTV=G*(1L+1L1)
      PLTV=G*(PLT+PLT1)
      CALL COOL(TTV,PLTV,4)
      RTA=R
      DPT=XJ*RTA*WA*(1.-TTV/TV)-DF*RTA/RSA*(TTV/TV)
      PLTX=PLT
      PLT=PLT1+DPT
      TLX=TL
      CALL COOL(HLT,PLT,-3)
      RTL=R
      TLS=SS(7)
      IF(ABS(PLTX-PLT).LT.CT(4).AND.ABS(TLX-TL).LE.CT(8)) GO TO 83
78  CONTINUE

C          MACH NO. LIMITATION PROCEDURE
80  IF (EML.LT.YM) GO TO (92,82,96),KD
82  IF (KU.LT.3) KU=KU+1
      VLS=YM*SVL
      HLS=HLT-VLS**2/G2/XJ
      CALL COOL(HLS,PL,-3)
      RS2=R
      AL=HLT/RS2/VLS
      Z=HLT/AL*DHL/RHOLB
      DO 84 K=1,5
      HCP=Z./H1*(AL-H4*G)
      RU=RI +CPI*HCP
      WX=ALP
      HCP=Z.*P2*RO-F
      WP=P1*RT+2.*HCP+HCP
      JHL=4.*AL/WP
      IF(ABS(WX-HCP).LT.CT(2)) GJ TO 96
84  H1=2.*RT+HCP
      GU TO 96

C          AREA MODIFICATION FOR TUBE SPLICE
86  IF (ANNEB-ANWB) 88,58,88
88  KA=1
      WR=ANWB/ANNEB
      AL1=WR*AL1
      RT1=WR*RT1
      WCP1=WR*HCP1
      H11=Z.*RT1+WCP1
      H41=P1*RT1**2
      DO 90 K=1,5
      HCP1=Z./H11*(AL1-H41*G)
      RU1=H11+CPI*HCP1
      WX1=WCP1
      WCP1=Z.*P1/ANWB*RU1-(Z.*T*1+BRAZ)
      WP1=P1*RT1+2.*HCP1+WCP1
      IF (ABS(WX1-WCP1).LT.CT(2)) GO TO 58
90  H11=Z.*RT1+WCP1
      GU TO 58
92  IF(RU.GT.41) GO TO 112

```

C AREA MODIFICATION FOR MINIMUM AREA

```

94 AL=H4/2.
RU=RI
DHL=1.222*RT
HCP=0.0
WCP=2.*RT

```

C EVALUATION PROCEDURE

```

95 Z=WLT/AL*DHL/RHOL8
DO 110 K91=1,MT
QA1=QA
TF=TLF
CALL CUOL (TLF,PL,4)
RHOLF=R
RL=Z/AM*R
PF=CP *AM /AK
CPL=CP
AKL=AK
CALL CUOL(TLS,PL,4)
RB=R
RLH=WLT/AL*DHL/AM
AB=AM/R
CALL CUOL(TWL,PL,4)
AW=AM/R
C11=1.+0.1457*AW/AB*C1
CC=C11
IF(RC*C2.EQ.0.0) GO TO 98
IF(RL*RZ.LT.6.7) GO TO 98
C22=(RL*RZ)**0.05
IF(RC.LT.0.0) C22=1.
CC=CC*C22

98 HLF=CUFL*AKL*RL**0.8*PF**0.4*CC/DHL
TWL=QCOM*RTD/RT/HLF+TL
TLF=G*(TWL+TL)
DO 106 K=1,MT
A=QCOM*RAUTW
T=TMET
TMET=G*(TWL+TWG)
TWG=A/KHET(1, TMET)+TWL
TGF=G*TWG+.28*TGS+.22*TGE
CALL CUOL (TGF,PGS,4)
RHUGF=R
RG=RG/.785/DHG/AM*RHUGF/RHJGS
AMG=AM
AKG=AK
PG=CP *AM /AK
HGF=CUFG*AK*RG**0.8*PG**0.3/DHG
QC= HGF*(TGE - TWG)
Q7=QLQM
JCOM=QC+QRAU
QTOL=QCOM*CT(7)
IF (ABS(QCOM-Q7).LE.QTOL) GO TO 103
GO TO 108
103 IF (ABS(TF-TLF).LE.CT(3)) GO TO 102
GO TO 110
102 IF (ABS(T-TMET).LE.CT(3)) GO TO 104
GO TO 106
104 NCT=2
JLIQS=QCOM*RTD/RT
GO TO 58
106 CONTINUE
GO TO 58

108 JCOM=G*(QCOM+Q7)
QA=G*(QLQM+Q1)*WALL/WLT+QG
QL=QA*WLT*ANWB
IF(N.EQ.1) GO TO 110
HLT=HLT1+QA
CALL CUOL (HLT,PLT,-3)
TL=SS(7)
110 CONTINUE
112 NCT=2
GO TO 118

```



```

C          CALC. OF TOTAL PRESSURE AT INLET
114 CALL COOL (TL,PL,3)
    VL=(WLT/R/AL)**2/G2
    PT=PL+VL*R
    CALL CUOL (TL,PT,3)
    HLT=H(6)
    HLS=HLT-VL/XJ
    DO 116 K=1,MT
    CALL CUOL (HLS,PL,-3)
    VLS=WLT/R/AL
    RS2=R
    PT=PL+VLS**2*R/G2
    CALL CUOL (TL,PT,3)
    HLT=H(6)
    HLS=HLT-VLS**2/G2/XJ
    CALL COOL (HLS,PL,-3)
    TLS=SS(7)
    SVL=SVVL
    EML=VLS/SVL
    IF(ABS(HX-HLS).LT.CT(6)) GO TO 118
    HX=HLS
116 CONTINUE
    GO TO 118

118 CALL STRESS
C          END OF PROGRAM CALCULATIONS
C          RESULTS REQUIRED FOR NEXT STATION CALCS.

PGS1=PGS
AL1=AL
D1 =DHG
AX1 =AX
UHL1=UHL
ANWED1=ANWED
RT1=RT
TW1=TW
HLT1=HLT
TLS1=TLS
PLT1=PLT
WCP1=WCP
RI1=RI
CPH1=CPH
PH11=PH1
WP1=WP
TL1=TL
TWG1=TWG
TWGG=TWG
TWG(N+1)=TWG
PL1 =PL
AKT=1MET
Q1=QCUM
RS=RS2
HLS1=HLS
RS1=RS2
TUT1=RT+HCP
JTUT=QTOT+QL
ATUT=ATUT+WALT
VLSF=VLS/12.0
DO 120 K=12,50
JJ=K-11
120 SEE(N,JJ)=C(K)
AKL=0.0
PF=0.0
RL=0.0
AMG=0.0
AKG=0.0
PG=0.0
RG=0.0

```

```

      OUTPUT
      IF(N.NE.1) GO TO 124
      WRITE (6,122)
122  FORMAT(2X,7HSEC.NO.,2X,7HQ/A OUT,4X,6HQ/A IN,3X,9HEFF.GAS T,2X,
      16HT.REF.,4X,7HT.MET.G,3X,7HT.MET.L,5X,6HLIQ.T.,
      24X,6HLIQ.P.,4X,7HLIQ.VEL,4X,7HMACH NO,3X,9HTUBE AREA/
      374X,5HTOTAL,5X,6HSTATIC/
      410X,18H(BTU./SQ.IN.-SEC.),4X,7H(DEG.R),3X,7H(DEG.R),3X,7H(DEG.R),
      53X,7H(DEG.R),5X,7H(DEG.R),3X,6H(P.S.I),4X,6HFT/SEC,15X,
      68H(SQ.IN.)///)
124  WRITE (6,126) V,(C(K),K=1,11)
126  FORMAT(3X,13,2F11.2,4F10.0,F11.1,2F10.0,F12.3,F10.4)
128  CONTINUE
      V=NUMB
      GO TO 132
130  N=N-1
      WRITE (6,131)
131  FORMAT(//25X,31H** PRESSURE BELOW MINIMUM VALUE)
132  WRITE (6,134)
134  FORMAT(1H1//2X,7HSEC.NO.,2X,10HFRI.P.DROP,2X,10HMDM.P.DROP,2X,
      1 8HFRI.FACT,7X,3MHGF,11X,3HHLF,10X,2HCL,9X,2HC2,8X,2HC3,7X,
      29HQ/SECTION,6X,7HQ/A NUC//13X,5H(P.S.I),8X,5H(P.S.I),17X,21H(BTU./SQ.IN
      3,SEC.DEG.R),39X,7HBTU/SEC,4X,13HBTU/SQ.IN.SEC//)
      DO 136 J=1,N
136  WRITE (6,138) J,(SEE(J,1), I=1,10)
138  FORMAT(3X,13,2F12.2,3F13.5,3F11.3,F12.1,F15.3)
      WRITE (6,140)
140  FORMAT(1H1//2X,7HSEC.NO.,5X,9HSHELL RAD,8X,
      1 11HTUBE RADIUS,6X,11HTUBE HEIGHT,6X,10HTUBE WIDTH,9X,7HHYD.D
      21A,7X,9HWALL AREA,6X,17HTOTAL TUBE HEIGHT//18X,5H(IN.),11X,5H(IN.)
      3,12X,5H(IN.),13X,5H(IN.),12X,5H(IN.),10X,7H(SQ.IN.),12X,5H(IN.)///)
      DO 142 J=1,N
142  WRITE (6,144) J,(SEE(J,1), I=1,17)
144  FORMAT(3X,13,7F17.4)
      WRITE (6,146)
146  FORMAT(1H1//2X,7HSEC.NO.,2X,6HLIQ.T.,3X,6HLIQ.P.,6X,
      1 12HLIQ.ENTHALPY,11X,11HLIQ.DENSITY,9X,6HRE GAS,5X,6HPR GAS,
      24X,6HRE LIQ,7X,6HRE LIQ,6X,6HPR LIQ/11X,6HSTATIC,3X,5HTOTAL,4X,6H
      3TATIC,6X,5HTOTAL,6X,6HSTATIC,5X,5HTOTAL,7X,4HFILM,7X,4HFILM,6X,
      44HBULK,9X,4HFILM,8X,4HFILM/11X,7H(UEG.R),2X,4HPSIA,5X,6HBTU/LB,6X,
      56HBTU/LB,9X,9HLS/CU.IN.///)
      DO 148 J=1,N
148  WRITE (6,150) J,(SEE(J,1), I=18,28)
150  FORMAT(3X,13,F10.1,F9.0,2F11.2,2F11.5,4E13.3,F9.3,2E13.3,F9.3)
      WRITE (6,152)
152  FORMAT(1H1//1X,7HSEC.NO.,1X,8HR OVER T,2X,10HTUBE DELTA,22X,
      1 18HTUBE WALL STRESSES,15X,9HVG.METAL,3X,5HYIELD,5X,
      27HCOEF.UF,6X,7HYDUNG'S/31X,7HLUNG.AV,3X,8HLUNG.OUT,4X,7HLONG.IN,
      34X,8HTANG.OUT,3X,7HTANG.IN,4X,5HTEMP.,3X,8HSTRENGTH,4X,7HLIN.EXP,
      46X,7HMODULUS/21X,5H(IN.),6X,5H(P.S.I),6X,5H(P.S.I),6X,5H(P.S.I),6X,5H(P.S.I)
      51,6X,5H(P.S.I),5X,5HDEG.R,4X,5H(P.S.I),6X,7H(IN/IN),7X,5H(P.S.I)///)
      DO 154 J=1,N
154  WRITE (6,156) J,(SEE(J,1), I=29,39)
156  FORMAT(2X,13,F10.3,F11.5,5F11.0,F9.0,F11.0,2E13.3)
      DELTT=TL-TLIN
      DELTP=PLIN-PL
      WRITE (6,158) QTOT,ATOT,WGHT,DELTT,DELTP
158  FORMAT(1H1//9X,27HTOTAL COOLANT HEAT PICKUP =,F10.2,2X,7HBTU/SEC
      1 //9X,27HTOTAL NOZZLE WALL AREA =,F10.2,2X,61SQ.IN.//9X,
      27HTOTAL NUZZLE WEIGHT =,F10.2,2X,3HLS//9X,27HTOTAL COOLANT
      3 TEMP.DELTA =,F10.2,2X,5HDEG.R//9X,27HTOTAL COOLANT PRESS.DELTA =
      4,F10.2,2X,3HPSI)
      WRITE (6,160)
160  FORMAT(//50X,5HTITLE//50X,7HRESULTS//50X,16HFUTURE REVISIONS//)
      GO TO 4
      END

```

```

SUBROUTINE COOL (X,Y,J)
COMMON/STATE1/SS(50)/STATE2/U(3)/STATE3/C(215)/STATE4/JK(5)
COMMON/ST/H(10)
COMMON XZ(6),TL
EQUIVALENCE (TL,TS)

EQUIVALENCE (P,SS(6)),(T,SS(26)),(NF,SS(5)),(CP,SS(31))
EQUIVALENCE (AK,SS(30)),(VL,SS(15)),(VG,SS(16)),(VF,SS(19))
EQUIVALENCE (AM,SS(27)),(HF,SS(17)),(NCAL,H(10))
P=Y
IF(J.NE.0) GO TO 10
NCAL=1
NF=1
U=-2.
U(3)=1.E-06
VL=.25
VG=.4.
SS(6)=.5
VF=.5
SS(8)=VF
CALL STATE 5
RETURN

10 NCAL=NCAL+1
IF(J.GT. 9) GO TO (11,11,11,12),J
SS(7)=TS
SS(12)=X
CALL STATE (J)
H(6)=SS(12)
H(7)=1./SS(8)
H(2)=SS(10)
H(5)=SS(9)
RETURN

11 SS(7)=X
CALL STATE (J)
H(6)=SS(12)
H(7)=1./SS(8)
H(5)=SS(9)
RETURN

12 SS(26)=X
CALL STATE (J)
H(2)=SS(31)
H(3)=SS(27)
H(4)=SS(30)
H(5)=SS(9)
H(6)=SS(12)
H(7)=1./SS(19)
H(8)=SS(28)
RETURN
END

```

```

SUBROUTINE STRESS
COMMON QCOM, Q1QS, TGE, TGF, TWGG, TWL, TL, PL, VLSF, EML, AL, DF, DM, FF, HGF,
1 HLF, C11, C22, C33, QL, QN, RD, RT, HCP, WCP, DHL, WALT, TOTHT, TLS, PT,
2 HLS, HLT, RS2, RTL, RG, PG, RLB, RL, PF, ROVT, UELT, SIGLON, SIGLOO,
3 SIGLOI, SIGLOU, SIGIN, TMET, SIGALM, ALPHA1, E
4 /INPUT/AX(50), D4G(50), ANWEH(50), PHI(50), TH(50), TWG(50),
5 TGS(50), PGS(50), CJEFG(50), CJEFL(50), RC(50), QRAU(50),
6 QGEN(50), SHELTH(50)
COMMON/INPUT/DEN, SEC, G, PI, PGS1, CPH, AMU, ES, WGH, N, RI
REAL KMET
IF(N. GT. 1) GO TO 9
RAU=57.29578
VT=0.0
VS=0.0
AT=0.0
AS=0.0
ENS=0.0
ENS=0.0

9 E=KMET(3, TMET)
A=KMET(4, TMET)
DS1=DS
ENS1=ENS
US=2.*(RI+HLP/CPH)
ENS=-6*(PGS+PGS1)*(DS1*DS1-DS*DS)
ENS=ENS/(4.*DS*CPH)+ENS1*DS1/DS*COS((PHI-PHI1)/RAD)
ENI=PGS*US*G/CPH

11 RX=RI+G*TH
E6=0.0
E7=E6
IF(SHELTH.EQ.0.0) GO TO 12
E6=(ENS-AMU*ENI)/ES/SHELTH
E7=(ENI-AMU*ENS)/ES/SHELTH
12 Z=RX*(PL-PGS)/E/TH
ALPHA1=KMET(4, G*(TMET+TL))
W=ALPHA1*(TMET-TL)
EB=W-AMU*Z
E9=Z+W
DEL=2.*((E9-AMU*(E6-E8))*RX-PI/ANWEH*E7*RI)
T11=L*(1.068*TH*DEL/RX**2/(1.-AMU**2)-A*(TWG-TWL)/Z./(1.-AMU))
T12=E*(Z-.2796*DEL*TH**2/RX**3/(1.-AMU**2))

SIGOU1=T12+T11
SIGIN=T12-T11
E15=E6-E8
SIGLUN=E*E15
SIGMBT=E*A*(TWG-TWL)/(2.*(1.-AMU))
SIGLOU=SIGLON-SIGMBT
SIGLOI=SIGLON+SIGMBT
SIGALM=KMET(2, TMET)
ROVT=RX/TH
ATU=AT
AT=TH*(2.*HLP+PI*RT)*ANWEH
VT=.5*SEL*(ATU+AT)+VT
SU=2.*RU+SHELTH*CPH
ASU=AS
AS=PI*SD*SHELTH
VS=0.*SEC*(ASU+AS)+VS
IF(N.EQ.1) RETURN
WGH=UEN*(VT+VS)
RETURN
END

REAL FUNCTION KMET(N, TL)
COMMON/TEMP1, TEMP2, X(10,4), XZ(50)
DIMENSION TEN(4)
DATA (TEN(I), I=1,4)/.0001, 1000., 100000., .000001/

T=TE
IF(TEMP1.GT.T) T=TEMP1
IF(TEMP2.LT.T) T=TEMP2
T=T/TEN(2)
KMET=X(8, N)
K=8
DO 1J J=1,7
K=K-1
10 KMET=X(K, N)+T*KMET
KMET=KMET*TEN(N)
15 RETURN
END

```

EVALUATION PROGRAM

```

C
C
C      EVALUATION PROGRAM FOR CONVECTIVELY COOLED NOZZLES
C
COMMON X(10,5),TEMP1,TEMP2,TEMP3
1  /INPUT/AX(50),DHG(50),ANWEB(50),PHI(50),TW(50),AREAL(50),
2  TGS(50),PGS(50),COEFG(50),COEFL(50),AREACR(50),ROUGH(50),
3  RC(50),QRAD(50),QGEN(50),SHELTH(50),TKCER(50),TESTC(50)
4  /OUTPUT/DELPF(50),DELP(50),CFLIQ(50),HGF(50),HLF(50),
5  C1(50),C2(50),C3(50),QSEC(50),QNUCPT(50),RADSH(50),
6  RADIUS(50),HEIGHT(50),WIDTH(50),DHL(50),AWALL(50),HIGH(50),
7  TLSTAT(50),PLTOT(50),HS(50),HT(50),ROS(50),RUT(50),
8  REGF(50),PRGF(50),REBULK(50),RELF(50),PRLF(50),ROVT(50),
9  DELT(50),SIGLON(50),SIGLOD(50),SIGLOI(50),SIGOUT(50),
A  SIGIN(50),TMET(50),SIGALM(50),ALPHA1(50),E(50)
B  /STATE1/STORE(50)/STATE2/UNITS,COMP,CONV/STATE3/CS(215)/
C  STATE4/JUNK(50)
DIMENSION DUMMYI(50,18),DUMMYO(50,39),CT(9)
EQUIVALENCE(DUMMYI,AX),(DUMMYO,DELPF),
1  (PST34,STORE(6)),(CPSTA4,STJRE(31)),(TSTAT4,STORE(26)),
2  (RSTA3,STORE(8)),(AMUST4,STORE(27)),(AKSTA4,STORE(30)),
3  (TSTA3,STORE(7)),(ENTH33,STORE(12)),(RSTF4,STORE(19))
REAL KMET
LOGICAL LESTC1, LESTC2, LESTC3, LESTC4, LESTC5
NAMELIST /STUFF/TW,DHG,AX,TGS,PGS,ANWEB,AREAL,COEFL,COEFG,PHI,QRAD
1  ,TKCER,TESTC,SHELTH,RC,AREACR,ROUGH,QGEN,NUMB,COMP,AMU,
2  TLIN,PLIN,BRAZ,WL,WG,DIAM,DEN,ES,TEMP1,TEMP2,TEMP3,X,
3  QEST,TCER,TWGE,TMET1,F1,AKR,CT/CONST/CT,X,TESTC,TEMP1,
4  TEMP2,TEMP3,QEST,TCER,TWGE,TMET1,F1,AKR
DATA PI,PI2,A,A1,A2,A3,A4,CT/3.1415927,1.5707963,0.083333333,
1  9337.932,0.017453292,1.3868612E-7,5.7870370E-4,3.0E-6,C.0002,
2  1.0,0.1,0.001,0.0001,0.001,0.1,0.0001/
DO 2 I=1,900
2  AX(I)=0.0
TEMP3=0.0
DO 4 I=1,10
DO 4 J=1,5
4  X(I,J)=0.0
4  WRITE(6,8)
8  FORMAT(1H1)
READ(5,10) LESTC1,LESTC2,LESTC3,LESTC4,LESTC5
10 FORMAT(5L5)
READ(5,STUFF)
CONV=1.0E-6
UNITS=-1.0
CALL STATES
QNM1=QEST
Q1=QEST
P=PLIN
TL=TLIN
TJ=TLIN
NXX=NUMB+1
TG=TGS(NXX)
TLENG=ABS(AX(NXX)-AX(2))
ARCON=DHG(NXX)**2/DIAM**2
ARDIV=DHG(2)**2/DIAM**2
WRITE(6,CONST)
WRITE(6,12)
12 FORMAT(1H1///1X,8HSEC.NU.,3X,12HAXIAL LENGTH,4X,9HENG.DIAM.,5X,
1  8HNO.TUBES,3X,9HANGLE PHI,4X,11HTUBE THICK.,4X,13HAREA PER.T
2  UBE,5X,13HSTAT.GAS TEMP,4X,14HSTAT.GAS PRESS//16X,5H(IN.),9X,
3  35H(IN.),20X,6H(DEG.),8X,5H(IN.),9X,8H(SQ.IN.),11X,8H(DEG. R),9X,
4  46H(PSIA)///)
DO 14 J=2,NXX
14 JJ=J-1

```

```

14 WRITE(6,16) JJ,(DUMMYI(J,I),I=1,8)
16 FORMAT(2X,I3,F16.4,F15.4,F12.1,F13.3,F14.4,F15.4,F19.1,F16.2)
WRITE(6,18)
18 FORMAT(1H1///1X,9H SEC.NO. ,2X,9HGAS COEF.,2X,10HCOOL.COEF.,2X,
1 10HAREA CORR.,3X,9HROUGHNESS,3X,11HRA.D OF CURV,4X,6HQ RAD.,
25X,8HNUC.HEAT,4X,12HSHELL.THICK.,2X,16HCOAT.THK.OR RES.//50X,5H(IN
3.),8X,5H(IN.),7X,8HBTU.PER.,3X,8HBTU.PER.,7X,5H(IN.),6X,8H(IN) OR
4,11HSQ.IN-SEC-R/75X,9HSQ.IN-SEC,2X,9HCU.IN-SEC,25X,8HPER.BTU.///)
DO 20 J=2,NXX
JJ=J-1
20 WRITE(6,22) JJ,(DUMMYI(J,I),I=9,17)
22 FORMAT(3X,I3,2X,2F11.4,F12.4,E15.3,E14.4,F11.3,2F13.3,F17.4)
WRITE(6,24) DEN,ES,AMU,BRAZ
24 FORMAT(1H1///1X,18HAVG.METAL DENSITY=F6.3,2X,9HLBS/CU.IN,3X,
1 22HSHELL YOUNG'S MODULUS=E10.3,2X,3HPSI,3X,16HPOISSON'S RAT
2IO=F6.3,3X,12HBRAZE THICK=F7.4,2X,5H(IN.))
WRITE(6,26) WG,WL,TGT,TLIN,PGS(NXX),PLIN,DIAM,TLENG,ARCON,ARDIV
26 FORMAT(1H1//9X,21HPROPELLANT FLOW RATE ,F9.4,2X,7HLBS/SEC,23X,
1 17HCOOLANT FLOW RATE,4X,F9.4,2X,7HLBS/SEC//9X,19HCHAMBER TEM
2PERATURE,3X,F8.1,2X,6HDEG.R ,24X,22HENTRANCE COOLANT TEMP.,
3F8.2,2X,6HDEG.R //9X,16HCHAMBER PRESSURE,6X,F8.1,2X,6HPSIA ,
424X,22HENTRANCE COOLANT PRESS,F8.1,2X,6HPSIA ///43X,15HTHRUAT DIA
5METER,13X,F9.4,2X,5H(IN.)/43X,19HTOTAL NOZZLE LENGTH,8X,F10.4,2X,
65H(IN.)/43X,26HCONVERGENT AREA RATIO A/A*,3X,F8.4,/43X,25HDIVERGEN
7T AREA RATIO A/A*,4X,F8.4//)
IF(LESTC1) GO TO 30
WRITE(6,28)
28 FORMAT(42X,16H C-1 IS NOT USED/)
GO TO 34
30 WRITE(6,32)
32 FORMAT(42X,16H C-1 IS USED //)
34 IF(LESTC2) GO TO 38
WRITE(6,36)
36 FORMAT(42X,16H C-2 IS NOT USED/)
GO TO 42
38 WRITE(6,40)
40 FORMAT(42X,16H C-2 IS USED //)
42 IF(LESTC3) GO TO 46
WRITE(6,44)
44 FORMAT(42X,16H C-3 IS NOT USED/)
GO TO 50
46 WRITE(6,48)
48 FORMAT(42X,16H C-3 IS USED //)
50 IF(LESTC4) GO TO 54
WRITE(6,52)
52 FORMAT(43X,21HTUBE IS ASSUMED ROUGH/)
GO TO 58
54 WRITE(6,56)
56 FORMAT(43X,22HTUBE IS ASSUMED SMOOTH/)
58 IF(LESTC5) GO TO 62
WRITE(6,60)
60 FORMAT(43X,34HASSUMED FLAT PLATE HEAT CONDUCTION///)
GO TO 66
62 WRITE(6,64)
64 FORMAT(43X,30HASSUMED RADIAL HEAT CONDUCTION///)
66 STORE(8)=0.5
STORE(15)=0.25
STORE(16)=4.0
68 ALSEC = 0.0
RAD1 = 0.0
HEIGHT=0.0
HEIGHT1 = 0.0
PEST=PLIN
TWI=0.0
TGLER=0.0
IT=1
ATUT=0.0
QTUT=0.0
CIRT=0.0
CTHH=0.0
CTRG=0.0
CTRR=0.0
CTRI=0.0
CTKQ=0.0
KKK=1
KK=1
K=1
70 DO 72 L=1,18
J=IT+1
72 DUMMYI(1,L)=DUMMYI(J,L)
IF(IT.EQ.1) GO TO 74
ALSEC=SQRT(((DHG-DHG1)*0.5)**2+(AX-AX1)**2)
74 ANGBRD=PHI*A2
COSA=COS(ANGBRD)
IT=IT+1
IF(LESTC.NE.0.0) GO TO 76
TOVERK=TKCER
TKCER=0.0

```

```

C          CALCULATION OF GEOMETRY
76 WEBT=2.0*TW+BRAZ
   GGAS=WG/((DHG**2)*PI/4.0)
   IF(IT.GT.NUMB) GO TO 80
   BNWEB=ANWEB(IT+1)
   IF(BNWEB.GE.ANWEB) GO TO 80
   PHI1=PI/BNWEB
   RADIUS=(PHI1*(DHG*0.5+(TW+TKCER)*COSA)-WEBT*0.5)/(1.0-PHI1*COSA)
   HOLD=2.0*AREAL-PI2*RADIUS**2+RADIUS*TW
   HEIGHT=HOLD/(2.0*RADIUS-TW)
78 RADSH=(HEIGHT+RADIUS+TW)*COSA+DHG*0.5
   WIDTH=2.0*PHI1*RADSH-WEBT
   THIGHT=HEIGHT
   HEIGHT=HOLD/(RADIUS+WIDTH/2.0-TW)
   XX=ABS(HEIGHT-THIGHT)
   CTG=CTG+1.0
   IF(CTG.GT.10.0) GO TO 84
   IF(XX.GT.CT(2)) GO TO 78
   HIGH=HEIGHT+RADIUS
   WP=PI2*RADIUS*2.0*HEIGHT+WIDTH/2.0-TW+RADIUS
   RADIUS=RADIUS/2.0
   GO TO 88
80 PHI1=PI/ANWEB
   RADIUS=(PHI1*(DHG*0.5+(TW+TKCER)*COSA)-WEBT*0.5)/(1.0-PHI1*COSA)
   HOLD=AREAL-PI2*RADIUS**2
   HEIGHT=HOLD/(2.0*RADIUS)
82 RADSH=(HEIGHT+RADIUS+TW)*COSA+DHG*0.5
   WIDTH=2.0*PHI1*RADSH-WEBT
   THIGHT=HEIGHT
   HEIGHT=HOLD/(RADIUS+WIDTH*0.5)
   XX=ABS(HEIGHT-THIGHT)
   CTG=CTG+1.0
   IF(CTG.GT.10.0) GO TO 84
   IF(XX.GT.CT(2)) GO TO 82
   HIGH=HEIGHT+RADIUS
   WP=PI*RADIUS*2.0*HEIGHT+WIDTH
   GO TO 88
84 WRITE(6,86)
86 FORMAT(///22X,36HITERATION LIMIT EXCEEDED ON GEOMETRY///)
   GO TO 268
88 CTG=0.0
   RAD=RADIUS+0.5*TW
   DHL=4.0*AREAL/WP
   AWALL=PI2*ALSEC*ANWEB*(RAD1+RADIUS+TW+TW1)*AREACR
   RRATSQ=(RADIUS/RC)**2
   IF(LESTC5) GO TO 90
   RADO=RADIUS
   RAUTW=TW
   IF(LESTC.LE.0.0) GO TO 92
   RADC=RADIUS
   RADCER=TKCER
   GO TO 92
90 RADO=RADIUS+TW
   RAUTW=RADO*ALOG(RADO/RADIUS)
   IF(LESTC.LE.0.0) GO TO 92
   RADC=RADO+TKCER
   RADCER=RADC*ALOG(RADC/RADO)
92 AREAL=AREAL*ANWEB
   GLIQ=WL/AREAL
   WLARDH=GLIQ*DHL
   TSTAT4=TGS
   PST34=PGS
   CALL STATE(4)
   RGO=A4/RST4
   IF(IT.NE.2) GO TO 94
   FFLIQ=0.0
   QNUC=0.0
   QNUCPT=0.0
   GLIQA=GLIQ
   GO TO 96
94 AVGW=(WP+WP1)/2.0
   AREALM=(AREAL+AREAL1)/2.0
   DHLAVG=4.0*AREALM/ANWEB/AVGW
   GLIQA=WL/AREALM
   QNUC=QGEN*SHELTH*ALSEC*PI*(RADSH+RADSH1+(SHELTH+SHELT1)*0.5)
   QNUCPT=QNUC/(ALSEC*PI*(RADSH+RADSH1)-WEBT*ANWEB)

```

```

C
          CALC FOR TEMP JF THE GAS WALL
96 IF(TESTC)108,98,100
98 TGCER=QEST*TOVERK+TWGE
   GU TO 108
100 AKCER=KMET(TCER,5)
   XTGER=TCER
   TGLER=(QEST/AKCER)*RADCER+TWGE
   TCER=(TGCER+TWGE)/2.0
   XX=ABS(TCER-XTGER)
   IF(XX.LT.CT(3)) GO TO 106
   CTRT=CTR1+1.0
   IF(CTR1-25.0) 100,102,102
102 WRITE(6,104)
104 FORMAT(///22X,44HITERATION LIMIT EXCEEDED ON AVG COATING TEMP///)
   GO TO 268
106 CTRT=0.0
108 TGE=(TGT-TGS)*AKR+TGS
   IF(TESTC)112,110,110
110 TGF=TGS+0.5*(TGCER-TGS)+0.22*(TGE-TGS)
   GO TO 114
112 TGF=TGS+0.5*(TWGE-TGS)+0.22*(TGE-TGS)
114 TSTAT4=TGF
   PST34=PGS
   CALL STATE(4)
   CPGF=CPSTA4
   AMUGF=AMUST4*A
   RGF=A4/RSTF4
   AKGF=AKSTA4*A
   PRGF=(CPGF*AMUGF)/AKGF
   TAKR=AKR
   AKR=PRGF**0.3333333
   XX=ABS(AKR-TAKR)
   CTRR=CTR1+1.0
   IF(CTRR.GT.10.0) GO TO 116
   IF(XX.GT.CT(5)) GO TO 108
   CTRR=0.0
   GO TO 120
116 WRITE(6,118)
118 FORMAT(///22X,43HITERATION LIMIT EXCEEDED ON RECOVERY FACTOR///)
   GO TO 268
120 REGF=((GGAS*DHG)/AMUGF)*RGF/RGO
   REEXG=KEGF**0.8
122 PRGEX=PRGF**0.3
   HGF=((PRGEX*COEFC*AKGF)/DHG)*REEXG
   IF(TESTC) 128,124,126
124 TWG=TGE-(QEST-QRAD)/HGF-QEST*TOVERK
   GO TO 130
126 TWG=TGE-(QEST-QRAD)/HGF-QEST*RADCER/AKCER
   GO TO 130
128 TWG=TGE-(QEST-QRAD)/HGF
130 TERMX=ABS(TWGE-TWG)
   ABS15=TWGE
   IF(ITERMX.LT.CT(8)) GO TO 142
   IF(TWG-TL) 132,132,134
132 Q=QEST*0.1
   GO TO 224
134 IF(CTR1.GT.0.0) GO TO 136
   TWGE=(TWG+TWGE)*0.5
   GO TO 138
136 CALL ITRAT(TWGE,TWG,TWGX1,TWGY1,TWGE)
138 TWGX1=ABS15
   TWGY1=TWG
   CTR1=CTR1+1.0
   IF(CTR1.LT.25.0) GO TO 96
   WRITE(6,140)
140 FORMAT(///22X,44HITERATION LIMIT EXCEEDED ON TEMP OF GAS WALL///)
   GO TO 268

```



```

      C          CALC. OF TEMP. OF LIQUID WALL
142  CTRI=0.0
      IF(TESTC.GT.0.0) QEST=QEST*RADC/RADO
144  AKM=KMET(TMET,1)
      TWL=TWG-((QEST/AKM)*RADTW)
      TMET=(TWG+TWL)/2.0
      IF(TMET-TL) 146,146,148
146  Q=QEST*0.1
      GO TO 224
148  TERMX=ABS(TMET-TMET)
      CTRI=CTRI+1.0
      IF(CTRI.GT.25.0) GO TO 150
      IF(TERMX.LT.CT(3)) GO TO 154
      TMET=TMET
      GO TO 144
150  WRITE(6,152)
152  FORMAT(///22X,44HITERATION LIMIT EXCEEDED ON TEMP OF LIQ WALL///)
      GO TO 268
154  CTRI=0.0
      QSEC=((QEST+QNM1)/2.0)*AWALL+QNJC
      QSECL=QSEC/WL
      C          CALCULATION OF THE COOLANT
      IF(IT.NE.2) GO TO 162
      IF(KK.GT.1) GO TO 206
      KK=2
      C3=1.0
      PL=P
      DELPM=C.0
      DELPF=0.0
      CFLIQ=0.0
      PST34=PL
      TSTA3=TL
      CALL STATE(3)
      ROS=A4/RSTA3
      ROST=ROS
156  PLTOT=PL+GLIQ*GLIQ*ROST/(ROS*ROS*772.176)
      PST34=PLTOT
      TSTA3=TL
      CALL STATE(3)
      HT=ENTH33
      ROT=A4/RSTA3
      HS=HT-A3*(GLIQ/ROS)**2
      ENTH33=HS
      PST34=PL
      CALL STATE(-3)
      EROS=ROS
      ROS=A4/RSTA3
      EROST=ROST
      ROST=(ROS+ROT)/2.0
      XX=ABS(ROS-EROS)
      XXX=ABS(ROST-EROST)
      YY=ROST*CT(9)
      CTRI=CTRI+1.0
      IF(CTRI.GT.10.0) GO TO 158
      IF(XX.GT.YY) GO TO 156
      IF(XXX.GT.YY) GO TO 156
      CTRI=0.0
      TLSTAT=TSTA3
      SONICV=STORE(9)
      GO TO 206

```

```

158 WRITE(6,160)
160 FORMAT(///22X,54HITERATION LIMIT EXCEEDED ON INITIAL COOLANT CONDI
ITIONS///)
GO TO 268
162 DELTH=QSEC*WL
IF(CTRQ.EQ.0.0) HS=HS1+DELTH
ENTH33=HS
PST34=PL
TSTA3=TLSTAT
CALL STATE(-3)
ROS=A4/RSTA3
HT=HT1+DELTH
164 HEST=HS
HS=HT-A3*(GLIQ/ROS)**2
XXX=ABS(HEST-HS)
YY=ABS(HS*CT(6))
CTRH=CTRH*1.0
IF(CTRH.GT.15.0) GO TO 168
IF(XXX.LT.YY) GO TO 172.
166 PST34=PL
ENTH33=HS
CALL STATE(-3)
ROS=A4/RSTA3
SONICV=STORE(9)
TLSTAT=TSTA3
GO TO 164
168 WRITE(6,170)
170 FORMAT(///22X,43HITERATION LIMIT EXCEEDED ON STATIC ENTHALPY///)
GO TO 268
172 CTRH=0.0
DELPN=GLIQA*(GLIQ/ROS-GOVERR)/386.088
PST34=(PL+P1)/2.0
ENTH33=(HS+HS1)/2.0
CALL STATE(-3)
TLAVG6=TSTA3
ROAVG=A4/RSTA3
TSTAT4=TSTA3
CALL STATE(4)
AMULAV=AMUST4*A
RESTAV=GLIQA*DHLAVG/AMULAV
IF(LESTC3) GO TO 174
C3=1.0
GO TO 176
174 C3=(RESTAV*RRATSQ)**.05
IF(C3.LE.1.0937) C3 = 1.0
176 F2=F1
IF(LESTC4) GO TO 178
FFLIQ=(1.0/(-4.0*ALOG10(ROUGH/DHLAVG/3.7+1.255/RESTAV/F1**0.5)))
1**2
GO TO 180
178 FFLIQ=(1.0/(4.0*ALOG10(F1**0.5*RESTAV)-0.40))**2.0
180 F1=FFLIQ
CTRR=CTRR+1.0
IF(CTRR.GT.10.0) GO TO 182
DELTF=ABS(F1-F2)
IF(DELTF.GT.CT(1)) GO TO 176
CTRR=0.0
CFLIQ=FFLIQ*C3
DELPF=GLIQA*GLIQA/ROAVG*CFLIQ*ALSEC/DHLAVG/193.044
PEST=PL
PL=P-DELPN-DELPF
ABSIS=PL
IF(PL-PLIN*C.3)186,186,190

```

```

182 WRITE(6,184)
184 FORMAT(///22X,43HITERATION LIMIT EXCEEDED ON FRICTION FACTOR///)
GO TO 268
186 PLIN=PLIN+50.0
P=PLIN
TL=TI
QEST=QI
QNM1=QI
WRITE(6,188)
188 FORMAT(///22X,28HNOZZLE COOLANT PRESSURE LUST////)
GO TO 68
190 XX=ABS(PEST-PL)
IF(CTRI.GT.25.0) GO TO 192
IF(XX.GT.CT(4)) GO TO 196
CTRI=0.0
GO TO 200
192 WRITE(6,194)
194 FORMAT(///22X,40HITERATION LIMIT EXCEEDED ON LIQ PRESSURE///)
GO TO 268
196 IF(CTRI.EQ.0.0) GO TO 198
CALL ITRAT(PEST,PL,PQX,PQY,PL)
198 PQX=PEST
PQY=ABSIS
CTRI=CTRI+1.0
GO TO 166
200 PST34=(PLTOT1+PLTOT)/2.0
ENTH33=(HT+HT1)/2.0
CALL STATE(-3)
ROAVGT=A4/RSTA3
TLAVGT=TSTA3
DELPT=ROAVGT*A1*DELTH*(TLAVGT-TLAVGS)/TLAVGS*DELPF*ROAVGT
1*TLAVGT/TLAVGS/ROAVG
PTEST=PLTOT
PLTOT=PLTOT1-DELPT
XX=ABS(PTEST-PLTOT)
CTRI=CTRI+1.0
IF(CTRI.GT.15.0) GO TO 202
IF(XX.GT.CT(4)) GO TO 200
CTRI=0.0
PST34=PLTOT
ENTH33=HT
CALL STATE(-3)
TL=TSTA3
ROT=A4/RSTA3
GO TO 206
202 WRITE(6,204)
204 FORMAT(///22X,46HITERATION LIMIT EXCEEDED ON LIQ TOTAL PRESSURE//)
GO TO 268
206 TSTAT4=TLSTAT
PST34=PL
CALL STATE(4)
AMUBLK=AMUST4*A
ROS=A4/RSTF4
REBULK=WLARDH/AMUBLK

```

```

C          CALC. OF HEAT FLUX
208 IF(TWL-TL) 208,238,210
208 Q=QEST*0.1
GO TO 224
210 TLF=(TL+TWL)/2.0
TSTAT4=TWL
CALL STATE(4)
AMUTWL=AMUST4*A
ROTWL=A4/RSTF4
TSTAT4=TLF
CALL STATE(4)
CPLF=CPSA4
AMULF=AMUST4*A
AKLF=AKSTA4*A
RELF=WLARDH*A4/(RSTF4*AMULF*ROS)
IF(LESTC2) GO TO 212
C2=1.0
GO TO 214
212 C2=(RELF*RRATSQ)**.35
IF(C2.LE.1.0937) C2=1.0
214 IF(LESTC1) GO TO 216
C1=1.0
GO TO 218
216 ZDVZ=(AMUTWL/ROTWL)/(AMU8LK/ROS)
C1=1.0+(.01457*ZDVZ)
218 PRLF=(CPLF*AMULF)/AKLF
REEXL=RELF**.8
PREX4=PRLF**.4
PAHLF=(PREX4*COEFL*AKLF/UHL)*REEXL
IF(RC)220,220,222
220 C2=1.0
222 HLF=PAHLF*C2*C1
QI=(TWL-TL)*HLF
Q=QI*RAJUS/RAJ0
224 ABSIS=QEST
TERMX=ABS(QEST-Q)
IF(ITERMX.GT.CT(7)) GO TO 226
CTRQ=0.0
GO TO 236
226 IF(CTRQ.GT.0.0) GO TO 228
QEST=(Q+QEST)*0.5
GO TO 230
228 CALL ITRAT(QEST,J,TQX1,TQY1,QEST)
230 TQX1=ABSIS
TQY1=Q
IF(LESTC.GT.0.0) QEST=QEST*RAJ0/RADC
CTRI=0.0
CTRQ=CTRQ+1.0
IF(CIRQ-25.0) 96,232,232
232 WRITE(6,234)
234 FORMAT(///22X,37HITERATION LIMIT EXCEEDED ON HEAT FLUX///)
GO TO 268
236 VEL=(ULI4/ROS)*A
AMACH=VEL/SONICV

```

```

C          CALCULATION OF STRESS
      TMETA=(TMET+TL)/2.0
      ALPHA1=KMET(TMETA,4)
      ALPHA2=KMET(TMETA,4)
      E=KMET(TMET,3)
      SIGALM=KMET(TMET,2)
      IF(IT.NE.2) GO TO 238
      SNS = 0.0
      GO TO 240
238 SNS=-0.125*(PGS1+PGS)*(DHG1**2-DHG**2)/(DHG*COXA)
      1+SNS=DHG1/DHG*COS(ANGBRD-ANGRD1)
240 SNPS1=PGS*DHG*0.5/COXA
      EPSLNM=(SNS-AMU*SNPS1)/(ES*SHELTH)
      EPSLNH=(SNPS1-AMU*SNS)/(ES*SHELTH)
      TERM1=(PL-PGS)*RAD/(E*TW)
      EPSLT=-TERM1*AMU+ALPHA1*(TMET-TL)
      DELT=((TERM1+ALPHA1*(TMET-TL))-AMU*(EPSLNM-EPSLT))*2.0*RAD
      1-(PI*EPSLNH/ANWEB)*(DHG+2.0*RAD/COXA)
      TERM2=E*ALPHA2*(TWG-TWL)/(2.0*(1.0-AMU))
      TERM3=1.0681*E*TW*DELT/((1.0-AMU**2)*RAD**2)-TERM2
      TERM4=TERM1+E-0.2796*E*TW**2*DELT/((1.0-AMU**2)*RAD**3)
      SIGOUT=TERM4+TERM3
      SIGIN=TERM4-TERM3
      EPSLTX=EPSLNM-EPSLT
      SIGLON=E*EPSLTX
      SIGLOI=SIGLON+TERM2
      SIGLUU=SIGLON-TERM2
      ANGRD1=ANGBRD
      PGS1=PGS
      IF(IT.NE.2) GO TO 242
      WGH=0.0
      GO TO 244
242 SHELTA=(SHELT1+SHELTH)/2.0
      WGH=WGH+PI2*ALSEC*SHELTA*DEN)*(DHG1+DHG+2.0*(HEIGHT1+
      HEIGHT+RAD1+RADIUS+TW+TW1+SHELTA)*COXA)+(ALSEC*ANWEB
      2*0.5*(TW+TW1)*DEN)*(PI2*(RAD1+RADIUS)+HEIGHT1+HEIGHT)
C          OUTPUT AND NEXT STATION
244 P=PL
      ROVT=RAD/TW
      ATOT=ATOT+AWALL
      QTOT=QTOT+QSEC
      IF(K.EQ.2) GO TO 250
      IF(TESTR) 248,248,246
246 IF(TCER.GT.TEMP3) K=2
248 IF(TMET.GT.TEMP2) K=2
      IF(TMETA.LT.TEMP1) K=2
250 IF(IT.GT.NUMB) GO TO 258
      HT1=HT
      HSL=HS
      GOVERR=GLIQ/ROS
      PLTOT1=PLTOT
      QUEST=Q
      QNM1=Q
      DHG1=DHG
      AX1=AX
      HEIGHT1=HEIGHT
      TW1=TW
      SHELTI=SHELTH
      RADSH1=RADSH
      AREAL1=AREAL
      IF(BNWEB-ANWEB) 252,256,254
252 WP1=2.0*(WP-HEIGHT-RADIUS+TW)
      RAD1=2.0*RADIUS
      KKK=2
      GO TO 258
254 WP1=WP/2.0+HEIGHT+RADIUS-TW
      RAD1=RADIUS/2.0
      KKK=2
      GO TO 258
256 WP1=WP
      RAD1=RADIUS
258 IF(IT.NE.2) GO TO 262
      WRITE(6,260)
260 FORMAT(2X,7HSEC.NO.,2X,7HQ/A OUT,4X,6HQ/A IN,3X,9HEFF.GAS T,2X,
      1 6HT.REF.,3X,8HT.COAT.G,3X,7HT.MET.G,3X,7HT.MET.L,5X,6HLIQ.T,
      2,4X,6HLIQ.P,4X,7HLIQ.VEL,4X,7HMACH NO/84X,5HTOTAL,5X,6HSTATIC/
      310X,18H(BTU./SQ.IN.-SEC.),4X,7H(DEG.R),3X,7H(DEG.R),4X,7H(DEG.R),
      43X,7H(VEG.R),3X,7H(DEG.R),4X,7H(DEG.R),3X,6H(PSIA),4X,6HFT/SEC.//)
262 DO 264 L=1,39
264 DUMMYU(IT,L)=DUMMYO(1,L)
      JJ=IT-1
      WRITE(6,266) JJ,Q,Q1,TGE,TGF,TGCER,TWG,TWL,TL,P,VEL,AMACH
266 FORMAT(3X,I3,2F11.2,5F10.0,F11.1,2F10.0,F12.3)
      IF(NUMB.GE.IT) GO TO 270
      GO TO 270

```

```

C          FINAL OUTPUT DATA
268 NXX=I-1
270 IF(KKK.EQ.1) GO TO 274
    WRITE(6,272)
272 FORMAT(//25X,4H***NOTE NOZZLE DESIGN CONTAINS A SPLICE//)
274 IF(K.EQ.1) GO TO 278
    WRITE(6,276)
276 FORMAT(//25X,6H*** NOTE TEMPERATURE RANGE EXCEEDED ON MATERIAL
1 PROPERTIES)
278 WRITE(6,280)
280 FORMAT(1H1//2X,7HSEC.NO.,2X,10HFRI.P.DROP,2X,10HMDM.P.DROP,2X,
1 8HFRI.FACT,7X,3HHGF,11X,3HHLF,10X,2HCL,9X,2HC2,8X,2HC3,7X,
29HQ/SECTION,6X,7HQ/A NUC//13X,5H(P>1),8X,5H(PS1),17X,21H(BTU/SQ.IN
3.SEC.DEG.R),39X,7HBTU/SEC,4X,13HBTU/SQ.IN.SEC//)
    DO 282 J=2,NXX
    JJ=J-1
282 WRITE(6,284) JJ,(DUMMY(J,I),I=1,10)
284 FORMAT(3X,I3,2F12.2,3F13.5,3F11.3,F12.1,F15.3)
    WRITE(6,286)
286 FORMAT(1H1//2X,7HSEC.NO.,6X,9HSHELL RAD,8X,
1 11HTUBE RADIUS,6X,11HTUBE HEIGHT,6X,10HTUBE WIDTH,9X,7HHYD.O
21A,7X,9HWALL AREA,6X,17HTOTAL TUBE HEIGHT//18X,5H(IN.),11X,5H(IN.)
3,12X,5H(IN.),13X,5H(IN.),12X,5H(IN.),10X,7H(SQ.IN),12X,5H(IN.)//)
    DU 288 J=2,NXX
    JJ=J-1
288 WRITE(6,290) JJ,(DUMMY(J,I),I=1,17)
290 FORMAT(3X,I3,7F17.4)
    WRITE(6,292)
292 FORMAT(1H1//2X,7HSEC.NO.,2X,6HLIQ.T.,3X,6HLIQ.P.,6X,
1 12HLIQ.ENTHALPY,11X,11HLIQ.DENSITY,9X,6HRE GAS,5X,6HPR GAS,
24X,6HRE LIQ,7X,6HRE LIQ,6X,6HPR LIQ/11X,6HSTATIC,3X,5HTOTAL,4X,6HS
3TATIC,6X,5HTOTAL,6X,6HSTATIC,5X,5HTOTAL,7X,4HFILM,7X,4HFILM,6X,
44HBULK,9X,4HFILM,8X,4HFILM/11X,7H(DEG.R),2X,4HPSIA,5X,6HBTU/LB,6X,
56HBTU/LB,9X,9HLBS/CU.IN//)
    DO 294 J=2,NXX
    JJ=J-1
294 WRITE(6,296) JJ,(DUMMY(J,I),I=18,28)
296 FORMAT(3X,I3,F10.1,F9.0,2F11.2,2F11.5,E19.3,F9.3,2E13.3,F9.3)
    WRITE(6,298)
298 FORMAT(1H1//1X,7HSEC.NO.,1X,8HR OVER T,2X,10HTUBE DELTA,22X,
1 18HTUBE WALL STRESSES,15X,9HAVG.METAL,3X,5HYIELD,5X,
27HCOEF.UF,6X,7HYOUNG'S/31X,7HLONG.AV,3X,8HLONG.OUT,4X,7HLONG.IN,
34X,8HTANG.OUT,3X,7HTANG.IN,4X,5HTEMP.,3X,8HSTRENGTH,4X,7HLIN.EXP,
46X,7HMODULUS/21X,5H(IN.),6X,5H(PS1),6X,5H(PS1),6X,5H(PS1),6X,5H(PS
51),6X,5H(PS1),5X,5HDEG.R,4X,5H(PS1),6X,7H(IN/IN),7X,5H(PS1)//)
    DO 300 J=2,NXX
    JJ=J-1
300 WRITE(6,302) JJ,(DUMMY(J,I),I=29,39)
302 FORMAT(2X,I3,F10.3,F11.5,5F11.0,F9.0,F11.0,2E13.3)
    DELT=TL-TLIN
    DELTP=PLIN-PL
    WRITE(6,304) QTOT,ATOT,WGHT,DELT,DELTP
304 FORMAT(1H1//9X,27HTOTAL COOLANT HEAT PICKUP =,F10.2,2X,7HBTU/SEC
1 //9X,27HTOTAL NOZZLE WALL AREA =,F10.2,2X,6HSQ.IN//9X,
27HTOTAL NOZZLE WEIGHT =,F10.2,2X,3HLBS//9X,27HTOTAL COOLANT
3 TEMP.DELTA =,F10.2,2X,5HDEG.R//9X,27HTOTAL COOLANT PRESS.DELTA =
4,F10.2,2X,3HPSI)
    WRITE(6,306)
306 FORMAT(//50X,5HTITLE//50X,7HRESULTS//50X,16HFUTURE REVISIONS//)
    GO TO 6
END
SUBROUTINE ITRAT(V,W,X,Y,Z)
    IF(V-X)2,1,2
    1 X=X+1.1
    2 DENOM=W-X
    SLOPE=(W-Y)/DENOM
    IF(SLOPE.EQ.1.0) GO TO 3
    DNMI=1-SLOPE
    Z=ABS ((X>SLOPE-Y)/DNMI)
    GO TO 4
    3 Z=W
    4 RETURN
END
REAL FUNCTION KMET(TX,N)
COMMON X(10,5),TEMP1,TEMP2,TEMP3
DIMENSION TEN(5)
DATA TEN/1.0E-4,1.0E3,1.0E6,1.0E-6,1.0E-4/
N=1, THERMAL CONDUCTIVITY
N=2, YIELD STRENGTH
N=3, YOUNGS MODULUS
N=4, THERMAL EXPANSION
N=5, THERMAL CONDUCTIVITY OF COATING
T=TX
IF(TEMP1.GT.T) T=TEMP1
IF(N.EQ.5) GO TO 1
IF(TEMP2.LT.T) T=TEMP2
GO TO 2
1 IF(TEMP3.LT.T) T=TEMP3
2 T=T/1000.0
KMET=(X(1,N)+T*(X(2,N)+T*(X(3,N)+T*(X(4,N)+T*(X(5,N)+T*(X(6,N)
1+T*(X(7,N)+T*(X(8,N)+T*(X(9,N)+T*(X(10,N)))))))))*TEN(N)
RETURN
END

```

REFERENCES

1. Benser, W. A.; and Graham, R. W.: Hydrogen Convective Cooling of Rocket Nozzles. Paper No. 62-AV-22, ASME, June 1962.
2. Bartz, D. R.: A Simple Equation for Rapid Estimation of Rocket Nozzle Convective Heat Transfer Coefficients. *Jet Propulsion*, vol. 27, no. 1, Jan. 1957, pp. 49-51.
3. Schacht, Ralph L.; Quentmeyer, Richard J.; and Jones, William L.: Experimental Investigation of Hot-Gas Side Heat-Transfer Rates for a Hydrogen-Oxygen Rocket. NASA TN D-2832, 1965.
4. Anon.: Phoebus-2 Monthly Progress Report for the Period February 15 through March 31, 1965. Rep. No. RP-MR-0001, Aerojet-General Corp., Apr. 1965.
5. Eckert, Ernst R. G.; and Drake, Robert M., Jr.: *Heat and Mass Transfer*. Second ed., McGraw-Hill Book Co., Inc., 1959.
6. Hess, H. L.; and Kunz, H. R.: A Study of Forced Convection Heat Transfer to Supercritical Hydrogen. *J. Heat Transfer*, vol. 87, no. 1, Feb. 1965, pp. 41-48.
7. Itō, H.: Friction Factors in Turbulent Flow in Curved Pipes. *J. Basic Eng.*, vol. 81, no. 2, June 1959, pp. 123-134.
8. Hendricks, R. C.; and Simon, F. F.: Heat Transfer to Hydrogen Flowing in a Curved Tube. *Multi-Phase Flow Symposium*, Norman J. Lipstein, ed., ASME, 1963, pp. 90-93.
9. Hendricks, R. C.; Simoneau, R. J.; and Friedman, R.: Heat-Transfer Characteristics of Cryogenic Hydrogen from 1000 to 2500 psia Flowing Upward in Uniformly Heated Straight Tubes. NASA TN D-2977, 1965.
10. McAdams, William H.: *Heat Transmission*. Third ed., McGraw-Hill Book Co., Inc., 1954.
11. Hall, Newman A.: *Thermodynamics of Fluid Flow*. Prentice-Hall, Inc., 1951 (3rd Printing, 1957).
12. Timoshenko, Stephen P.; and Gere, James M.: *Theory of Elastic Stability*. Second ed., McGraw-Hill Book Co., Inc., 1961.
13. Pfluger, Alf (Ervin Galantay, trans.): *Elementary Statics of Shells*. Second ed., F. W. Dodge Corp., 1961.
14. Roark, Raymond L.: *Formulas for Stress and Strain*. Third ed., McGraw-Hill Book Co., Inc., 1954.

15. Anon.: Materials Properties Data Book. Rep. No. 2275, Aerojet General Corp., July 1964.
16. Harry, David P., III: Formulation and Digital Coding of Approximate Hydrogen Properties for Application to Heat-Transfer and Fluid-Flow Computations, NASA TN D-1664, 1963.

"The aeronautical and space activities of the United States shall be conducted so as to contribute . . . to the expansion of human knowledge of phenomena in the atmosphere and space. The Administration shall provide for the widest practicable and appropriate dissemination of information concerning its activities and the results thereof."

—NATIONAL AERONAUTICS AND SPACE ACT OF 1958

NASA SCIENTIFIC AND TECHNICAL PUBLICATIONS

TECHNICAL REPORTS: Scientific and technical information considered important, complete, and a lasting contribution to existing knowledge.

TECHNICAL NOTES: Information less broad in scope but nevertheless of importance as a contribution to existing knowledge.

TECHNICAL MEMORANDUMS: Information receiving limited distribution because of preliminary data, security classification, or other reasons.

CONTRACTOR REPORTS: Technical information generated in connection with a NASA contract or grant and released under NASA auspices.

TECHNICAL TRANSLATIONS: Information published in a foreign language considered to merit NASA distribution in English.

TECHNICAL REPRINTS: Information derived from NASA activities and initially published in the form of journal articles.

SPECIAL PUBLICATIONS: Information derived from or of value to NASA activities but not necessarily reporting the results of individual NASA-programmed scientific efforts. Publications include conference proceedings, monographs, data compilations, handbooks, sourcebooks, and special bibliographies.

Details on the availability of these publications may be obtained from:

SCIENTIFIC AND TECHNICAL INFORMATION DIVISION
NATIONAL AERONAUTICS AND SPACE ADMINISTRATION
Washington, D.C. 20546